AD_____

Award Number: DAMD17-00-1-0394

TITLE: Negative Regulation of Tumor Suppressor p53 Transcription
in Breast Cancer Cells

PRINCIPAL INVESTIGATOR: Jingwen Liu, Ph.D.

CONTRACTING ORGANIZATION: Palo Alto Institute for Research &
Education, Incorporated
Palo Alto, California 94304

REPORT DATE: July 2004

TYPE OF REPORT: Final

PREPARED FOR: U.S. Army Medical Research and Materiel Command
Fort Detrick, Maryland 21702-5012

DISTRIBUTION STATEMENT: Approved for Public Release;
Distribution Unlimited

The views, opinions and/or findings contained in this report are
those of the author(s) and should not be construed as an official
Department of the Army position, policy or decision unless so
designated by other documentation.

20050407 147

REPORT DOCUMENTATION PAGE

1. AGENCY USE ONLY (Leave blank)	2. REPORT DATE July 2004	3. REPORT TYPE AND DATES COVERED Final (1 Jul 2000 – 30 Jun 2004)

4. TITLE AND SUBTITLE
Negative Regulation of Tumor Suppressor p53 Transcription in Breast Cancer Cells

5. FUNDING NUMBERS
DAMD17-00-1-0394

6. AUTHOR(S)
Jingwen Liu, Ph.D.

7. PERFORMING ORGANIZATION NAME(S) AND ADDRESS(ES)
Palo Alto Institute for Research & Education, Incorporated
Palo Alto, California 94304

E-Mail: Jingwen.liu@med.va.gov

8. PERFORMING ORGANIZATION REPORT NUMBER

9. SPONSORING / MONITORING AGENCY NAME(S) AND ADDRESS(ES)
U.S. Army Medical Research and Materiel Command
Fort Detrick, Maryland 21702-5012

10. SPONSORING / MONITORING AGENCY REPORT NUMBER

11. SUPPLEMENTARY NOTES

12a. DISTRIBUTION / AVAILABILITY STATEMENT
Approved for Public Release; Distribution Unlimited

12b. DISTRIBUTION CODE

13. ABSTRACT (Maximum 200 Words)

The original proposed specific tasks of this Idea grant were threefold: (1) to identify the cis-acting elements and the trans-acting factors that are responsible for the cytokine oncostatin M (OM)-induced suppression of p53 transcription in breast cancer cells, (2) to determine whether ERK and STAT3 play essential roles in OM-mediated suppression of p53 transcription, and (3) to over express p53 in a tetracycline regulated expression system. These 3 tasks have been successfully accomplished. We have identified a novel cis-regulatory element, designated as PE21, that mediates the OM-induced suppression of p53 transcription. By conducting electrophoretic mobility shift assay connected with UV-crosslinking, we have detected a protein of 87 kDa that specifically binds to the PE21 element. We have demonstrated that blocking STAT3 transactivating activity by the expression of a dominant negative mutant of STAT3 (dnStat3) reversed the OM inhibitory effects on p53 promoter activity and p53 protein expression, indicating an involvement of STAT3 in OM-mediated negative regulation of the p53 transcription. In addition, to determine functional roles p53 in the process of proliferation and differentiation of breast cancer cells, we generated stable cell lines (MCF-7 ptsp53) that express p53Val^{135} temperature-sensitive mutant. We found that overexpression of functional p53 in MCF-7 cells leads to growth .

14. SUBJECT TERMS
Tumor suppressor p53, transcriptional regulation, cell signaling

15. NUMBER OF PAGES
52

16. PRICE CODE

17. SECURITY CLASSIFICATION OF REPORT Unclassified	18. SECURITY CLASSIFICATION OF THIS PAGE Unclassified	19. SECURITY CLASSIFICATION OF ABSTRACT Unclassified	20. LIMITATION OF ABSTRACT Unlimited

Table of Contents

INTRODUCTION

Oncostatin M (OM), a 28 kDa glycoprotein, is a cytokine produced by activated T lymphocytes and macrophages (1). Previous studies showed that OM inhibits the growth of several breast cancer cell lines. OM-treated breast cancer cells show a reduced growth rate that is accompanied by an increased proportion of cells in G_0/G_1 phase and a concomitant decrease in the number of cells in S phase. In addition, a variety of morphological changes associated with the differentiated phenotype appeared after OM treatment (2-4). However, OM treatment does not lead to apparent apoptosis. Since the p53 tumor suppressor protein plays important roles in cellular proliferation, differentiation and apoptosis (5), we examined the effects of OM on p53 expression in breast cancer cells. Surprisingly, we found that p53 expression was down regulated by OM in MCF-7 cells that express the wt functional p53 (6). Treatment of MCF-7 cells with OM for 5 days reduced p53 protein expression by more than 50% as compared to the control and the viable cell numbers were concurrently decreased by about 70%. In addition to OM, we found that the p53 expression in MCF-7 cells was also suppressed by PMA, a differentiation-inducing agent for these cells. Further investigations demonstrate that the down regulation of p53 protein as well as mRNA expressions by OM occurs at the transcriptional level and is mediated through a specific OM-responsive cis-acting element (PE21) of the p53 promoter (7).

Based upon these observations, we initially hypothesized that p53 plays a positive role in apoptosis, but it could have a negative role in the differentiation process in breast tumor cells. Decreasing p53 expression might be a factor that contributes to the cell commitment to undergo growth arrest/differentiation and to prevent apoptosis in response to OM exerted stress. In order to investigate the relationship between p53 expression and the growth inhibition of breast cancer cells, and to determine whether p53 plays a negative role in the OM-induced growth arrest of breast cancer cells, in this study, we utilized the temperature-sensitive (ts) p53 mutant p53Val[135] to establish a cell system where the transactivating function of p53 can be turned on or turned off by culturing cells at either permissive temperature 32°C or at the non-permissive temperature 37°C (8-10). It has been well documented that at 37°C p53Val[135] transfectants express exogenous p53 in a mutant conformation that acts as a dominant negative mutant and inhibits the function of the endogenous p53 (11, 12). In contrast, at permissive temperature 32°C, the p53Val[135] mutant resumes normal conformation and behaves as the wt p53. Previous reports in literature showed that ectopic expression of the ts p53 mutant had different effects on cell cycle in different cell lines. In many cases, cells expressing the p53Val[135] were arrested primarily in the G_0/G_1 phase of the cell cycle, suggesting that p53 plays a specific role at G_1 (11-15). It has been shown that transfection of p53Val[135] into Hs578T human breast cancer cells resulted in the G_1 cell cycle arrest (13). However, a few reports had showed that a second cell cycle block at G_2/M occurred in human fibroblasts by overexpression of the wt p53 (16; 17). This suggests that p53 may have an important role in regulating the G_2-M transition. In addition, p53Val[135] overexpression at 32°C induces apoptosis in Jurkat (18) and U-937 cells (19). Presently, it is not totally clear what factors are involved in the determination of cell fate in response to p53 overexpression.

In the third year of funding, we have focused our investigation on the relationship between OM-induced cell growth and p53 expression using the MCF7-pts-p53 cell system.

4

Body

Identification of PRC1 as the p53 target gene uncovers a novel function of p53 in the regulation of cytokinesis

The protein p53 is the most important tumor suppressor identified to date. The essential roles of p53 as a gatekeeper to maintain mammalian cell homeostasis and to prevent malignant transformation (1) is well indicated by its frequent mutations occurring in the majority of human tumors including breast tumor (2-4). The loss of wild type (wt) p53 is clearly an important event in breast tumorigenesis (5; 6). However, the exact mechanisms by which loss of p53 normal function leads to cancer formation and progression are not fully understood. In mammalian cells, the correct cell division is controlled by checkpoints at G1/S transition, G2/M transition, and mitosis. Many studies have indicated p53 being an important integral part of these checkpoints (7). Accumulated p53 in response to DNA damage or through experimental overexpression has been shown to cause growth arrest at G1 (8-10) and/or G2 (11-14) or to induce apoptosis (15; 16). In some cases, overexpression of the wt p53 induces cellular senescence (17-19). However, at present it is not fully understood what factors are involved in the determination of cell fate in response to high cellular levels of p53. Moreover, the p53 downstream target genes mediating different cellular responses to p53 have not been completely characterized.

We have stably transfected a temperature-sensitive (ts) p53 mutant p53Val[135] in MCF-7 breast cancer cells to establish a cell system (MCF7-ptsp53) where the transactivating function of p53 can be turned on or turned off by culturing cells at either permissive temperature 32°C or at the non-permissive temperature 37°C (20-22). Interestingly, flow cytometric analysis of the DNA content shows that overexpression of the transcriptionally active p53 at 32°C arrested the growth of MCF-7 cells by exclusively increasing the percentage of cells in the G2/M phase without affecting G0/G1 phase or inducing apoptosis (23). Thus, this cell line provides us a relatively unique system to characterize p53-initiated molecular events occurring at the G2/M phase. In order to identify novel p53 regulated genes that are responsible for the p53-mediated G2/M arrest, we performed cDNA microarray analyses to compare the gene profiles of MCF7-ptsp53 cells cultured at either 37°C or at 32°C. Using the criteria of 2-fold as a cut off line, the expressions of 14 genes were shown differentially regulated by wt p53 overexpression but not by nonspecific temperature switch (23). Interestingly, none of the p53 regulated genes is related to apoptosis. However, 4 genes that previously have demonstrated to be involved in G2/M arrest were affected by the overexpression of wt p53 including p21, cdc2, cyclin B2, and PRC1. The former three genes have been demonstrated in a number of studies to be involved in p53-mediated G2 arrest (11; 24-27). However, PRC1 is a newly characterized cell cycle protein and its regulation by p53 or by other agents that affect cell cycle have not been reported.

The terminal stage of the cell cycle is cytokinesis. During the process of cytokinesis, cells divide their organelles, cytoplasm, plasma membrane, and other cell contents into two daughter cells (28). PRC1, a recently characterized mitotic spindle-associated Cdk substrate, has been shown to have an exclusive role in cytokinesis (29; 30). Microinjection of anti-PRC1 antibodies into HeLa cells blocked cellular cleavage without affecting nuclear division, which resulted in binucleated cells (29). The essential role of PRC1 in cell cleavage was also demonstrated by using PRC1 small interfering RNA (siRNA) to block its expression (30). It was shown that in the absence of the PRC1 protein, cells were able to progress normally in mitosis to

metaphase and underwent normal chromatid segregation in anaphase. However, cells lacking PRC1 always showed aberrant anaphase spindle morphology and became increasingly binucleate with time. Further studies demonstrate that PRC1 regulates cytokenesis by stabilizing the midzone microtubule bundle and permitting completion of cell cleavage. The requirement of PRC1 for cell cleavage can also be inferred from its expression pattern. PRC1 expression levels are high during S and G2/M and drop dramatically after cells exit mitosis and enter G1 (Jiang et al., 1998). However, the factors control the cell cycle-specific expression of PRC1 are largely unknown.

In this study, we have extensively examined the functional role of p53 in the regulation of PRC1 expression. Through several different lines of investigation, we provide strong evidence to demonstrate that PRC1 gene transcription is negatively regulated by p53. Our new findings suggest that p53 as the gatekeeper to maintain mammalian homeostasis may exert its function to control the final checkpoint for cell division at the stage of cytokinesis by transcriptional suppression of PRC1.

RESULTS
Overexpression of p53 downregulates PRC1 gene expression in MCF-7 cells
To identify specific wt p53 regulated genes, we performed 4 sets of microarray analysis. First, gene expression profiles of MCF7-ptsp53 grown at 32°C and 37°C were compared. Second, MCF7-ptsp53 grown at 32°C was compared to untransfected parental MCF-7 cells grown at 37°C. Third, MCF7-ptsp53 grown at 37°C was compared to untransfected parental MCF-7 cells grown at 37°C. The last set of experiment was designed to assess the effect of temperature switch (37°C → 32°C) on general gene expression of MCF-7 cells, as a negative control for the specific changes induced by p53 overexpression. The array results showed that the PRC1 mRNA level in MCF7-ptsp53 cells cultured at 32°C was decreased by 70% as compared to cells cultured at 37°C (Fig. 1A, bar 1) and was decreased by 78% as compared to MCF-7 cells cultured at 37°C (bar 2). On the contrary, the temperature switch had no effect on PRC1 mRNA expressions in MCF-7 cells (bar 4). The data also indicated that overexpression of mutant p53 (ptsp53 ^{Val135}) did not significantly affect PRC1 mRNA expression, as MCF7-ptsp53 and MCF-7 cells cultured at 37°C expressed similar amounts of PRC1 mRNA (bar 3). These results demonstrated an inverse relationship between p53 transcriptional activity and PRC1 expression.

To follow up on this observation, northern blot analysis was performed to detect the changes of PRC1 mRNA levels after the ptsp53 cells were switched from 37°C to 32°C. The results in Fig. 1B show that the PRC1 mRNA was downregulated by wt p53 in a time-dependent manner. The level of PRC1 mRNA began to drop by 6 h of culturing in the permissive temperature. By 24 h at 32°C, only 40% of the mRNA remained, and a residual level of the PRC1 mRNA could be detected after 48 h. Again, the temperature switching had no effect on PRC1 mRNA expression in the parental and the mock-transfected control clone (neo). We further conducted a quantitative real-time PCR assay using cDNAs prepared from mRNAs isolated from different samples. The results confirmed the kinetics of p53-mediated downregulation of PRC1 mRNA expression (Fig. 1C). Examination of PRC1 protein levels in these cells led to corroborated findings in that the PRC1 protein level was decreased to 31% of control at 24 h and further decreased to 15% at 48 h by temperature shift-down (Fig. 1D) only in MCF7-ptsp53 cells but not in parental MCF-7 cells.

Overexpression of p53 downregulates PRC1 gene expression in other cell lines

The above experiments were carried out in MCF-7 breast cancer cell line. To further confirm the correlation between p53 overexpression and downregulation of PRC1 gene expression, different cell systems were used. T47D and HeLa cells were cotransfected with a wt p53 expression vector pBSp53 and pEGFP or mock transfected (pEGFP plus pBS empty vector). Two days post transfection, cells were subjected to cell sorting using GFP as a marker for transfection. After separation, GFP positive cells were collected and total cell lysates as well as total RNA were harvested. Fig. 2A. (middle panel) and Fig. 2B confirmed the increased protein levels and the transactivating activities of p53 in pBSp53 transfected cells. Fig. 2A also shows that exogenous expressed wt p53 reduced PRC1 protein level by 52% in T47D and by 67% in HeLa cells, as compared to that in untransfected or mock transfected cells.

Real-time PCR to detect PRC1 mRNA levels in pBSp53 transfected cells confirmed the results of western blot (Fig. 2C). Together, these results demonstrate that down regulation of PRC1 mRNA and protein expression by p53 are not limited to MCF7-ptsp53 cells.

Suppression of PRC1 expression upon treatment with chemotherapeutic drugs 5'-fluorouracil (5-FU) and doxorubicin (Dox)

In addition to overexpression of the wt p53, we were interested in determining whether PRC1 expression could be repressed in a physiological environment with an elevated level of endogenous p53. To investigate this, we treated HCT116 p53$^{+/+}$ and HCT116 p53$^{-/-}$ with the therapeutic drugs 5-FU at 50 µg/ml or doxorubicin at 2 µg/ml for 24 h. We also treated MCF-7, T47D, and HeLa cells with 5-FU at an effective dose of 10 µg/ml, which has been shown to increase cellular p53 protein levels in several cell lines (Chun et al., 2003). Following the treatment, the p53 and PRC1 protein levels were examined by western blotting. Fig. 3A and 3C (top panel) showed that the therapeutic drugs only effectively induce endogenous p53 expression in HCT116 p53$^{+/+}$ and MCF-7 cells that have functional p53; whereas p53 was not induced in HCT116 p53$^{-/-}$ cells which are p53 null, and T47D which does not have functional p53. P53 protein level in HeLa cells was also not induced due to the expression of the human papillomavirus E6 protein, which targets p53 for degradation. The induction of endogenous p53 by 5-FU or doxorubicin considerably repressed PRC1 protein expression in HCT116 p53$^{+/+}$ and MCF-7 cells, whereas the PRC1 expressions in HCT116 p53$^{-/-}$, T47D and HeLa cells were not changed by the same treatment (Fig 3A and 3C middle panel). The real-time PCR assay to measure PRC1 mRNA levels in different cell lines after the drug treatments obtained similar data (Fig. 3B and 3D). These results are consistent with those achieved by exogenous expression of p53 and clearly demonstrate a regulatory role of p53 on PRC1 expression.

Downregulation of PRC1 gene expression by p53 overexpression results in binucleation

PRC1 is a microtubule binding and bundling protein essential to maintain the mitotic spindle midzone. Mollinari et al have shown that complete suppression of PRC1 by siRNA in HeLa cells resulted in about 10% cells became binucleated after 24 h treatment of siRNA (Mollinari et al., 2002). We sought to determine whether the decreased PRC1 expression caused by p53 overexpression has similar inhibitory effects on cell division. First, by performing wt p53 immunostaining and DAPI staining we examined the cell p53 level as well as the nuclei of MCF7-ptsp53 and regular MCF-7 cells that had been cultured at 32°C for two days. Under this condition, we found that over 95% of the ptsp53 cells cultured at 32°C overexpressed wt p53 and

approximately 3% of these cells had two nuclei per cell (Fig. 4, top panel). In contrast, we could not find any binucleated cells in MCF-7 cells (image not show). We have tried to detect the cell PRC1 level by immunostaining, but we could not obtain a specific staining by the current PRC1 antibody. Next, we extended this observation to HCT116 p53$^{-/-}$ cells after transfection of pBSp53 and pEGFP and enrichment of transfected cells by cell sorting. We found that about 95% of the transfected cells overexpressed wt p53 and 2% of these cells became binucleated (Fig. 4 middle panel), whereas in mock-transfected HCT116 p53$^{-/-}$ cells, few cells showed binucleation. Similar experiments of transfection and cell sorting were performed in HeLa cells. We detected binucleation in 5.4% of HeLa cells after transfection with the wt p53 as compared to the mock-transfected HeLa cells that contained less than 0.5% of binucleated cells. Fig. 4 bottom left panel showed the phase contrast image of pBSp53 transfected HeLa cells, bottom right showed DAPI staining.

P53 suppresses PRC1 promoter activity

To determine an inhibitory effect of p53 on PRC1 gene transcription, we first isolated a 3 kb genomic fragment of PRC1 gene covering from –2964 to +76 relative to the transcription start site. This was accomplished by a PCR reaction using RPCI 11 human genomic clone as a template. The PCR product was subcloned into the pGL3-basic luciferase reporter. The resulting plasmid was named PRC1-3kb. The ATG translation start codon was excluded from the fragment to ensure the correct translation of luciferase gene product.

HCT116 p53$^{-/-}$, MCF-7, T47D and HeLa cells were cotransfected with PRC1-3kb along with the pRSV-Luc normalizing vector. In all four cell lines, PRC1-3kb showed the luciferase activities. In MCF-7, the PRC1-3kb luciferase activity was 20 fold of the promoterless vector pGL3-basic. In HCT116 p53$^{-/-}$, T47D, and HeLa cells, the PRC1-3kb luciferase activities were over 100 fold of pGL3-basic (data not shown). These results indicate that the isolated 3 kb fragment contains the functional PRC1 promoter. The fact that the PRC1 promoter activity was 5-fold lower in MCF-7 cells that express functional wt p53 than that in HCT116 p53$^{-/-}$, HeLa, and T47D cells implies that the PRC1 promoter activity is subjected to the negative regulation by endogenous p53.

To examine the effect of p53 on PRC1 transcription, we transfected PRC1-3kb in the presence of different amounts of pBSp53 into HCT116 p53$^{-/-}$ or T47D cells. Two days after transfection the PRC1 promoter activities in transfected cells were determined. Fig. 5A and 5B show that p53 inhibited PRC1-3kb promoter activity in a dose dependent manner in HCT116 p53$^{-/-}$ cells and T47D cells. PRC1-3kb promoter activity was nearly completely suppressed by the highest dose of pBSp53 in both cell lines. In a parallel experiment, p53 reporter vector p53Luc was cotransfected with different amounts of pBSp53 into HCT116 p53$^{-/-}$ cells. The result in Fig. 5C demonstrated the dose-dependent increase of p53 transactivating activity in these transfected cells. We also determined the time-dependent effect of p53 expression on PRC1 promoter activity in T47D cells. PRC1 promoter activity was decreased to 34.1% of control at 16 h and further decreased to 6.1% at 48 h by exogenous expression of p53 (Fig. 5D). At each time point, pBS empty vector was used as a control to pBSp53.

The effects of p53 overexpression on PRC1 promoter activities in MCF-7 and HeLa cells were further examined. In MCF-7, cotransfection of pBSp53 with PRC1-3kb reduced the luciferase activity by 49% as compared to that of the empty vector transfected cells. In HeLa cells, 45% reduction in PRC1 promoter activity was observed after cotransfection of PRC1-3kb with pBSp53 (data not shown).

Localization of the p53 responsive region to the proximal section of the PRC1 promoter

To understand how p53 regulates PRC1 transcription, the identification of p53-responsive cis-regulatory elements on PRC1 promoter is of importance. To this end, serial deletions of the 5' flanking region of PRC1-3kb promoter were made. Fig. 6 illustrates the nucleotide sequence spanning the PRC1 proximal promoter region from –281 to + 76 and a schematic diagram of the deletion constructs. T47D cells were transfected with these truncated constructs individually with pBSp53 or with the empty vector pBS, and assayed for luciferase activities. Fig. 7A compared the basal promoter activity of the deletion constructs with the activity of the full promoter construct PRC1-3kb. These results, summarizing 6 separate transfections, showed that deletion of the 5'-flanking region from 3 kb to -282 did not affect the PRC1 promoter basal activity at all. However, additional deletion of 67 nucleotides drastically reduced the promoter activity by more than 80%. Further deletions to –9 gradually reduced the promoter activity to the baseline. These data demonstrate that the functional regulatory elements controlling the basal transcription of PRC1 gene reside within a 272 bp region between –281 to -10. P53 was able to repress the promoter activities of PRC1-281 and PRC1-214 to the same extent as PRC1-3kb (Fig. 7B), but it lost responsiveness to the promoter constructs PRC1-163, PRC1-99, and PRC1-9. To confirm the presence of the p53-responsive element within the region of –214 to –163, we made an internal deletion construct (PRC1-281-del) that does not contain the fragment between –216 to –161. The results in Fig. 8 show that deletion of this region increased the basal promoter activity (Fig. 8A) but significantly reduced the response to p53-mediated suppression (Fig. 8B). These data provide additional evidence to support the functional role of this region in p53-mediated downregulation of PRC1 transcription.

Sequence analysis using MatInspector failed to detect a consensus or a homologous p53 binding site within the whole 272 bp basal promoter region or within the p53-responsive region (-214 to –163). This p53-responsive region, however, does contain a GC-rich sequence (-206 to –199) and a putative NF-kB site (-195 to –181). Thus, site-directed mutagenesis on the promoter construct PRC1-281 was performed to individually mutate the GC rich stretch (muGC) or the NF-kB site (muNF-kB). The contributions of these sequences to the basal and p53-repressed PRC1 promoter activity were assessed by transfection of the wt and the mutated constructs into T47D cells in the absence or the presence of pBSp53. The upper panel of Fig. 9 shows that nucleotide alternation within the GC rich sequence reduced the basal PRC1 promoter activity by 65% and mutation within the NF-kB site moderately lowered the promoter activity by 37%. However, none of these mutations individually abolished the p53-mediated repression of the promoter activity (Fig. 9, lower panel). These data suggests that the GC rich region and the NF-kB site are important for the PRC1 promoter basal activity but they are expendable for the p53-mediated suppression of the PRC1 transcription.

P53 interacts with PRC1 promoter in vivo

To determine whether p53 could interact with the proximal region of the PRC1 promoter in vivo, we performed chromatin immunoprecipitation (ChIP) experiments. The MCF7-ptsp53

cell system was used for this purpose. MCF7-ptsp53 cells cultured at 37°C or 32°C for 48 h were treated with formaldehyde to generate covalently cross-linked DNA-protein complex within the cells. Cross-linked chromatin was then immunoprecipitated with antibody against p53. Normal rabbit IgG was used as a non-specific binding control. PCR amplification was then performed on the immunoprecipitated DNA and on the total input DNA. Primers were designed to amplify the region from −281 to +76 of the PRC1 gene that contained the full promoter activity as well as the p53 responsive region. Primers to amplify the p53 responsive region within the p21 promoter were used as a positive control (Kaeser et al., 2002). Fig. 10 showed that PRC1 and p21 chromatins were specifically immunoprecipitated with anti-p53 antibody only from MCF7-ptsp53 cells maintained at 32°C (Fig. 10, right panel) that express the functional p53 but not from cells cultured at 37°C that expressed the mutant p53 (Fig. 10, left panel). These data clearly indicate the in vivo association of wt p53 with PRC1 gene promoter and provide additional evidence to support the regulatory role of p53 in PRC1 gene transcription.

In conclusion, we have identified a new p53 target gene PRC1 whose transcription is subject to the negative regulation of p53. Regarding to the physiological significance of PRC1 repression by p53, we hypothesize that in addition to G1/S and G2/M checkpoints, p53 as the most important tumor suppressor may provide a final checkpoint control for cell division at the stage of cytokinesis by repressing the transcription of the PRC1 gene whose expression is required for cell cleavage at the end of mitosis, thereby preventing premature entry into another round of cell proliferation. Hence, the effects of p53 on blocking cytokinesis may provide additional protection to maintain genomic integrity and to prevent cancer formation in situations of failed G1 or G2 checkpoints.

KEY RESEARCH ACCOMPLISHMENTS

- Establishment of stable cell line (MCF-7 ptsp53) that can turn on or off the wt p53 expression by temperature switch
- Identified a noveL p53 target gene PRC1

REPORTABLE OUTCOMES

4 manuscripts have been published on top journals

- Li C, Kraemer FB, Ahlborn TE, and Liu J: Oncostatin M–induced growth inhibition and morphological changes of MDA-MB231 breast cancer cells are mediated through the MEK/ERK signaling pathway. *Breast Cancer Res Treat*. 66:111-121, 2001
- Li C, Ahlborn TE, Tokita K, Boxer LM, Noda A, and Liu J: The Critical Role of the PE21 Element in Oncostatin M-Mediated Transcriptional Repression of the p53 Tumor Suppressor Gene in Breast Cancer Cells. *Oncogene* 20:8193-8202, 2001.
- Zhang F, Li C, Halfter H, and Liu J: Delineating an oncostatin M-activated STAT3 signaling pathway that modulates gene expression and cellular responses in MCF-7 cells. *Oncogene* 22:894-905, 2003
- Li C, Zhang F, and Liu J: Identification of PRC1 as the p53 target gene uncovers a novel function of p53 in the regulation of cytokinesis. *Oncogene*. 2004 Nov 08

Reference List

1. Levine, A.J. p53, the cellular gatekeeper for growth and division. Cell, *88*: 323-331, 1997.

2. Vogelstein, B. and Kinzler, K.W. p53 function and dysfunction. Cell, *70*: 523-526, 1992.

3. Harris, C.C. Structure and function of the p53 tumor suppressor gene: Clues for rational cancer therapeutic strategies. J.Natl.Cancer Inst., *88*: 1442-1455, 1996.

4. Tarapore, P. and Fukasawa, K. p53 mutation and mitotic infidelity. Cancer Inves., *18*: 148-155, 2000.

5. Malkin, D., Li, F.P., and Strong, L.C.e.a. Germ line p53 mutations in a familial syndrome of breast cancer, sacromas, and other neoplasms. Science, *250*: 1233-1238, 1990.

6. Hollstein, M., Sidransky, D., and Vogelstein, B. p53 mutations in human cancer. Science, *253*: 531991.

7. Bargonetti, J. and Manfredi, J. Multiple roles of the tumor suppressor p53. Curr.Opin.Oncol., *14*: 86-91, 2002.

8. Willers, H., McCarthy, E., Wu, B., Wunsch, H., Tang, W., Taghian, D., Xia, F., and Powell, S. Oncogene, *19*: 632-639, 2000.

9. Agami, R. and Bernards, R. Distinct initiation and maintenance mechanisms cooperate to induce G1 cell cycle arrest in response to DNA damage. Cell, *102*: 55-66, 2000.

10. Wesierska-Gadek, J. and Schmid, G. Overexpressed poly(ADP-ribose) polymerase delays the release of rat cells from p53-mediated G1 checkpoint. J.Cell.Biochem., *80*: 85-103, 2000.

11. Taylor, W., DePrimo, S., Agarwal, A., Agarwal, M., SchÖnthal, A., Katula, K., and Stark, G. Mol.Bio.of the Cell, *10*: 3607-3622, 1999.

12. Agarwal, M., Agarwal, A., Taylor, W., and Stark, G.R. p53 controls both the G2/M and the G1 cell cycle checkpoints and mediates reversible growth arrest in human fibroblasts. Proc.Natl.Acad.Sci.USA, *92*: 8493-8497, 1995.

13. Taylor, W.R. and Stark, G.R. Regulation of the G2/M transition by p53. Oncogene, *20*: 1803-1815, 2001.

14. Nakamura, S., Gomyo, Y., Roth, J.A., and Mukhopadhyay, T. C-terminus of p53 is required for G2 arrest. Oncogene, *21*: 21072002.

15. Vousden, K. p53:Death star. Cell, *103*: 691-694, 2000.

16. Kokontis, J.M., Wagner, A.J., O'Leary, M., Liao, S., and Hay, N. A transcriptional activation function of p53 is dispensable for and inhibitory of its apoptotic function. Oncogene, *20*: 6682001.

17. Sugrue, M.M., Shin, D.Y., Lee, S.W., and Aaronson, S.A. Wildtype p53 triggers a rapid senescence program in human tumor cells lacking functional p53. Proc.Natl.Acad.Sci.USA., *94*: 9648-9653, 1997.

18. Jung, M.-S., Yun, J., Chae, H.-D., Kim, J.-M., Kim, S.-C., Choi, T.-S., and Shin, D.Y. p53 and its homologous, p63, and p73, induce a replicative senesence through inactivation of NF-Y transcription factor. Oncogene, *20*: 5818-5825, 2001.

19. Dubrez, L., Coll, J., Hurbin, A., Fraipont, F., Lantejoul, S., and Favrot, M. Cell cycle arrest is sufficient for p53-mediated tumor regression. Gene Therapy, *8*: 1705-1712, 2001.

20. Michalovitz, D., Halevy, O., and Oren, M. Conditional inhibition of transformation and of cell proliferation by a temperature-sensitive mutant p53. Cell, *62*: 671-680, 2002.

21. Martinez, J., Georgoff, I., and Levine, A.J. Cellular location and cell cycle regulation by a temperature-sensitive p53 protein. Genes & Dev., *5*: 151-159, 1991.

22. Milner, J. and Medcalf, E. Temperature-dependent switching between "wild-type" and "mutant" forms of p53Val135. J.Mol.Biol., *210*: 481-484, 1990.

23. Li, C., Shridhar, K., and Liu, J. Molecular characterization of oncostatin M-induced growth arrest of MCF-7 cells expressing a temperature-sensitive mutant of p53. Breast Cancer Research and Treatment, *80*: 23-37, 2003.

24. Kruse, K., Wasner, M., Reinhard, W., Ulrike, H., Dohna, C., MÖssner, J., and Engeland, K. The tumor suppressor protein p53 can repress transcription of cyclin B. Nucleic Acids Res, *28*: 4410-4418, 2000.

25. Dulic, V., Stein, G.H., Farahi, F.D., and etal Nuclear accumulation of p21cip1 at the onset of mitosis: a role at the G2/M-phase transition. Mol Cell Bio, *18*: 546-557, 1998.

26. Yin, X.-Y., Grove, L., Datta, N.S., Katula, K., Long, M.W., and Prochownik, E.V. Inverse regulation of cyclinn B1 by c-mycand p53 and induction of tetraploidy by cyclin B1 overexpression. Cancer Res., *61*: 64932001.

27. Manni, I., Mazzaro, G., Gurtner, A., Mantovani, R., Haugwitz, U., Krause, K., Engeland, K., Sacchi, A., Soddu, S., and Piaggio, G. NF-Y mediates the transcriptional inhibition of the cyclin B1, cyclin B2, and cdc25C promoters upon induced G2 arrest. J.Biol.Chem., *276*: 5570-5576, 2001.

28. Stright, A.F. and Field, C.M. Microtubules, membranes and cytokinesis. Current Biology, *10*: R760-R7702000.

29. Jiang, W., Jimenez, G., Wells, N., Hope, T., Wahl, G., Hunter, T., and Fukunaga, R. PRC1: a human mitotic spindle-associated CDK substrate protein required for cytokinesis. Mol.Cell, *2*: 877-885, 1998.

30. Mollinari, C., Kleman, J.-P., Jiang, W., Schoehn, G., Hunt, T., and Margolis, R.L. PRC1 is a microtubule binding and bundling protein essential to maintain the mitotic spindle midzone. J.Cell Biology, *157*: 1175-1186, 2002.

FIGURE LEGENDS

Figure 1. Overexpression of the wt p53 downregulates PRC1 gene expression in MCF-7 breast cancer cell lines.
(A) Comparison of the PRC1 mRNA levels by microarray. MCF7-ptsp53 and MCF-7 cells were cultured at 37°C or 32°C for 4 days respectively. Total RNA isolated from both cell lines were labeled with either cy3-dCTP or cy5-dCTP according to different experiment designs. The graph illustrates the ratio of PRC1 mRNA expression level in the paired samples. Bar 1, MCF7-ptsp53 at 32°C versus MCF7-ptsp53 at 37°C; Bar 2, MCF7-ptsp53 at 32°C versus MCF-7 at 37°C; Bar 3, MCF7-ptsp53 at 37°C versus MCF-7 at 37°C; Bar 4, MCF-7 at 32°C versus MCF-7 at 37°C.
(B) Northern blot: MCF-7, MCF-7-neo and MCF7-ptsp53 were seeded at 37°C. After switching to 32°C, cells were harvested at different times as indicated. Total RNA was isolated and 15 µg per sample was analyzed for PRC1 mRNA by northern blot. The membrane was stripped and hybridized to a human GAPDH probe.
(C) Real-time PCR: The relative amounts of PRC1 mRNA harvested from MCF-7 or ptsp53 cells cultured at 32°C for various times were measured by a quantitative real-time RT-PCR assay using a PRC1 specific fluorogenic probe from Gorilla Genomics. The amount of PRC1 mRNA in cells cultured at 37°C was defined as 100, and the amount of PRC1 mRNA at different time points was plotted relative to that value. The data shown are derived from 3 separate experiments.
(D) Western blot: MCF7-ptsp53 or MCF-7 seeded at 37°C was switched to 32°C at the same time and total cell lysates were harvested at different time points as indicated. Fifty µg protein per sample was analyzed for PRC1 protein expression by western blot. The membrane was stripped and reprobed with anti-α-actin for normalizing differences in protein loading.

Figure 2. Suppression of PRC1 expression by p53 in different cell lines. T47D or HeLa cells were cotransfected with pBSp53 and pEGFP vector or mock transfected with pBS empty vector plus pEGFP. Two days after transfection, pEGFP expressing cells were selected by fluorescent activated cell sorting. Two third of sorted cells were used for protein extraction and the rest of the cells were lysed for RNA isolation. Total cell lysate and total RNA were also harvested from untransfected cells as control. (A). The PRC1 protein was detected by western blotting with anti-PRC1 rabbit serum and the p53 protein was detected with DO-1 antibody (Santa Cruz). (B). T47D and HeLa cells were cotransfected with p53Luc plus pBS vector or pBSp53 along with the normalizing vector pRSVluc. 48 h after transfection, the luciferase activities were analysed. (C). The relative amount of PRC1 mRNA was measured by the real-time quantitative RT-PCR. The amount of PRC1 mRNA or protein signals in untransfected cells (T47D) or mock-transfected cells (HeLa) was defined as 100%.

Figure 3. Repression of PRC1 expression by endogenous p53 activated in response to chemotherapeutics. HCT116 p53$^{+/+}$ and HCT116 p53$^{-/-}$ cells were treated with 5-FU (50 µg/ml)or Doxorubicin (2 µg/ml) for 24 h. MCF-7, T47D, and HeLa cells were treated with 10 µg/ml of 5-FU for 48 h. Total cell lysate as well as total RNA were isolated from these samples. (A). Western blot analyses of p53, PRC1 protein expressions in HCT116 p53$^{+/+}$ and HCT116 p53$^{-/-}$ cells treated or untreated with drugs. The amount of p53 in untreated cells is expressed as 1; the amount of PRC1 in untreated cells is expressed as 100%. Note that p53 was not induced by chemotherapeutics in p53 null cells and PRC1 level in this cell line was not changed either. (B). Real-time quantitative PCR analyses of PRC1 mRNA levels in HCT116 p53$^{+/+}$ and in HCT116 p53$^{-/-}$ cells untreated and treated with drugs. The amount of PRC1 mRNA level in

untreated cells is expressed as 100%. (C). Western blot analyses of p53 and PRC1 protein expressions in MCF-7, T47D, and HeLa cells treated or untreated with 5-FU. P53 protein was induced by 5-FU in MCF-7 cells but was not changed in T47D and HeLa cells; and the PRC1 level in MCF-7 was decreased by 60% after the drug treatment but was not changed in other cell lines. (D). Real-time quantitative PCR analyses of PRC1 mRNA levels in MCF-7 and HeLa cells untreated and treated with 5-FU. PRC1 mRNA levels in untreated cells are expressed as 100%.

Figure 4. Suppression of PRC1 expression by p53 leads to binucleation. To detect binucleated cells after p53 expression, MCF7-ptsp53 cells cultured at 37°C were switched to 32°C for two days prior to staining with pAb246 p53 antibody (Green) and DAPI (blue) (top panel). HCT116 p53$^{-/-}$ (middle panel) and HeLa cells (bottom panel) were transfected with pBSp53 or the empty vector in the presence of pEGFP. Two days after transfection, positive transfected cells were selected by cell sorting and were cultured overnight. Next day, cells were fixed with cold methanol and stained with DO-1 p53 antibody and FITC-conjugated rabbit anit-mouse IgG (green) and DAPI to visualize the DNA (blue). The green signal of EGFP could not be detected after fixing cells, so the green signals are solely due to the positive staining of p53. Cell images under phase contrast and under fluorescent microscope were recorded by a CCD digital camera PENGUIM 600CL. Red arrows indicate binucleated cells.

Figure 5. P53 suppresses PRC1 promoter activity
(A, B) Dose-dependent suppression of PRC1 promoter activity by p53: HCT116 p53$^{-/-}$ (A) or T47D cells (B) seeding in 24 well culture plates were cotransfected with PRC1-3kb reporter DNA, pBSp53 (with indicated amount of plasmid), and a normalizing vector pRSV-Luc for 48 h. The normalized PRC1 promoter luciferase activity in the absence of p53 expression is expressed as 100%.
(C) Dose-dependent activation of p53Luc by p53. HCT116 p53$^{-/-}$ cells seeding in 24 well culture plates were cotransfected with p53Luc reporter DNA, pBSp53 (with indicated amount of plasmid) and a normalizing vector pRSV-Luc for 48 h. The normalized p53 reporter luciferase activity in the absence of p53 expression is expressed as 100%.
(D) Time-dependent suppression of PRC1 promoter activity by p53 in T47D: T47D cells seeding in 24 well culture plates were cotransfected with PRC1-3kb reporter DNA, pBSp53 (or pBS vector as control), and normalizing vector pRSV-Luc. Cells were harvested at different intervals after transfection. At each time point, the normalized PRC1-3kb luciferase activity in the pBS empty vector cotransfected cells is expressed as 100%.

Figure 6. Nucleotide sequence of the proximal 5'-flanking region of PRC1 gene and a diagram of the PRC1 promoter deletion constructs. In A, the first nucleotide in exon 1 is putatively signed as the transcription start site and is indicated by an arrow. The arrowheads indicate the truncation sites. The defined p53 responsive region is bold and underlined. In B, PRC1 genomic fragments with different 5' deletions were cloned into pGL3-basic luciferase vector.

Figure 7. Truncation analyses of PRC1 basal promoter activity and p53-mediated suppression of the PRC1 promoter activity.

(A) Comparison of the PRC1 promoter activities driven by different lengths of the 5'-flanking sequences: T47D cells were transfected with different PRC1 promoter deletion constructs along with the pRSV-Luc normalizing vector. Cell lysates were harvested 48 h after transfection and the firefly luciferase activity and the renilla luciferase activity were measured using the dual luciferase assay kit. The data shown are summarized results of 6 independent transfection assays in which triplicate wells were used in each condition. The PRC1-3kb promoter activity is defined as 100%, other promoter constructs' activities are presented as percentage of that value.

(B) Localization of the p53-responsive region of PRC1 promoter: T47D cells were transfected with different PRC1 promoter constructs and pRSV-Luc with pBSp53 or with pBS empty vector. Forty-eight h post transfection, cells were harvested and the luciferase activities were analyzed. The normalized luciferase activity of each construct in the pBSp53 transfected cells were comp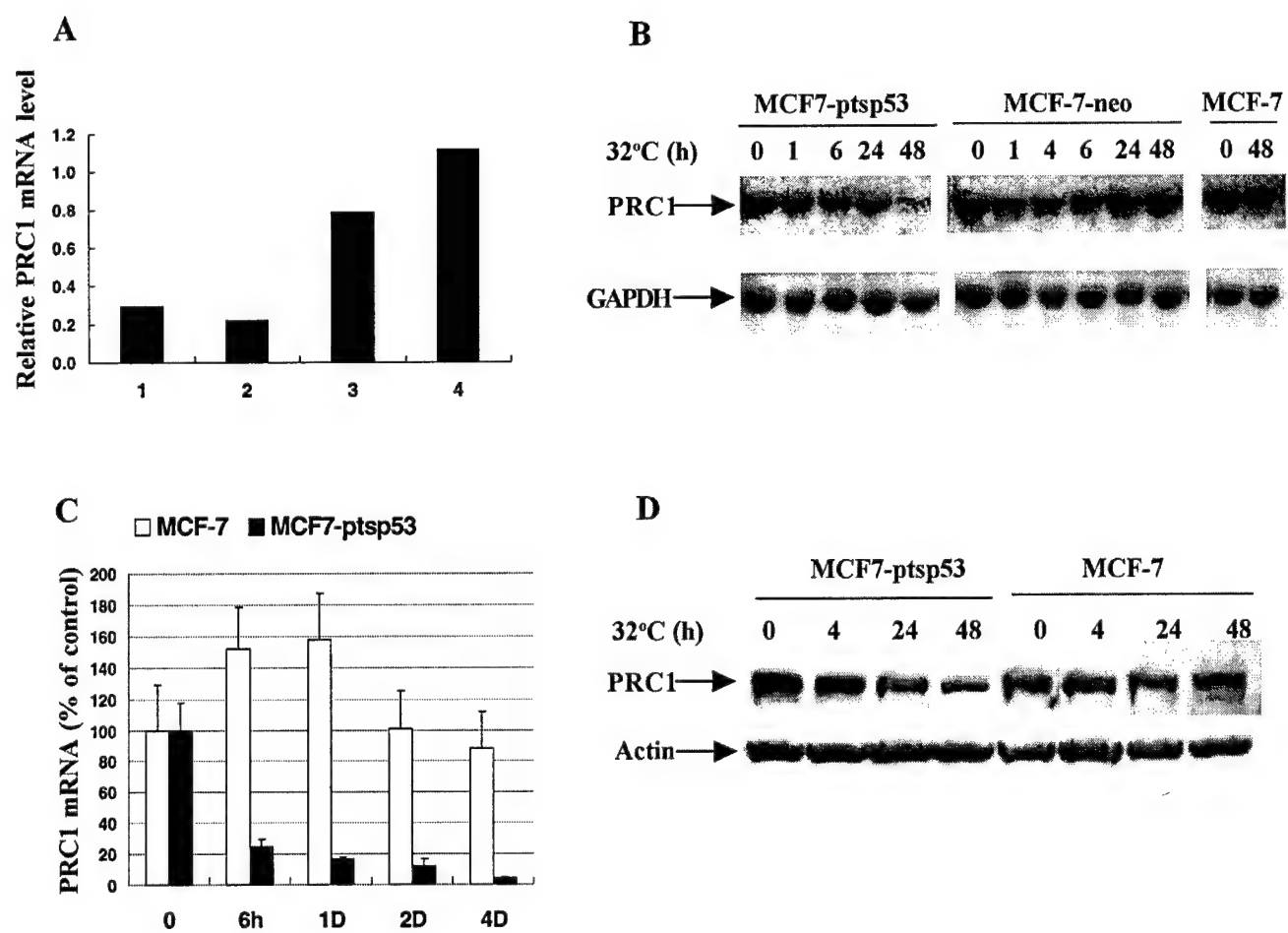ared to that of the pBS vector which is expressed as 100%. The data shown are summarized results of 4 independent transfection assays in which triplicate wells were used in each condition. The different responses to p53 between PRC1-214 and PRC1-163 are statistically significant ($P<0.05$). In these assays, pGL3-basic vector is included to filter out nonspecific effects of p53 on luciferase activity.

Figure 8. Loss of p53 response by deletion of the PRC1 promoter region of –216 to –163.

(A) Comparison of the basal PRC1 promoter activities in different constructs.

The function of –214 to –163 region on the basal PRC promoter activity was assessed by transient transfect PRC1-281-del (the region from –216 to-161 was deleted from PRC1-281) as well as other PRC1 promoter constructs into the T47D cells. PRSV-Luc was cotransfected as a normalizing plasmid. Cell lysates were harvested 48 h after transfection and the luciferase activities were measured using the dual luciferase assay kit. The normalized PRC1-281 promoter activity is defined as 100%, other promoter constructs' activities are presented as percentage of that value.

(B) p53-mediated suppression. T47D cells were transfected with different PRC1 promoter constructs and pRSV-Luc with pBSp53 or with pBS empty vector. Forty-eight h post transfection, cells were harvested and the luciferase activities were analyzed. The normalized luciferase activity of each construct in the pBSp53 transfected cells was compared to that of the pBS vector which is expressed as 100%.

Figue 9. The proximal GC-rich motif and NF-kB site are important for basal PRC1 transcriptional activity but they are not essential for p53-mediated suppression. The effects of p53 on the wt PRC1 promoter construct PRC1-281 and the two mutant constructs were assessed by transient transfection of these plasmids with pBSp53 or with pBS control vector respectively into T47D cells. Luciferase reporter assays were conducted as described in Fig. 7. The data (mean ± sd) were derived from four separate transfection experiments. In the upper panel, the normalized luciferase activity of PRC1-281 is expressed as 100%. In the lower panel, the luciferase activity of each vector in pBS control-transfected cells is expressed as 100%.

Figure 10. Chromatin immunoprecipitation of PRC1 promoter. MCF7-ptsp53 cells were cultured at 37°C or at 32°C for two days. ChIP was performed with antibody against p53. Normal rabbit IgG was included in the assay as a negative control for nonspecific binding. P53 binding was tested by using PRC1 specific primers; p21 primers were used as a positive control

for p53 binding. *Bound* represents the DNA coimmunoprecipated with antibody, while *input* represents the starting material before immunoprecipitation.
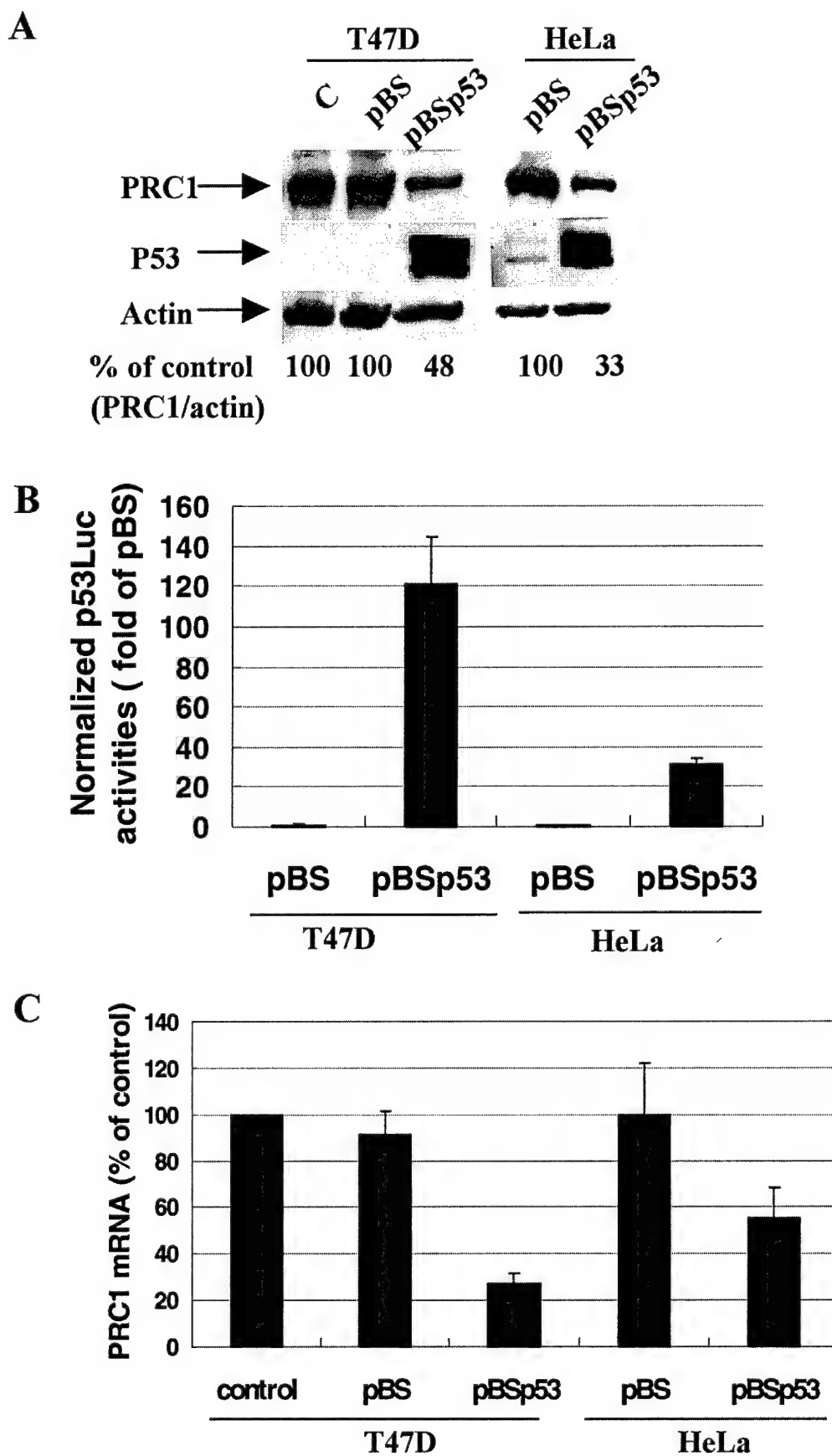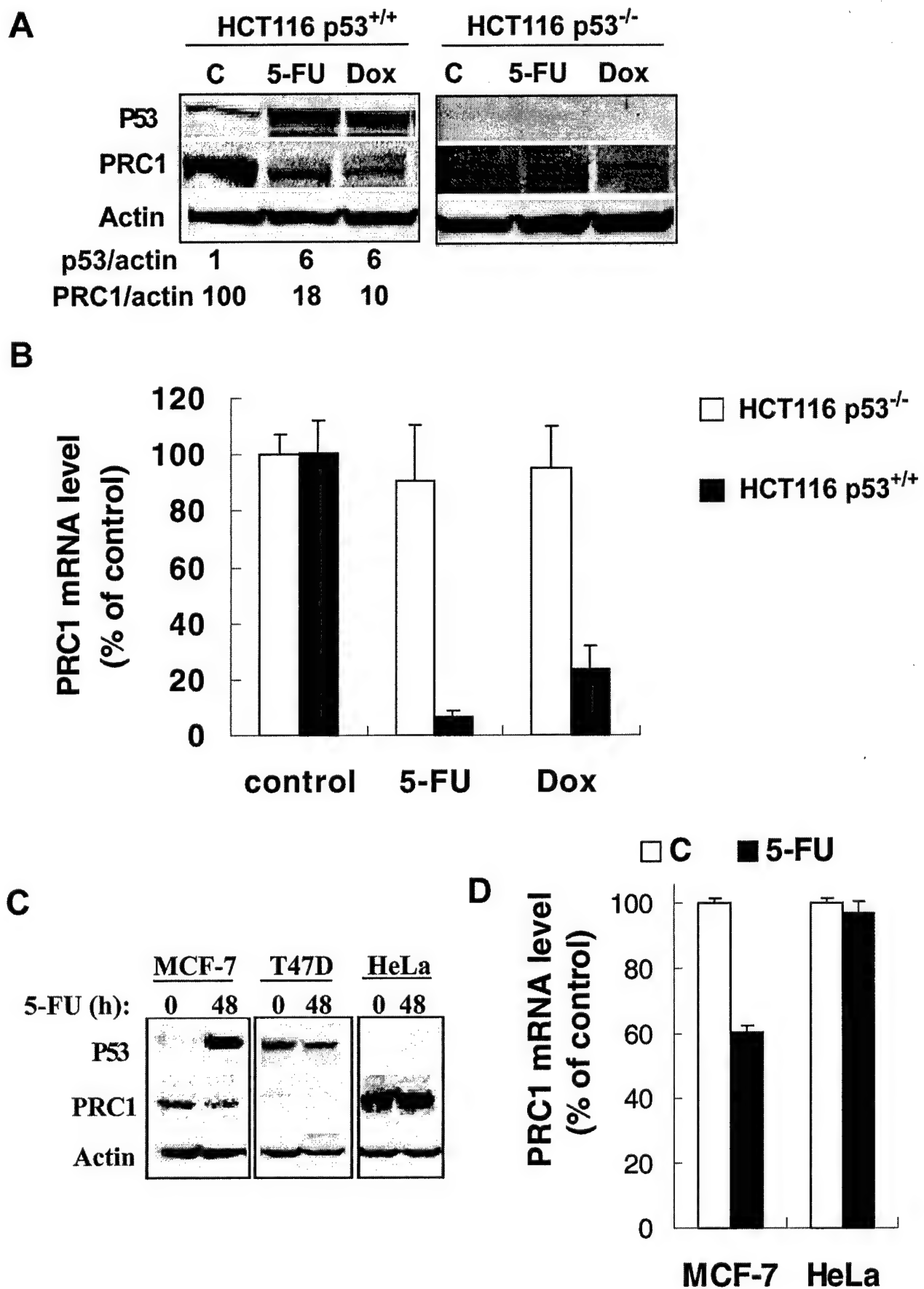
Figure 1

A

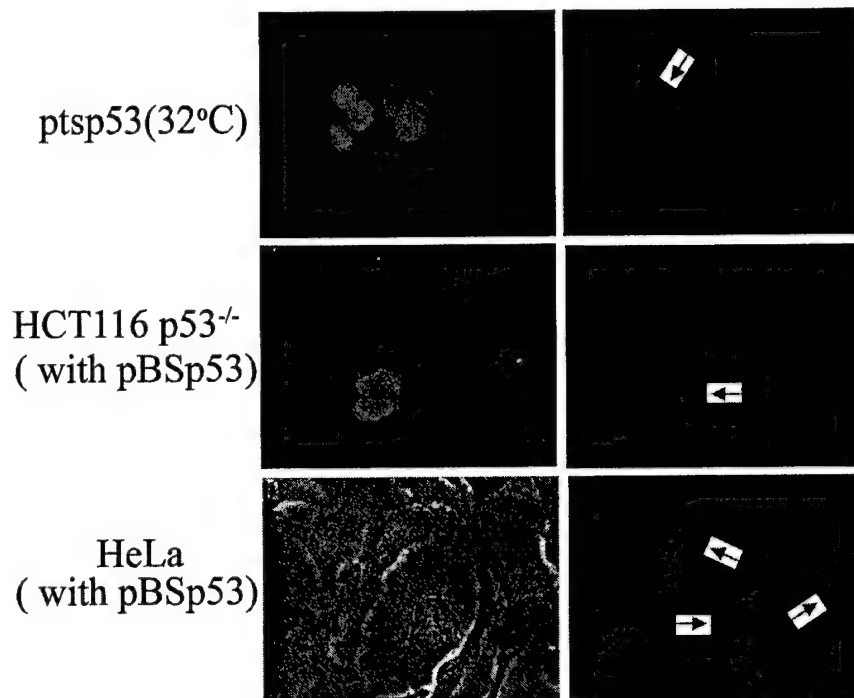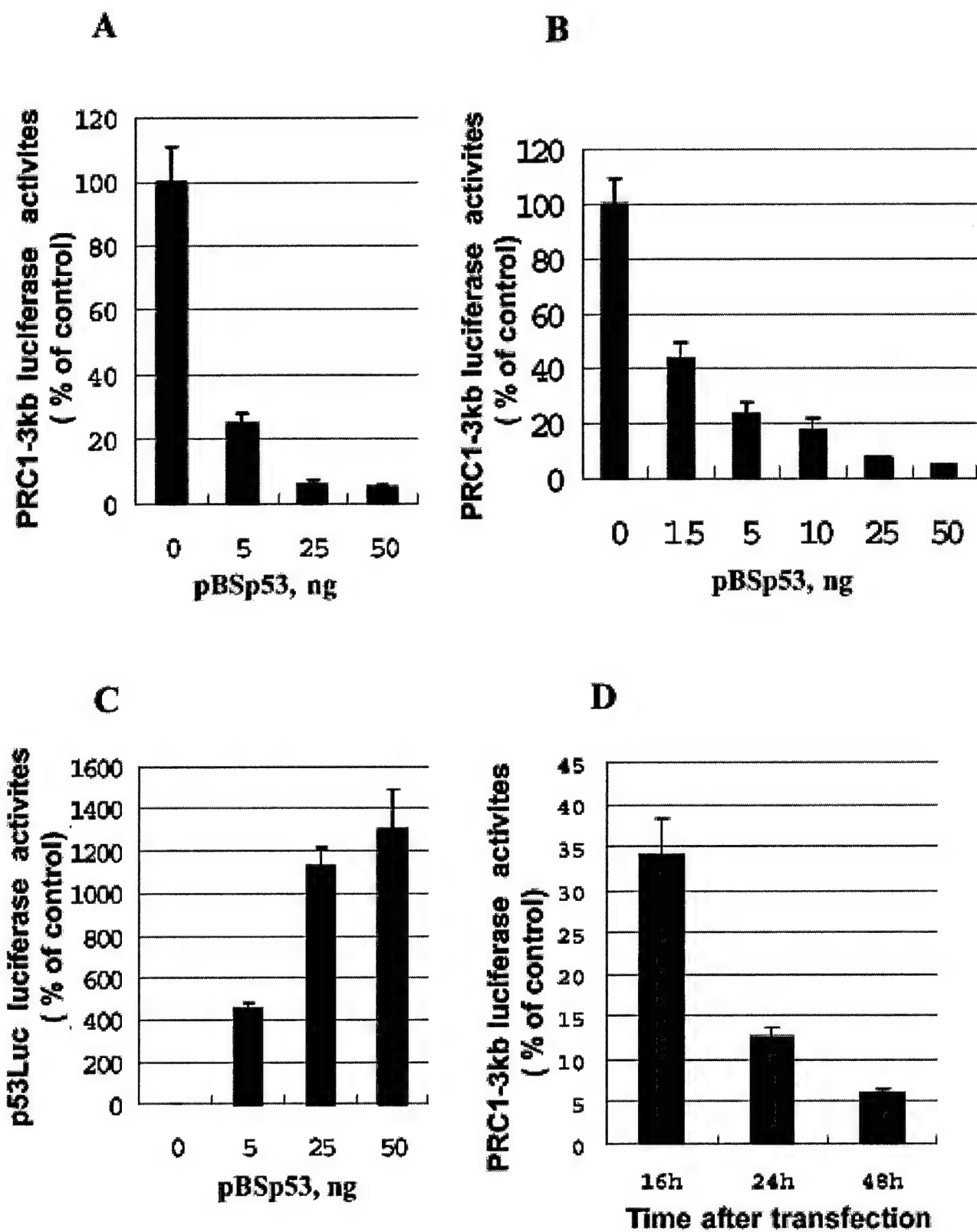**B**

C

D

Figure 2

A

B

C

Figure 3

A

HCT116 p53^{+/+}

HCT116 p53^{-/-}

	C	5-FU	Dox
p53/actin	1	6	6
PRC1/actin	100	18	10

B

C

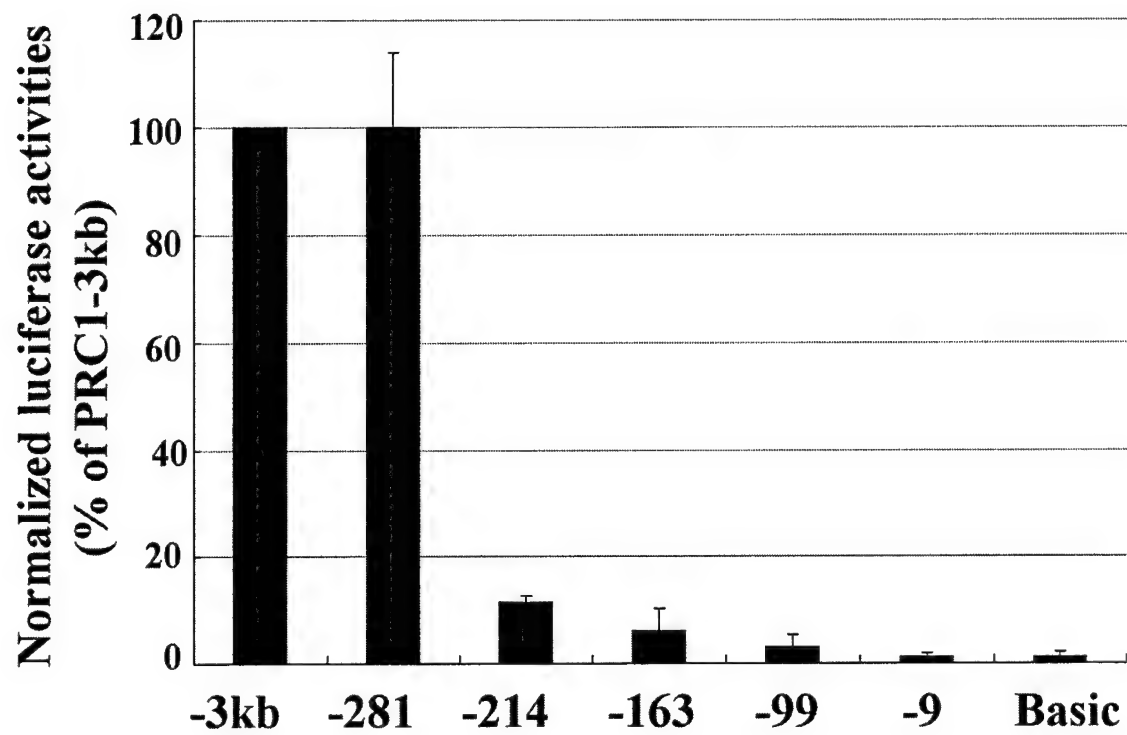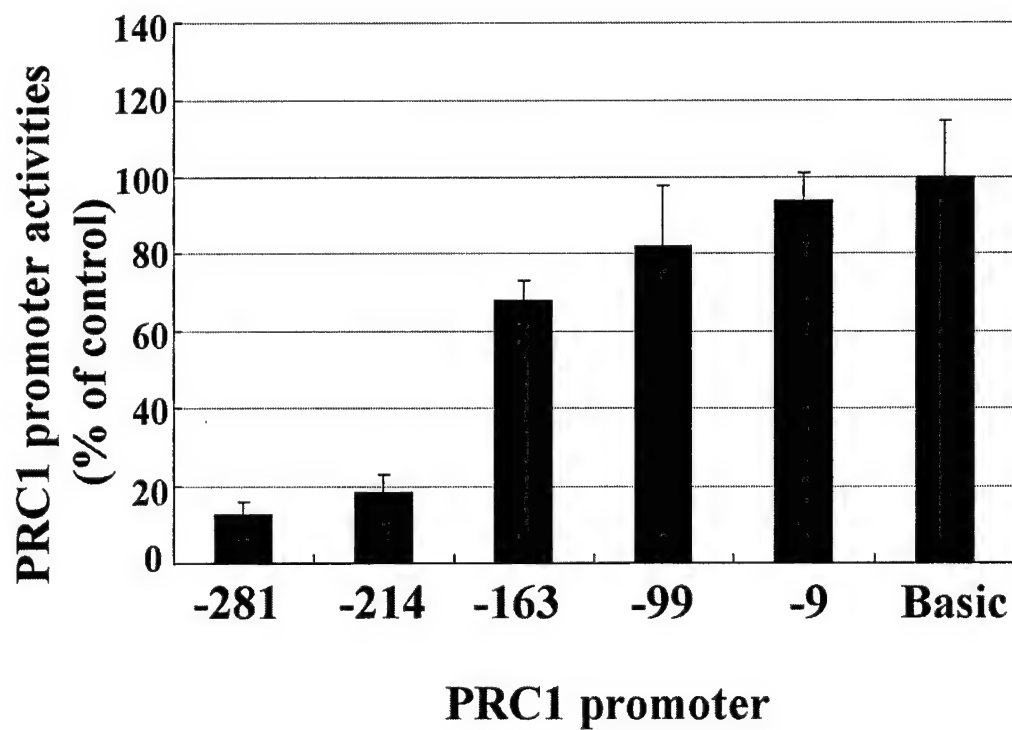**D**

Figure 4

ptsp53(32ºC)

HCT116 p53$^{-/-}$
(with pBSp53)

HeLa
(with pBSp53)

Figure 5

A

B

C

D

Figure 6

A

```
CTTGAGGCTGCCGCCAAGCCAGGGAAGCGGGAGGCGCAGGCCACGCCCGG        -232

CCACTCACAGACAGTGACGTCATCCCCCGCCGCCACTCCGGCGCTTCCCA        -182
                  ▼
GGCCCTGCTCGCGAGTCCCCACCCCGATTGCGCACCCGCGACTTCAGCCC        -132
                ▼
GAGGGGCGGGGATTTTCTTGGAGCGACGGGACGCGACGCCAATCGCGACG        -82
                           ▼
AGGCTTCGCCCCGTGGCGCGGTTTGAAATTTTGCGGGGCTCAACGGCTCG        -32

CGGAGCGGCTACGCGGAGTGACATCGCCGGTGTTTGCGGGTGGTTGTTGC        +19
                  ▼
TCTCGGGGCCGTGTGGAGTAGGTCTGGACCTGGACTCACGGCTGCTTGGA        +69

GCGTCCG                                                  +76
```
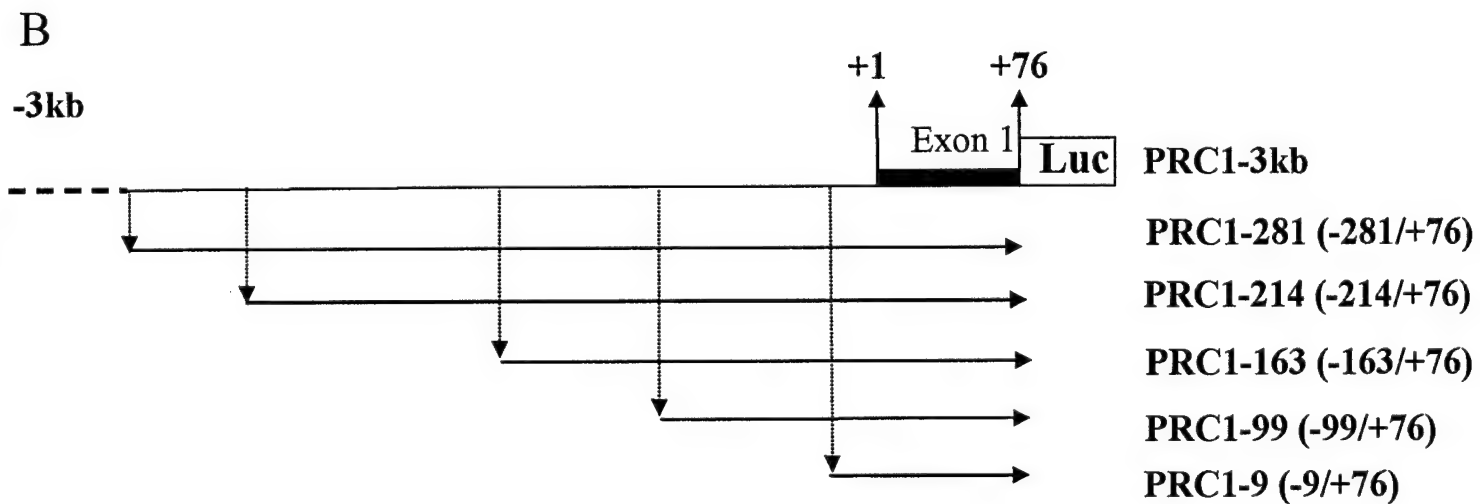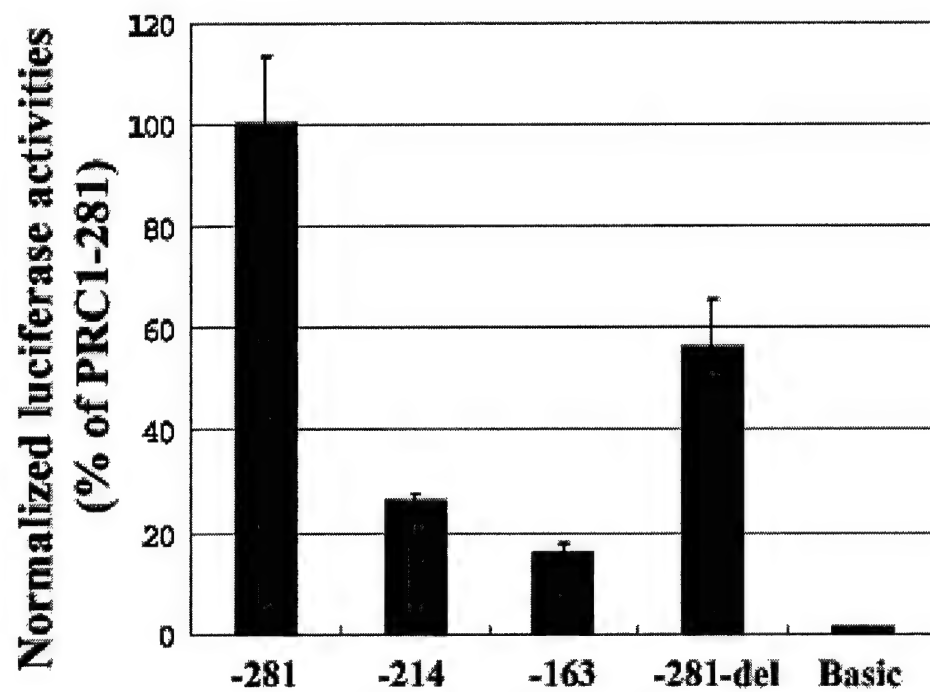
B

Figure 7

Figure 8

A

B

Figure 9

A

B

Figure 10

MCF7-ptsp53   37°C   32°C
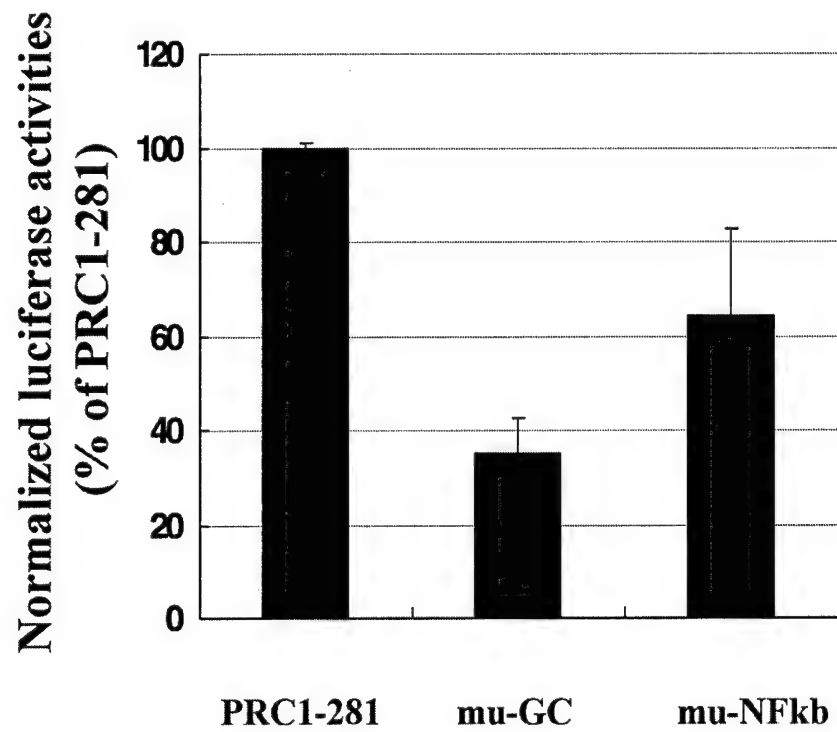
a-IgG   a-p53   a-IgG   a-p53

PRC1, bound
PRC1, input
P21, bound
P21, input
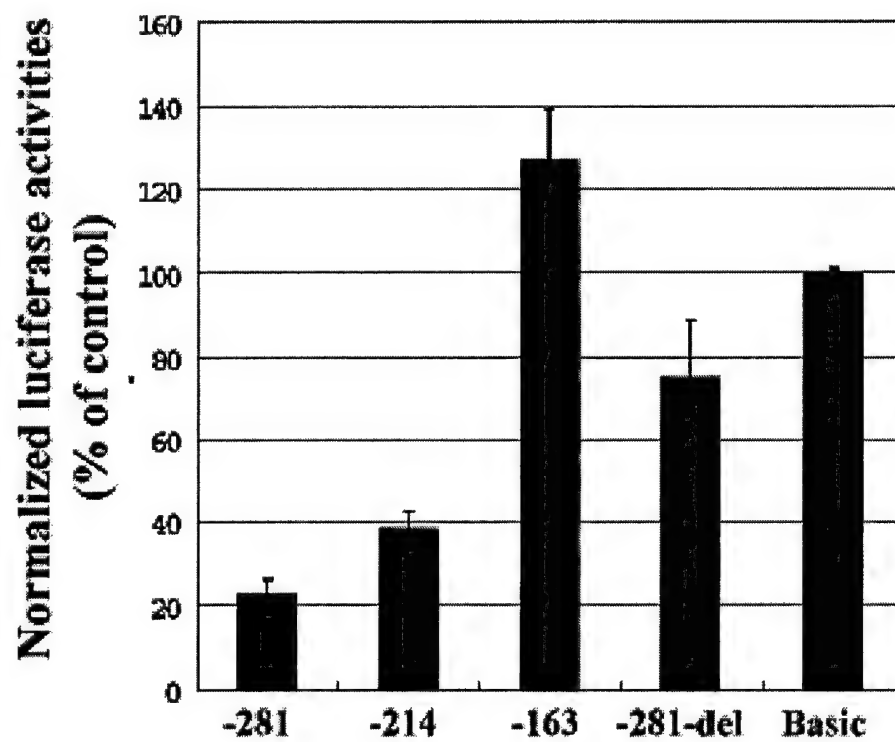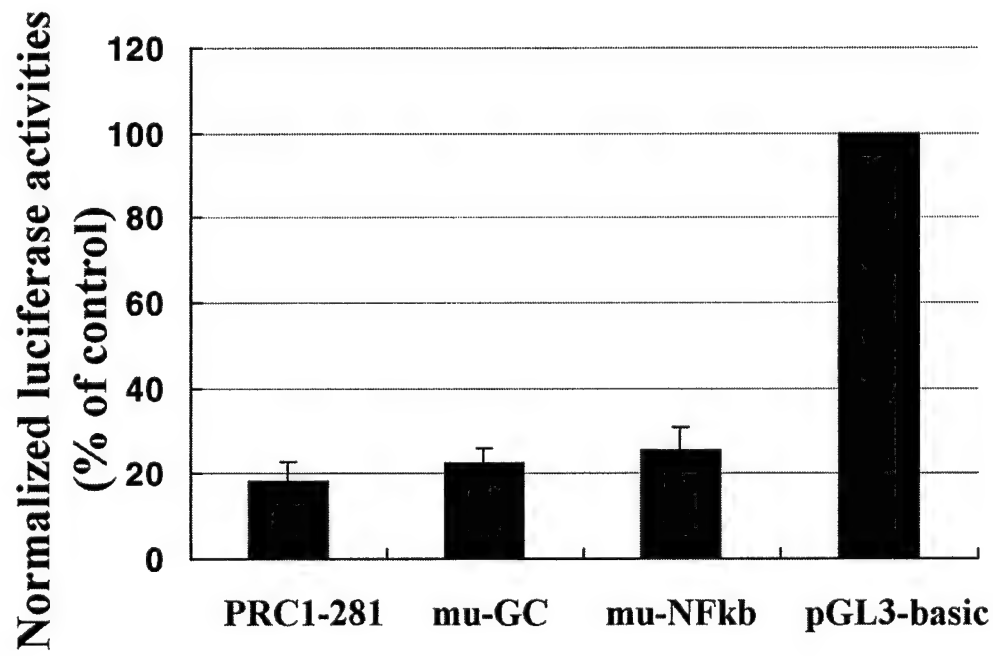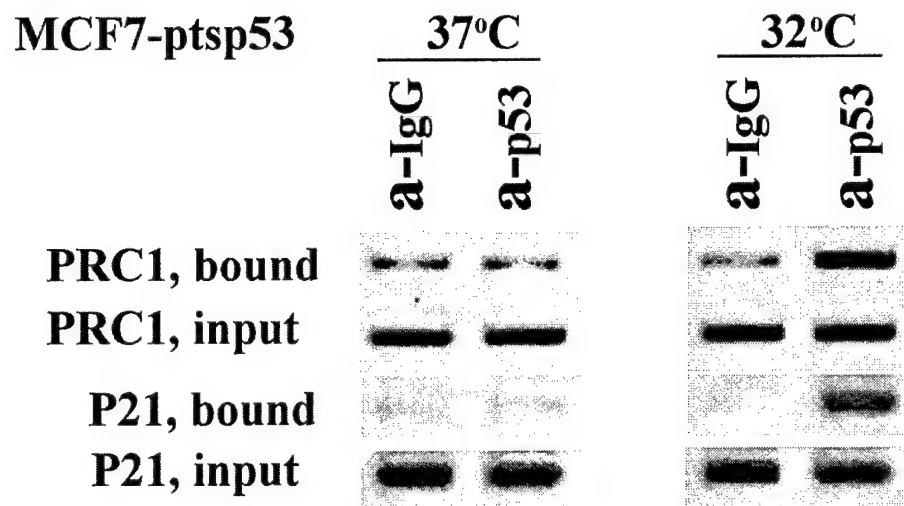
Delineating an oncostatin M-activated STAT3 signaling pathway that coordinates the expression of genes involved in cell cycle regulation and extracellular matrix deposition of MCF-7 cells

Fang Zhang[1], Cong Li[1], Hartmut Halfter[2] and Jingwen Liu*,[1]

[1]Department of Veterans Affairs Palo Alto Health Care System, Palo Alto, CA 94304, USA; [2]Department of Neurology and Internal Medicine A (Oncology), Westfälische Wilhelms-Universität Münster, Münster, Germany

A number of studies have demonstrated that the STAT pathway is an important signaling cascade utilized by the IL-6 cytokine family to regulate a variety of cell functions. However, the downstream target genes of STAT activation that mediate the cytokine-induced cellular responses are largely uncharacterized. The aims of the current study are to determine whether the STAT signaling pathway is critically involved in the oncostatin M (OM)-induced growth inhibition and morphological changes of MCF-7 cells and to identify STAT3-target genes that are utilized by OM to regulate cell growth and morphology. We show that expression of a dominant negative (DN) mutant of STAT3 in MCF-7 cells completely eliminated the antiproliferative activity of OM, whereas expression of DN STAT1 had no effect. The growth inhibition of breast cancer cells was achieved through a concerted action of OM on cell cycle components. We have identified four cell cycle regulators including c-myc, cyclin D1, c/EBPδ, and p53 as downstream effectors of the OM-activated STAT3 signaling cascade. The expression of these genes is differentially regulated by OM in MCF-7 cells, but is unaffected by OM in MCF-7-dnStat3 stable clones. We also demonstrate that the OM-induced morphological changes are correlated with increased cell motility in a STAT3-dependent manner. Expression analysis of extracellular matrix (ECM) proteins leads to the identification of fibronectin as a novel OM-regulated ECM component. Our studies further reveal that STAT3 plays a key role in the robust induction of fibronectin expression by OM in MCF-7 and T47D cells. These new findings provide a molecular basis for the mechanistic understanding of the effects of OM on cell growth and migration.

*Correspondence: J Liu. (154P), VA Palo Alto Health Care System, 3801 Miranda Avenue, Palo Alto, CA 94304, USA:
E-mail: jingwen.liu@med.va.gov

Introduction

STAT proteins are important signaling molecules for many cytokines, such as IL-6 family cytokines (Hirano et al., 1997; Heinrich et al., 1998), and numerous growth factors, including EGF (Leaman et al., 1996). STAT proteins possess dual functions that not only transmit a signal from the cell surface to the nucleus after cytokine engagement of cognate cell surface receptors, but also regulate gene expression by direct binding to STAT-recognition sequence in the promoter region of the target genes (Bowman et al., 2000). Although seven members of the STAT family have been characterized in mammalian cells, in general only a single STAT protein or a subset of family members is specifically activated by individual cytokines.

STAT3 and STAT1 are the main STAT proteins activated by the IL-6 cytokine family in a variety of cell types including hepatocytes (Kiuchi et al., 1999; Li et al., 2002; Marsters et al., 2002), chondrocytes (Catterall et al., 2001), astrocytes (Schaefer et al., 2000), endothelial cells (Mahboubi and Pober, 2002), glioblastoma cells (Halfter et al., 2000), melanoma cells (Kortylewski et al., 1999), and breast cancer cells (Badache et al., 2001; Li et al., 2001a, b; Grant et al., 2002). A number of recent studies have shown that activation of STAT3 and STAT1 by the same cytokine, such as oncostatin M (OM), leads to different biological outcomes in different cell types, suggesting that the expression of genetic programs initiated by STAT activation is heavily influenced by cellular context.

OM is a member of IL-6 cytokine family produced by activated T cells and macrophages (Zarling et al., 1986; Brown et al., 1987; Grove et al., 1991). Similar to IL-6 or LIF, OM is pleiotropic and participates in diversified cellular processes such as wound healing (Duncan et al., 1995; Bamber et al., 1998), inflammatory response (Wahl and Wallce, 2001), and cellular proliferation and differentiation (Douglas et al., 1997; Liu et al., 1997; Horn et al., 1990; Grove et al., 1993; Zhang et al., 1994; Halfter et al., 1998). OM manifests its function through specific binding to OM receptors, including the OM-specific receptor (OSMR) and the LIF receptor (LIFR). Additions of OM to cells in culture immediately induce the dimerization of receptor subunits, OSMRβ and

GP130. This results in phosphorylation and activation of receptor-associated JAK family kinases, leading to activation of several intracellular signaling pathways. Although the STAT1 and STAT3 proteins and the MAP kinase ERK are coactivated simultaneously by OM in every cell type that expresses the OM-high-affinity receptor (OSMR), there are conflicting reports as to which signaling cascade is critically linked to a defined OM-induced cellular functional change.

Previously, we have shown that the OM-induced growth suppression and morphological changes of breast cancer cell line MDA-MB231 can be totally abrogated by blocking ERK activation with the MAP kinase kinase-1 (MEK-1) inhibitors (Li et al., 2001a, b, c). By contrast, MEK inhibitors PD98059 and U0126 were not able to abolish the OM anti-proliferative activity or to reverse the morphological changes in MCF-7 cells, implying that other signaling pathways activated by OM in MCF-7 cells are responsible for its actions.

It has been reported in several studies that the OM antiproliferative activity is accompanied by the induction of morphological changes of breast cancer cells (Liu et al., 1997; Spence et al., 1997; Douglas et al., 1998; Halfter et al., 1998). In general, the OM-treated cells displayed disrupted intercellular cell junctions. Cells became scattered. The morphological changes could be partially attributed to cellular differentiation, as the accumulation of neutral lipid, a marker of differentiation, was detected in OM-treated MCF-7 cells (Douglas et al., 1998; Grant et al., 2002). However, a recent study conducted in T47D cells has suggested that the scattered phenotype is associated with an increased cell migration towards OM (Badache and Hynes, 2001). OM, acted as a chemoattractant, induced T47D cells to migrate in the absence of STAT3 activation. The mechanisms that underlie the effect of OM on cell migration of T47D cells remain elusive.

The aims of the current study are to determine whether the STAT signaling pathway is critically involved in the OM-induced growth inhibition and morphological changes of MCF-7 cells and to identify STAT3-target genes that are utilized by OM to regulate cell growth and motility.

Result

Blockade of OM-induced STAT3 and STAT1 transactivation by dominant negative STAT mutant proteins

OM activates both STAT3 and STAT1 in MCF-7 cells. To determine whether STAT3 or STAT1 activation is a key event in the OM-induced growth inhibition of MCF-7 cells, we established stable MCF-7 clones that express a dominant negative STAT3 mutant (dnStat3, Y705F) or a dominant negative STAT1 mutant (dnStat1, Y701F). MCF-7 clones (neo) transfected with the empty vector (pEFneo) were also generated and were used in this study as negative controls to access

the possible side effects associated with antibiotic selection.

To determine the effect of mutant STAT proteins on OM-induced STAT DNA binding activity, gel shift and supershift assays using a ^{32}P-labeled oligonucleotide probe (c-FosSIE), containing the high-affinity STAT3 binding site of c-fos gene promoter, were performed with nuclear extracts prepared from MCF-7 stable clones that were untreated or treated with OM for 15 min. As shown in Figure 1a, in MCF-7-neo cells, OM induced the formation of three specific DNA–protein complexes (lane 2). Supershift assays with antibodies specific to STAT1 or to STAT3 showed that the complex C3 was completely supershifted by anti-STAT1 antibody (lane 3), suggesting that C3 is the homodimer of STAT1. The C2 complex was supershifted by both anti-STAT1 and anti-STAT3 (lane 5), thereby demonstrating that C2 is the heterodimer of STAT1 and STAT3. The low-intensity band C1 was completely supershifted by anti-STAT 3 antibody (lane 4), demonstrating its identity as the STAT3 homodimer. The OM-induced STAT binding activity was markedly reduced in clones of dnStat3 (lanes 8–11) and dnStat1 (lanes 12–15) as compared to the neo clone (lanes 1–7) and untransfected MCF-7 cells (data not shown). Low levels of STAT1 binding activity were observed in uninduced neo (lane 1) and dnStat3 (lane 8) clones, suggesting that some of the STAT1 protein exist in a constitutively activated form in MCF-7 cells.

To further demonstrate a blockade of STAT3 transactivating activity by the mutant dnStat3 a STAT3 luciferase reporter (pTKlucS3) was transiently trans-fected into MCF-7-neo and dnStat3 clones. Cells, 40 h after transfection, were treated with OM for 4 h and luciferase activities were measured. As shown in Figure 1b, OM induced an eight-fold increase in the promoter activity of pTKlucS3 in the neo clone, but this induction was completely abolished in the clone of dnStat3.

We next examined the effect of OM on ERK activation in MCF-7 and stable clones. Western blot analysis detected comparable levels of activated ERK in parental MCF-7 cells and stable clones (Figure 2). These results clearly demonstrate that expression of the DN STATs specifically abolished STAT DNA binding and transactivating activity without subverting the OM-induced MEK/ERK signaling pathway.

### Expression of dnStat3 but not dnStat1 abolished the antiproliferative activity of OM

The impact of dnStat3 or dnStat1 expression on OM-induced growth suppression was first evaluated by cell proliferation assays that measured the binding of a fluorescent dye to cellular nucleic acids, which produces fluorescent signals in proportion to the cell number. Figure 3a shows that the cellular proliferation of MCF-7, the neo clones, and the clones expressing dnStat1 was inhibited by 60–75% as compared to control after incubation with OM for 5 days, whereas the growth rate of dnStat3 clones was unaffected by OM. To further
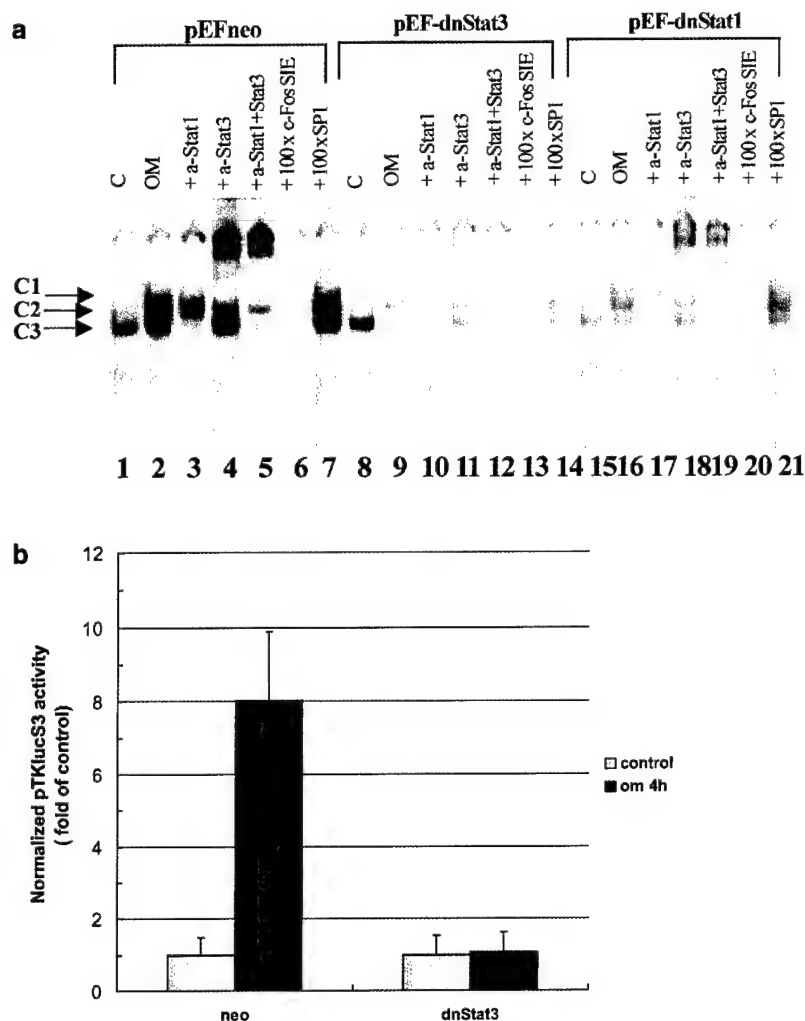
Figure 1 Blocking STAT DNA binding and transactivation by STAT mutant proteins. (a) EMSA analyses of nuclear proteins interacting with the STAT binding site. Nuclear extracts were prepared from MCF-7-neo clone, pEFneo-dnStat1 clone, and pEF-dnStat3 clone that were untreated (lanes 1), or treated with OM (15 min) (lanes 2–15). A double-stranded oligonucleotide, designated as c-FosSIE, was radiolabeled and incubated with 10 μg of nuclear extract per reaction for 10 min at 22°C in the absence (lanes 1, 2, 7, 8, 14, 15) or presence of 100-fold molar amounts of unlabeled competitor DNA (lanes 6, 7, 13, 14, 20, 21). For supershift, antibodies were incubated with nuclear extracts at 22°C for 30 min prior to the addition of the probe. The reaction mixtures were loaded onto a 6% polyacrylamide gel and run in TGE buffer at 30 mA for 3 h at 4°C. (b) Analysis of STAT3 reporter luciferase activity. The STAT3 reporter pLucTKS3 was cotransfected with pRL-SV40 into neo or dnStat3 clones. Cells, 40 h after transfection, were treated either with OM (50 ng/ml) or with OM dilution buffer for 4 h prior to harvesting cell lysates. Luciferase activities in total cell lysates were measured using the Promega Dual Luciferase Assay System. Absolute firefly luciferase activity was normalized against renilla luciferase activity to correct for transfection efficiency. The normalized luciferase activity is expressed as the fold of luciferase activity in untreated control cells. The data presented are derived from three separate transfections in which triplicate wells were used in each condition
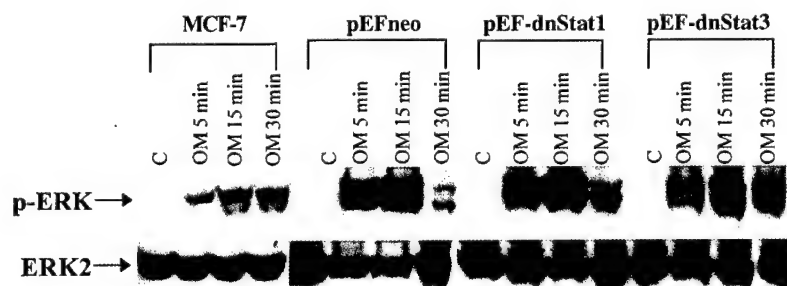
Figure 2 Activation of MAP kinases ERK1 and ERK2 by OM in MCF-7 and stable clones. MCF-7, neo, dnStat1, and dnStat3 clones cultured in medium containing 0.5% FBS were stimulated with 50 ng/ml OM. At the indicated times, cells were scraped into lysis buffer and cell extracts were prepared. Soluble proteins (30 μg/lane) were applied to SDS–PAGE. Detection of phosphorylated ERK1 and ERK2 and the nonphosphorylated ERK2 was performed by immunoblotting
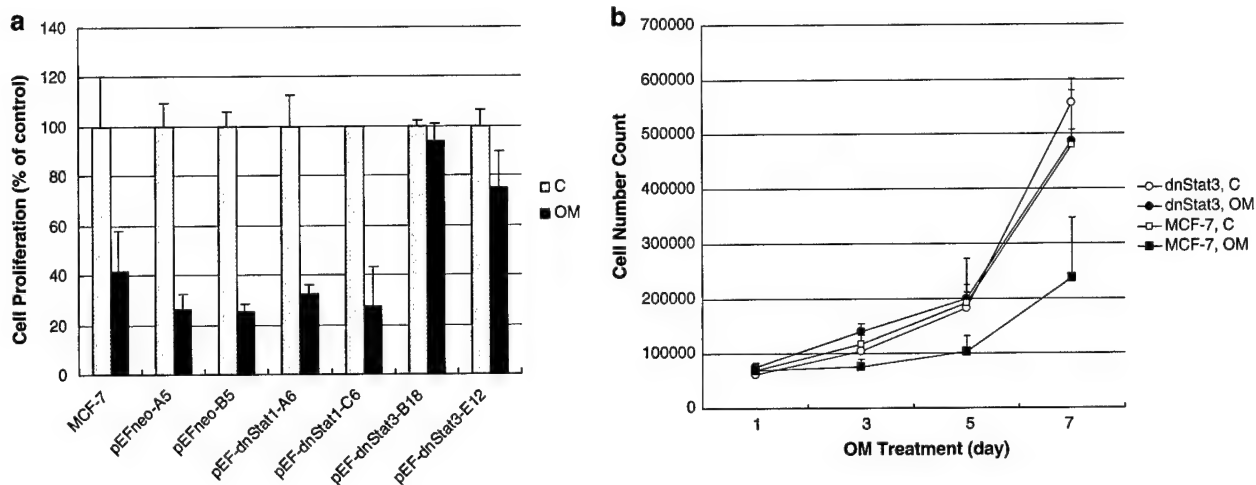
Figure 3 Abrogation of OM antiproliferative activity by expression of DN STAT3 in MCF-7 cells. (**a**) Untransfected parental MCF-7, two independently isolated neo, dnStat1, and dnStat3 clones were cultured in 96-well plates at a density of 2000 cells/well in 0.1 ml RPMI containing 2% FBS with or without 50 ng/ml OM for 5 days. The medium was removed and cells were washed with PBS. A volume of 200 μl of Cyquant GR dye mixed with cell lysis buffer was added to each well. The fluorescent signals were then measured using a fluorescence microplate reader. (**b**) Cells of MCF-7 and dnStat3 clone were cultured in 24-well culture plates at a density of 7×10^3 cells/well in 0.5 ml RPMI containing 2% FBS with or without 50 ng/ml of OM for different days. At the indicated time, cells were trypsinized and viable cells (trypan blue excluding cells) were counted. Values are mean of triplicate wells. The figure shown is representative of 4–5 separate experiments

verify the blocking effect of DN STAT3 on OM growth inhibitory activity, a time course of cell growth rate in the absence or the presence of OM was conducted by direct accounting of the viable cell numbers of MCF-7 cells and the dnStat3 clone. Figure 3b shows that OM exerted a time-dependent inhibitory effect on MCF-7 cells. By 7 days of the OM treatment, the number of viable cells was decreased by more than 50% as compared to control. Consistent with the results of Figure 3a, the growth of dnStat3 cells was not inhibited by OM through the entire duration of the experiment. These results demonstrate that expression of the dominant negative mutant of STAT3 but not STAT1 blocked the OM-mediated growth arrest in MCF-7 cells.

OM regulates c-myc gene expression through STAT3-dependent and independent mechanisms

c-*myc* is a potent oncogene, the expression level of which is directly correlated with cellular growth status (Kelly *et al.*, 1983; Carroll *et al.*, 2002). Recent studies further identify c-*myc* as a target gene of STAT3 (Kiuchi *et al.*, 1999; Bowman *et al.*, 2001). OM and IL-6 regulates c-*myc* mRNA expression in a biphasic manner with an early induction and a subsequent suppression (Liu *et al.*, 1992, 1997; Minami *et al.*, 1996; Spence *et al.*, 1997). To determine the role of STAT3 in OM-regulated transcription of c-*myc*, Northern blot analysis was conducted to detect levels of the c-*myc* mRNA after short and long exposures to OM in MCF-7 and stable clones. Figure 4a shows that OM treatment over a 3-day time course decreased the levels of c-*myc* mRNA by 60–80% in MCF-7, neo, and dnStat1 clones but not in dnStat3 clones. Interest-

ingly, contrary to the long exposure, the transient induction of c-*myc* mRNA by OM was not abolished by overexpression of dnStat3 or dnStat1 (Figure 4b). A brief incubation of cells with OM stimulated c-*myc* expression to comparable levels (2–4 fold) in the MCF-7, neo, dnStat1, and the dnStat3 clones. These results suggest that OM downregulates c-*myc* transcription through a STAT3-dependent mechanism, whereas the immediate effect of OM on upregulation of c-*myc* is independent of the STAT3 signaling cascade.

Identification of STAT3 target genes c/EBPδ and cyclin D1 as novel OM-regulated genes that participate in OM-mediated growth repression

Previous investigations have shown that OM treatment resulted in an accumulation of breast cancer cells in the G_0/G_1 phase of the cell cycle (Douglas *et al.*, 1998; Grant *et al.*, 2002). The molecular mechanisms underlying the OM effects on cell cycle have not been clearly defined. Since cyclin D1 (Sinibaldi *et al.*, 2000; Sauter *et al.*, 2002) and c/EBPδ (Yamada *et al.*, 1997) are known target genes of STAT3 activation, and their gene products are important regulators in the $G_0/G1$ phase of the cell cycle, we sought to determine whether OM regulates cyclin D1 and c/EBPδ in MCF-7 cells and whether this regulation requires STAT3 activity. Figure 5 shows that OM reciprocally modulates cyclin D1 and c/EBPδ expression. OM increased c/EBPδ protein expression to levels of three- to fivefold of control in MCF-7, the neo, and dnStat1 clones, whereas the c/EBPδ expression in dnStat3 cells was not induced by OM (Figure 5a). The expression of cyclin D1 was inhibited by OM in MCF-7 cells and this inhibition was

a
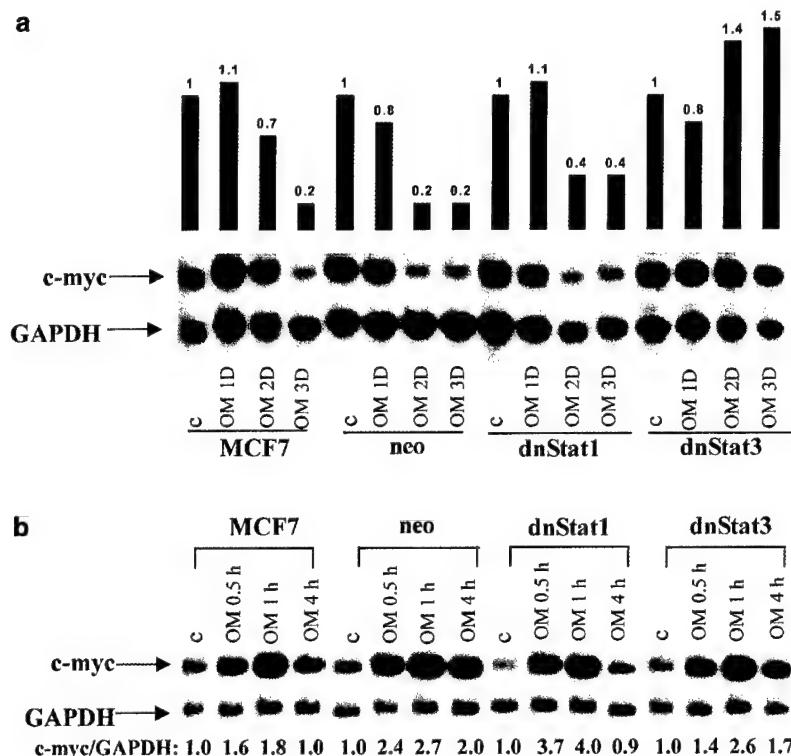
Figure 4 Detection of c-*myc* mRNA expression in MCF-7, neo, dnStat1 and dnStat3 clones by Northern blot analysis. Cells cultured in 60 mm dishes were treated with OM for 1–3 days (**a**) or for a short period of time (**b**). By the end of treatment, cells were lysed and total RNA was isolated. Total RNA of 15 μg per sample was analysed for c-*myc* mRNA by Northern blot. The membrane was stripped and rehybridized to a human GAPDH cDNA probe. The figure shown is representative of three separate experiments
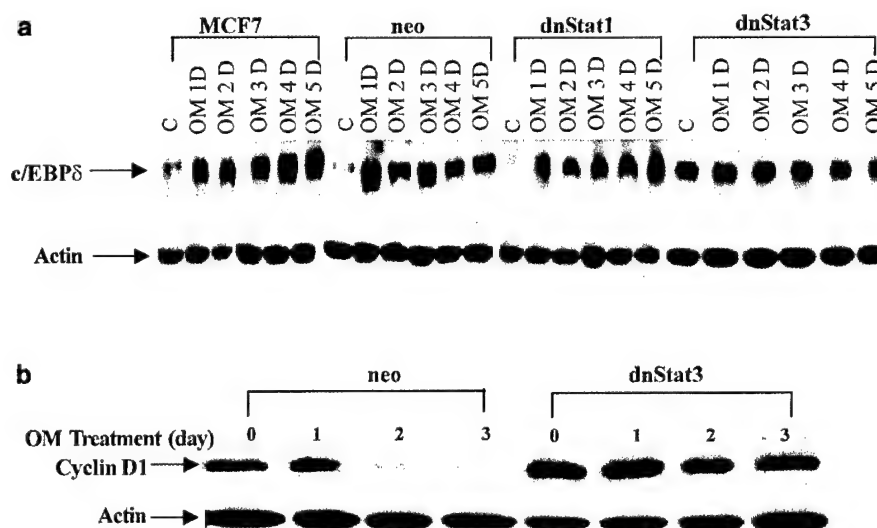

Figure 5 Western blot analyses of c/EBPδ and cyclin D1 protein expressions in MCF-7 and stable clones. Cells cultured in medium containing 2% FBS were incubated with 50 ng/ml OM for the indicated times and total cell lysate was harvested at the end of treatment. Soluble proteins (50 μg/lane) were applied to SDS–PAGE. Detections of c/EBPδ (**a**) and cyclin D1 (**b**) were performed by immunoblotting and autoradiography. Immunoblotting of the membranes with anti-β-actin mAb was conducted to normalize the amounts of protein being analysed

abrogated by overexpression of dnStat3 (Figure 5b). These results demonstrate that OM exerts its effect on cell growth by direct regulation of critical cell cycle components through the STAT3 signaling pathway.

STAT3 participates in OM-mediated downregulation of p53

OM downregulates p53 expression in MCF-7 cells by inhibiting the gene transcription (Liu *et al.*, 1999; Li *et al.*,

2001a, b, c). Since blocking the MEK/ERK pathway only partially reversed the OM inhibitory effect on p53 protein expression, it is possible that other signaling pathways could also be involved. To evaluate the role of STAT3 in p53 transcription, a p53 promoter luciferase reporter construct pGL3-p53 was cotransfected with pEF-dnStat3 or with a control vector (pEFneo) into MCF-7 cells along with pRL-SV40 for normalization of variations in transfection efficiency. Cells were treated with OM or OM dilution buffer for 40 h and dual luciferase activities were measured in total cell lysates. The p53 promoter activity was decreased by 50% in OM-treated cells in the absence of pEF-dnStat3. Expression of dnStat3 reversed the OM inhibitory effect on p53 promoter activity (Figure 6a). We further examined p53 protein levels in MCF-7 neo and dnStat3 clones untreated or treated with OM. Western blot analysis shows that while OM treatment lowered p53 protein level to 35% of control in the neo clone, the level of p53 protein in the dnStat3 clone was not decreased by OM treatment (Figure 6b). Taken together, these results demonstrate that activation of STAT3 signaling pathway is a necessary step in the OM-mediated regulation of p53 transcription.
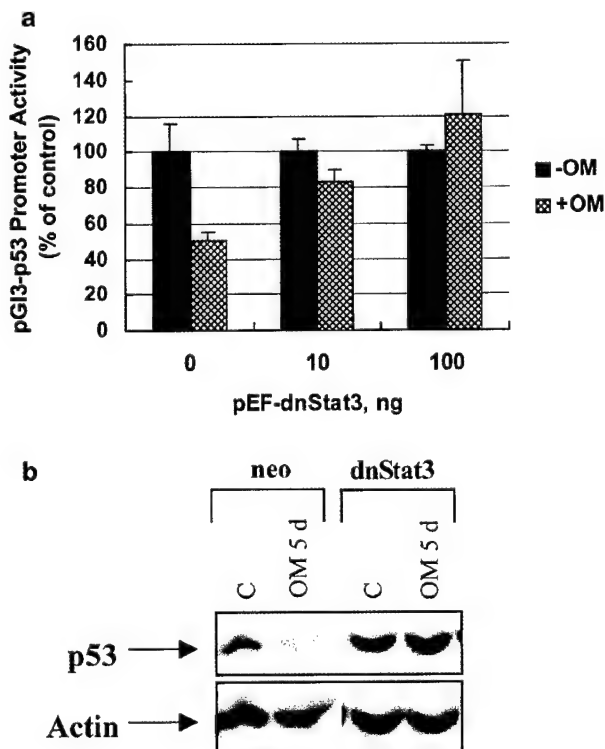

Figure 6 Evaluation of the role of STAT3 in OM-mediated downregulation of p53 promoter activity and protein expression. (a) The p53 promoter reporter pGL3-p53 was cotransfected with pEF-dnStat3 or with pEFneo into cells along with the normalizing vector pRL-SV40. Transfected cells were treated either with OM (50 ng/ml) or with OM dilution buffer for 40 h prior to harvesting cell lysates. The normalized luciferase activity is expressed as the percentage of luciferase activity in untreated control cells. (b) Cells were cultured in the presence or absence of OM for 5 days and harvested. Western blot analysis of p53 protein expression was conducted using total cell lysates

OM-induced morphological changes are associated with increased cell motility and expression of fibronectin in a STAT3-dependent manner

Figure 7 shows OM-induced morphological changes that appeared in MCF-7, neo clone, and dnStat1 clone, but not in dnStat3 clones. The tight cell-to-cell junctions in MCF-7 cells was severely disrupted by OM. Cells became flat and larger, and also developed cell extensions and membrane protrusions. These changes subtly surfaced after 1 day of OM treatment and were predominant after 3 days. However, in dnStat3 clones morphological changes were not readily detected even after 5 days. After a longer period of culture (7 days) in the presence of OM, slight morphological changes were noticed. The OM-induced morphological changes were reversible, as cells slowly resumed original cell shape after withdrawal of OM from the culture medium.

We were interested to know whether the OM-induced phenotype is related to changes in the extracellular matrix (ECM) composition. Using Western blot analysis, we examined several ECM proteins including P-cadeherin, E-cadeherin, and fibronectin that are known to play important roles in cell morphology and migration. We found that the protein level of E-cadeherin was not changed by OM and the level of P-cadeherin was only slightly increased after OM treatment (data not shown). In contrast, OM induced a robust time-dependent expression of fibronectin in MCF-7 cells and a much weak induction of fibronectin in the dnStat3 clone (Figure 8a). To determine whether the effect of OM on fibronectin expression is confined to MCF-7 cells, we examined fibronectin expression in another two breast cancer cell lines T47D and SKBR-3 to which OM also induces similar morphological changes (data not shown). Figure 8b shows that the expression of fibronectin in these two cell lines were strongly induced by OM as well. Moreover, the induction of fibronectin by OM was not detected in T47D-dnStat3 cells that stably express the dnStat3 mutant (Figure 8c) and these cells failed to show the distinct morphological changes upon OM treatment. These results strongly suggest that fibronectin is a downstream effector of the OM-activated STAT3 signaling cascade and expression of fibronectin may change the cell morphology.

Finally, we examined the involvement of STAT3 pathway in cell migration. Boyden chamber assays were performed to examine the direct effect of OM on cell motility. Cells were pretreated with OM for different days, trypsinized, counted, and seeded onto the top chamber; cells were then allowed to migrate through the membrane in the absence of any chemoattractant. As shown in Figure 9a, OM induced a time-dependent increase in the number of migrated cells. After a 2-day treatment, the number of migrated cells increased more than 12-fold of control. To determine the involvement of STAT3 in this newly discovered property of OM, the migration assay was conducted using DN STAT3 cells that were untreated or treated
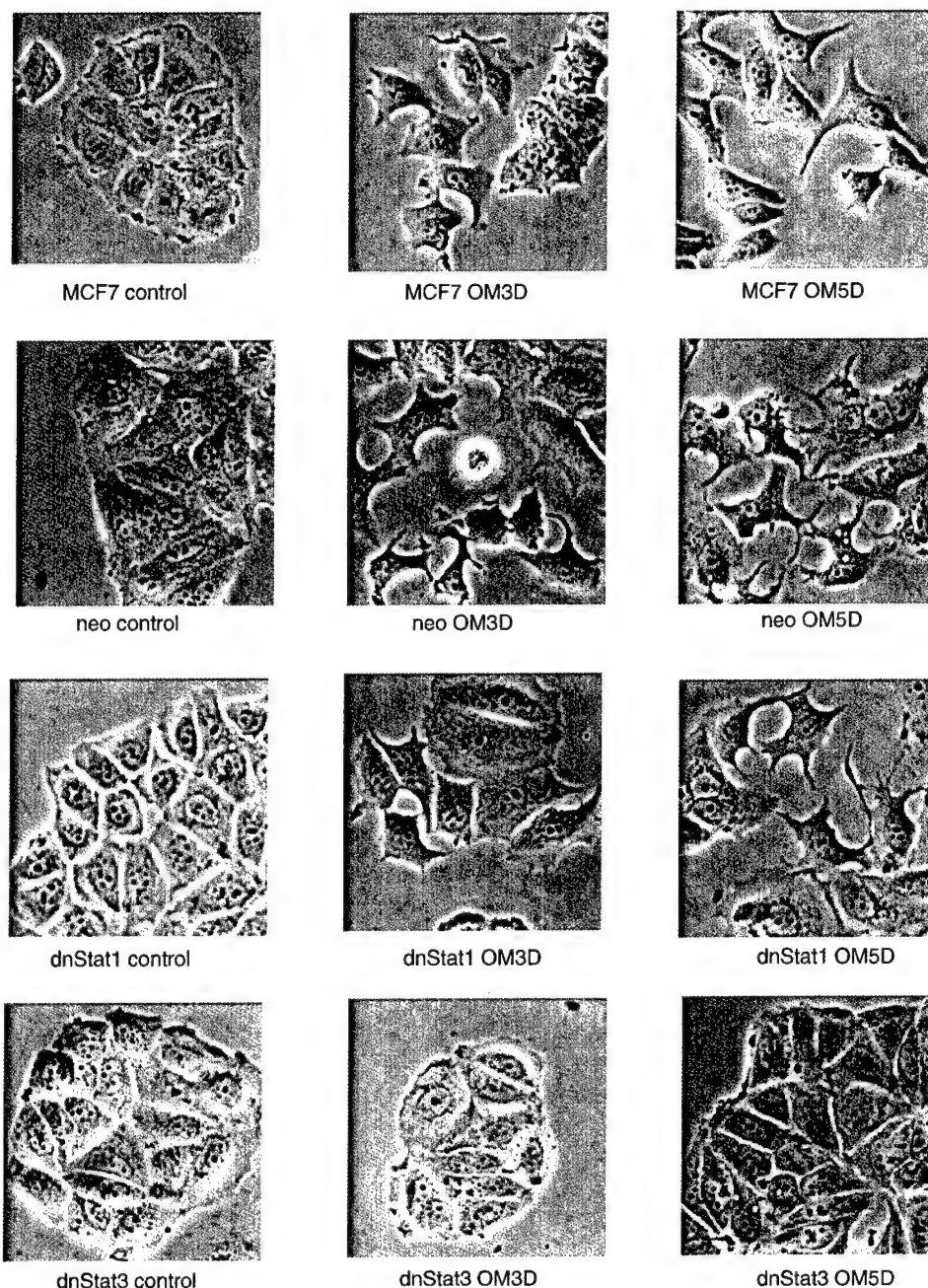
Figure 7 Detection of OM-induced morphological changes in MCF-7, neo, and dnStat1 clones but not in the dnStat3 clone. Cells were cultured in medium containing 2% FBS with or without OM for 3–5 days. Photographs were taken at the indicated time of OM treatment by using the Penguin 600CL digital camera at a magnification of 200. The loss of OM-induced morphological changes in T47D-dnStat3 cells was also observed

with OM. Figure 9b shows that the cell motility of dnStat3 clones was not stimulated at all even after 6 days of OM treatment.

Previously, using OM as a chemoattractant added to the bottom chamber, Badache *et al* has shown that expression of DN STAT3 did not affect the migration of T47D cells (Badache and Hynes, 2001). To determine whether DN STAT3 expression in MCF-7 cells is able to block the cell migration towards OM, MCF-7 and the dnStat3 clone were directly seeded onto the top

chambers without prior exposure to OM. OM or its dilution buffer as control was added to the bottom chambers. Cells were allowed to migrate for 24 h and the migrated cells were stained and counted. Figure 9c shows that OM as a chemoattractant induced the migration of dnStat3 clone and MCF-7 to similar extents. This corroborated the observation made in T47D cells. Thus, our results, for the first time, demonstrate that OM affects the intrinsic cell motility through a STAT3-dependent mechanism, whereas the

a

b

c
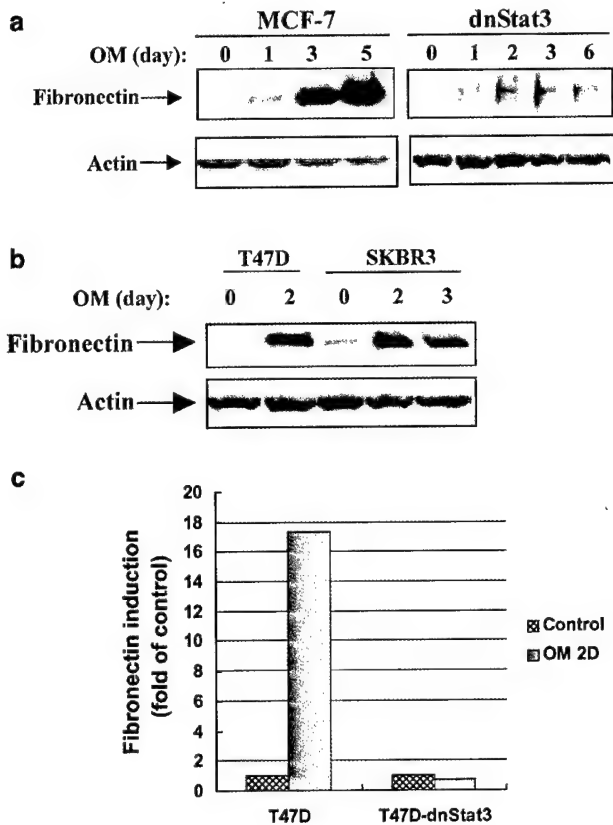
Figure 8 Western blot analysis for fibronection expression. The effects of OM on fibronectin expression were examined in wild-type STAT3 and the dnStat3 clones. MCF-7, MCF7-dnStat3 (a), T47D, SKBR-3 (b) cells were treated with OM. At the indicated time, cell was harvested and total cell lysates of 50 μg per sample were used to analyse fibronectin expression by Western blot analysis. In (c), T47D and T47D-dnStat3 cells were cultured in the absence (control) or presence of OM for 4 days and the expression of fibronection was examined by Western blot using total cell lysate. Data are expressed as fold increase relative to control

mechanism of chemoattraction mediated by OM is independent of STAT signaling pathway.

Discussion

The STAT pathway and the MEK/ERK pathway are two major signaling cascades utilized by IL-6 cytokine family to elicit a variety of biological response (Heinrich et al., 1998). Depending on cell types, activation of the same pathway can lead to different biological outcomes. It is conceivable that the downstream targets of ERK or STAT are differentially activated in different cell lines. Each signaling pathway may regulate a unique set of genes whose functions dictate the outcome induced by the cytokine in a cell line-specific manner. From this point of view, identification of target genes of a specific signaling cascade is of importance. It can provide insight to understand the mechanisms of cytokine's action at the molecular levels and may help predict outcomes in an uncharacterized system.

In this study, by utilizing dominant negative mutants of STAT3 and STAT1 we demonstrate that STAT3 but not STAT1 activation is a critical event in the OM-mediated growth inhibition of MCF-7 cells. Our results are consistent with the finding in A375 melonoma cells whose growth was strongly inhibited by OM in a STAT3 but not a STAT1-depdendent mechanism (Kortylewski et al., 1999). While it has been shown that STAT1 activation by IL-4 results in reduced growth rates in human colon carcinoma cell lines (Chang et al., 2000), it appears that activation of Stat1 by OM alone does not lead to changes in gene transcription and cell function. However, since blocking STAT3 DNA binding activity could affect the binding activity of STAT1 protein, our data cannot absolutely rule out the functional role of STAT1 in OM signaling. Additional experiments to block STAT3 and STAT1 expression by different approaches will be needed to reach a firm conclusion.

Recent investigations have identified c-myc as the downstream effector of STAT3 signaling (Kiuchi et al., 1999; Bowman et al., 2001). By using the dnStat3 clone, we found that the OM-induced biphasic regulation of c-myc is both STAT3-dependent and STAT3-independent. Our finding that dnStat3 blocks the OM-induced suppression of c-myc transcription recapitulates the observation obtained previously in M1 cells (Minami et al., 1996). It was shown that IL-6-induced down-regulation of c-myc in M1 cells was obviated by dnStat3 expression. Unexpectedly, the rapid induction of c-myc mRNA expression by OM in MCF-7 cells was not affected by dnStat3. The induction of c-myc mRNA (three- to four fold of control) by OM was completely abolished by actinomycin D (data not shown), implying a nature of transcriptional activation. The E2F binding site of the c-myc promoter, located at $+98$ to $+106$ bp, was shown to interact with STAT3 and to mediate the inducing activity of IL-6 on c-myc promoter activity (Kiuchi et al., 1999). We have analysed a series of c-myc promoter luciferase reporters that contain the wild-type E2F or the mutated E2F sites in a transient transfection system of MCF-7 cells. We did not observe a significant induction of the c-myc promoter activity by OM regardless of the status of the E2F site (our unpublished data). Our results suggest that OM may stimulate c-myc transcription through some regulatory mechanisms such as chromatin remodeling that might not be readily accessed by the transient transfection of plasmid DNA. The mechanisms underlying the STAT3-independent activation of c-myc transcription by OM is currently under investigation in our laboratory.

In addition to c-myc, we have identified another two cell cycle regulators, c/EBPδ and cyclin D1, that function in the $G_0/G1$ phase of the cell cycle. c/EBPδ has an important role in the induction of G_0 growth arrest in mammary epithelial cells (Hutt et al., 2000) and cyclin D1 expression promotes cell cycle progression (Sherr and Roberts, 1999). OM through the STAT3 signaling cascade coordinately regulates the expression of c/EBPδ and cyclin D1. Although the direct role of these proteins individually in the OM-mediated growth arrest of MCF-7 cells has not been demonstrated in this
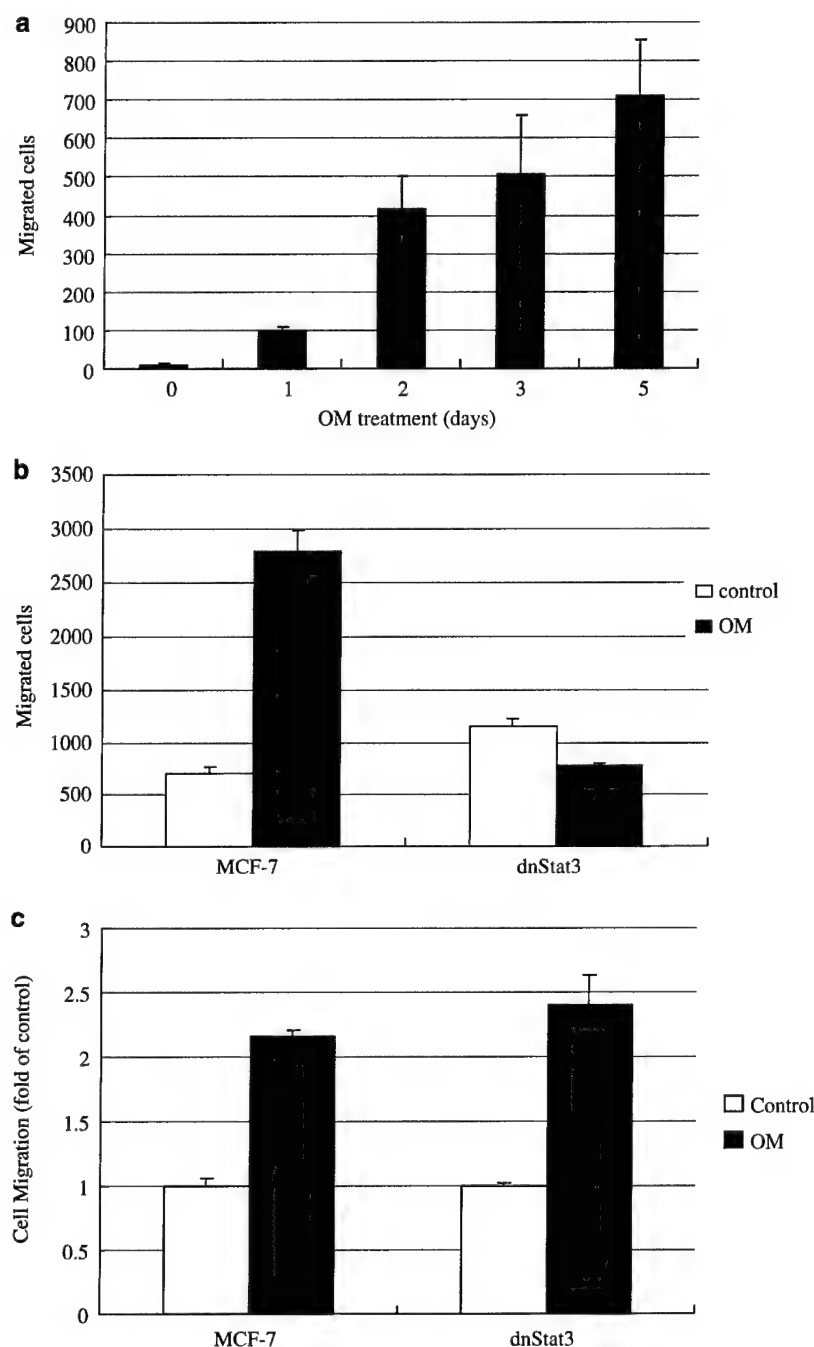
Figure 9 OM increases the intrinsic cell motility through the STAT3-signaling cascade. The effects of OM on cell motility were examined in MCF-7 and the dnStat3 clone. In (a), MCF-7 cells were pretreated with OM for different days at a concentration of 50 ng/ml. At the end of treatment, cells were trypsinized and counted. Cells were then seeded onto the top chamber at a density of 0.15×10^6 per chamber. The top chamber and the bottom chamber both contained 2% FBS RPMI. Migrated cells were counted after 6 h. In (b), MCF-7 and MCF7-dnStat3 cells were cultured in the absence (control) or presence of OM for 6 days. The ability of cell to migrate was determined as described in (a). In (c), cells without prior exposure to OM were seeded onto the top chamber which contained 2% FBS RPMI. OM at a concentration of 50 ng/ml was added to the bottom chamber that contained 2% FBS RPMI. Cells were allowed to migrate towards OM for 24 h. The migrated cells were fixed, stained, and counted. Data are expressed as fold increase relative to control

study, we postulate that the reduced growth rate of MCF-7 cells results from a concerted regulatory action of OM on several cell cycle components, leading to an accumulation of cells at the $G_0/G1$ phase.

Recently, there is emerging information to link STAT3 signaling pathway with p53. It was shown that the expression of the wild-type p53 in breast cancer cells inhibited STAT3-dependent transcriptional activity

(Lin *et al.*, 2002). Another reporter showed that Hep3B cells stably expressing a temperature-sensitive p53 species (p53-Val-135) displayed a reduced response to IL-6 when cultured at the wild-type p53 permitting temperature (Rayanade *et al.*, 1997). Later studies revealed that the reduction of cellular response to IL-6 was because of a p53-caused masking of STAT3 and STAT5, but not STAT1 (Rayanade *et al.*, 1998). In this study, we showed that blocking STAT3 activity by dnStat3 reversed the OM inhibitory effect on p53 transcription, demonstrating an involvement of STAT3 in OM-mediated negative regulation of the p53 transcription. Our previous investigation has identified the regulatory sequence (PE21) of p53 promoter as the OM-responsive element that mediates the OM effect on p53 transcription (Li *et al.*, 2001a, b, c). However, we did not detect STAT3 in the protein complex bound to the PE21 region by supershift using anti-STAT3 antibody (our unpublished data). This is not surprising, as the sequence of PE21 motif is not related to the STAT canonical sequence (Noda *et al.*, 2000). We speculate that the effect of STAT3 on p53 transcription is likely indirect and might be mediated through other downstream effectors of STAT3. Nevertheless, our novel finding that STAT3 participates in p53 transcription brings new insight into the interaction between the STAT signaling machinery and p53. It is possible that a reciprocal interaction exists: p53 regulates STAT3 phosphorylation and transactivating activity and the STAT3 affects p53 function by controlling p53 transcription.

OM has been implicated in the process of wound healing, which involves cell proliferation, migration, and remodeling of ECM. In dermal fibroblasts, OM stimulates the production of ECM components such as collagen and glycosaminoglycan (Duncan *et al.*, 1995). OM has been reported to stimulate the synthesis of tissue inhibitor of metalloproteinases 1 and 3 (Kerr *et al.*, 1999; Li *et al.*, 2001a, b, c). In endothelial cells, OM-promoted cell migration is associated with induction of the urokinase plasminogene activator (uPA) and uPA receptor (Strand *et al.*, 2000). In this study, we provide the first evidence that OM strongly induces fibronectin protein production. Analysis of fibronectin mRNA in untreated and OM-treated cells showed that OM increased the levels of fibronectin mRNA to the order of 20–30-fold (data not shown). The induction at this order of magnitude is likely to be transcriptional. Fibronectin is a multifunctional adhesive glycoprotein (Makogonenko *et al.*, 2002). It affects cell adhesion and migration. The OM-induced cell migration is likely to be mediated through the interaction of fibronectin with other ECM components. In MCF-7 cells, the OM-induced morphological changes, increased intrinsic cell motility, and production of fibronectin are all inhibited by DN STAT3. Our studies suggest that STAT3 signaling cascade may play important roles in ECM remodeling in breast cancer cells.

In summary, our studies have defined c-*myc*, cyclin D1, c/EBPδ, and p53 as the downstream effectors of the OM-activated STAT3 signaling cascade that participate in the process of growth regulation. Furthermore, we have unraveled the importance of STAT3 activation in OM-induced migration of breast cancer cells and identified a new OM-regulated ECM component fibronectin. These results provide a better understanding of the molecular mechanisms whereby OM regulates cell growth and differentiation.

Materials and methods

Cells and reagents

Human breast cancer cell lines MCF-7, T47D, and SKBR-3 were obtained from American Type Culture Collection (Manassas, VA, USA) and cultured in RPMI-1640 medium supplemented with 10% heat-inactivated fetal bovine serum (FBS). The T47D-dnStat3 cells were kindly provided by Dr Ali Badache at Friedrich Miescher Institute, Basel, Switzerland, and the effects of OM on these cells have been described (Badache and Hynes, 2001). The plasmids pEFneo and pEFneo-dnStat1 (Y701F) (Chang *et al.*, 2000) were obtained from Dr Xin-Yuan Fu at Yale University. The plasmid pEF-dnStat3 (Y705F) (Minami *et al.*, 1996) was provided by Dr Shizuo Arika at Osaka University. The specific STAT3 luciferase reporter plasmid pLucTKS3 (Zhang *et al.*, 1996) and the control reporter pLucTK were provided by Dr Richard Jove at the University of South Florida College of Medicine, Tampa, FL, USA. Antibodies directly to STAT3, STAT1, ERK2, cyclin D1, c/EBPδ, p53, c-*myc*, and fibronectin were obtained from Santa Cruz and the antiphosphorylated ERK was obtained from Cell Signaling Technology.

Generation of stable clones for STAT3 and STAT1 mutant proteins

To generate stable MCF-7 clones that constitutively express an FLAG-tagged dominant negative (DN) form of STAT3 (Y705F), plasmid pEF-dnStat3 and a empty vector containing a neomycin-resistant gene (pEFneo) were cointroduced into MCF-7 cells using the transfection reagent Effectene (Qiagen, Valencia, CA, USA). Cells were selected in 300 μg/ml G418. Several clones were picked, expanded in the presence of G418, and analysed for dnSTAT3 expression with anti-FLAG antibody by immunostainning. To generate MCF-7 clones expressing a DN form of STAT1 (Y701F), plasmid pEFneo-dnStat1 was transfected into MCF-7 cells and several independent clones were selected and characterized for dnStat1 expression by Western blot. MCF-7-neo clones were established by introducing the empty vector pEFneo into MCF-7 cells. These clones were used as negative controls in this study.

For each stable cell lines, at least two independent clones were analysed by Western blot analysis for the expression of mutant STAT proteins, by gel shift for STAT DNA binding activity, and by growth assays to determine the response to OM treatment. Significant clonal variations were not observed.

Electrophoresis mobility shift assays (EMSA) to detect STAT DNA binding activity in cells expressing the wild-type or the mutant STAT proteins

MCF-7 stable clones were seeded at 5–8 $\times$ 10^6 cells/100 mm and cultured in medium containing 0.5% FBS overnight. Cells were then untreated or treated with OM for 15 min. Nuclear extracts were prepared by the method of Dignam *et al* (1983) except that the buffer A was supplemented with 1 mM Na$_3$VO$_4$ and 1 μg per ml each pepstatin and leupeptin. Nuclear extracts were quick frozen by liquid nitrogen and stored in aliquots.

Protein concentrations were determined using a modified Bradford assay using BSA as a standard (Pierce). EMSA and supershift assays were conducted as previously described (Li *et al.*, 2001a, b, c) using a double-stranded oligonucleotide probe (c-FosSIE) containing the high-affinity STAT-binding site (m67) derived from the c-*fos* gene promoter (Wagner *et al.*, 1990). A double-stranded oligonuleotide probe containing an SP1 binding site was used in the assay for the assessment of nonspecific bindings.

Transfection and reporter assays

Cells cultured in 24-well plates at a density of 0.12×10^6 cells per well were transiently transfected with a total of 200 ng of reporter DNA and 2 ng of pRL-SV40 (Renilla, Promega) per well mixed with the Effectene reagent. Cells were switched to medium containing 0.5% FBS overnight, stimulated with OM for indicated length of time, and harvested, 24 h after transfection. Luciferase activities in total cell lysates were measured using the Promega Dual Luciferase Assay System. Absolute firefly luciferase activity was normalized against renilla luciferase activity to correct for transfection efficiency. Triplicate wells were assayed for each transfection condition and at least three independent transfection assays were performed for each reporter construct. The STAT3 luciferase reporter constructs contain seven copies of specific STAT3 binding sites corresponding to the region $-123/-85$ of the c-reactive protein (CRP) promoter (Zhang *et al.*, 1996). The p53 promoter luciferase reporter pGL3-p53 contains a 599 bp fragment of the human p53 promoter region and exon 1 (-426 to $+172$) (Li *et al.*, 2001a, b, c).

Cell growth assay

Cell number count was conducted in monolayer culture in 24-well Costar culture plates. Cells were plated at an initial density of 7×10^3 cells/well in 0.5 ml medium supplemented with 2% FBS. OM was added 24 h after initial seeding. The culture media were replenished every 2 days. At the end of treatment, cells were trypsinized and then viable cell numbers were counted using a hemocytometer. Cell proliferation assay conducted in 96-well culture plates with an initial seeding of 2×10^3 cells/well was measured using CyQUANT Cell Proliferation Assay Kit (C-7026) obtained from Molecular Probes and a fluorescence microplate reader with the parameters of 480 nm excitation and 520 nm emission.

Western blot analysis

For detection of activated ERK, cells were cultured in medium containing 0.5% FBS for overnight prior to OM stimulation. For detection of cycline D1, c/EBPδ, p53, and fibronectin expression, cells were cultured in medium containing 2% FBS with or without OM for various lengths of time. Cells in 60-mm culture dishes were lysed with 0.1 ml of cold lysis buffer (20 mM HEPES, pH 7.4, 30 mM *p*-nitrophenyl phosphate, 10 mM NaF, 10 mM MgCl$_2$, 2 mM EDTA, 5 mM dithiothreitol, 0.1 mM Na$_3$VO$_4$, 0.1 mM Na$_2$MnO$_4$, 10 mM Sodium B-glycerolphosphate, 10 nM Okadiac acid, 10 nM cypermethrin, 1 mM

phenylmethylsulfonyl fluoride, 5 μg/ml aprotinin, 1 μg/ml leupeptin, and 1.25 μg/ml pepstatin). Approximately 50 μg protein of total cell lysate per sample was separated on 10–15% SDS–PAGE, transferred to nitrocellulose membrane, followed by Western blot analysis. The signals detected using an enhanced chemiluminescence (ECL) detection system were quantitated with a BioRad Fluor-S MultiImager System. Densitometric analysis of autoradiographs in these studies included various exposure times to ensure linearity of signals.

RNA isolation and Northern blot analysis

Cells were lysed in Ultraspec RNA lysis solution (Biotecxs Laboratory, Houston, TX, USA) and total cellular RNA was isolated according to the vendor's protocol. Approximately 15 μg of each total RNA sample was used to analyse c-*myc* mRNA. The RNA blots were first hybridized to a 2 Kb human c-*myc* cDNA probe that was ^{32}P-labeled using the Primer-It II Random Primer Labeling kit (Stratagene) and then stripped and reprobed with a ^{32}P-labeled human GAPDH probe to ensure that equivalent amounts of RNA were being analysed. Hybridization signals were visualized by a BioRad Phosphor-Imager and were quantified by the Quantity One program.

Analysis of OM-induced morphological changes

MCF-7 and stable clones were cultured in the absence or presence of OM. At indicated times, cell morphology was examined under a phase contrast microscope equipped with a Penguin 600CL digital camera.

Migration assays

Cell motility was examined in a Boyden chamber assay using 8-μm-pore polycarbonate membrane. The migrated cells were fixed and stained using the kit Hema 3 manual staining system obtained from Fisher Scientific. Cells were counted under an inverted microscope in 10 different ×100-power fields in triplicate wells.

Abbreviations:
ECM, extracellular matrix; EMSA, electrophoretic mobility shift assay; ERK, extracellular signal regulated kinase; GAPDH, glyceraldehyde-3-phosphate dehydrogenase; IL-6, interleukin-6; OM, oncostatin M; STAT, signal transducer and activator of transcription.

References

Badache A and Hynes N. (2001). *Cancer Res.*, **61**, 383–391.

Bamber B, Reife R, Haugen H and Clegg C. (1998). *J. Mol. Med.*, **76**, 61–69.

Bowman T, Broome M, Sinibaldi D, Wharton W, Pledger W, Sedivy J, Irby R, Yeatman T and Courtneidge, SJR. (2001). *Proc. Natl. Acad. Sci. USA*, **98**, 7319–7324.

Bowman T, Garcia R, Turkson J and Jove R. (2000). *Oncogene*, **19**, 2474–2488.

Brown TJ, Lionbin MN and Marquardt H. (1987). *J. Immunol.*, **139**, 2977–2983.

Carroll J, Swarbrick A, Musgrove E and Sutherland R. (2002). *Cancer Res.*, **62**, 3126–3131.

Catterall J, Carrere S, Koshy P, Degnan B, Shingleton W, Brinckerhoff C, Rutter J, Cawston T and Rowan A. (2001). *Arthritis Rheum.*, **44**, 2296–2310.

Chang TL, Peng X and Fu X. (2000). *J. Biol. Chem.*, **275**, 10212–10217.

Dignam JD, Lebovitz RM and Roeder RC. (1983). *Nucleic Acids Res.*, **11**, 1475–1489.

Douglas AM, Goss GA, Sutherland RL, Hilton DJ, Berndt MC, Nicola NA and Begley CG. (1997). *Oncogene*, **14**, 661–669.

Douglas AM, Grant SL, Goss GA, Clouston DR, Sutherland RL and Begley CG. (1998). *Int. J. Cancer*, **75**, 64–73.

Duncan MR, Hasan A and Berman B. (1995). *J. Invest. Dermatol.*, **104**, 128–133.

Grant SL, Hammacher A, Douglas AM, Goss GA, Mansfield R, Heath J and Begley C. (2002). *Oncogene*, **21**, 460–474.

Grove RI, Eberthardt C, Abid S, Mazzucco CE, Liu J, Todaro GJ, Kiener PA and Shoyab M. (1993). *Proc. Natl. Acad. Sci. USA*, **90**, 823–827.

Grove RI, Mazzucco CE, Allegretto N, Kiener PA, Spitalny G, Radka SF, Shoyab M, Antonaccio M and Warr GA. (1991). *J. Lipid Res.*, **32**, 1889–1897.

Halfter H, Lotfi R, Westermann R, Young P, Ringelstein E and Stögbauer F. (1998). *Growth Factors*, **15**, 135–147.

Halfter H, Stögbauer F, Friedrich M, Serve S, Serve H and Ringelstein E. (2000). *J. Neurochem.*, **75**, 973–981.

Heinrich PC, Behrmann I, Muller-Newen G, Schaper F and Graeve L. (1998). *Biochem. J.*, **334**, 297–314.

Hirano T, Nakajima K and Hibi M. (1997). *Cytokine Growth Factor Rev.*, **8**, 241–252.

Horn D, Fitzpatrick WC, Gompper PT, Ochs V, Bolton-Hanson M, Zarling JM, Malik N, Todaro GJ and Linsley PS. (1990). *Growth Factors*, **2**, 157–165.

Hutt J, O'Rourke J and DeWille J. (2000). *J. Biol. Chem.*, **275**, 29123–29131.

Kelly K, Cochran BH, Stiles CD and Leder P. (1983). *Cell*, **35**, 603–610.

Kerr C, Langdon C, Graham F, Gauldie L, Hara T and Richard CD. (1999). *J. Interferon Cytokine Res.*, **19**, 1195–1205.

Kiuchi N, Nakajima K, Ichiba M, Fukada T, Narimatsu M, Mizuno K, Hibi M and Hirano T. (1999). *J. Exp. Med.*, **189**, 63–73.

Kortylewski M, Heinrich P, Mackiewicz A, Schniertshauer U, Klingmüller U, Nakajima K, Hirano T, Horn F and Behrmann I. (1999). *Oncogene*, **18**, 3742–3753.

Leaman D, Leung S, Li X and Stark G. (1996). *FASEB J.*, **10**, 1578–1588.

Li C, Ahlborn TE, Kraemer FB and Liu J. (2001a). *Breast Cancer Res. Treat.*, **66**, 111–121.

Li C, Ahlborn TE, Tokita K, Boxer L, Noda A and Liu J. (2001b). *Oncogene*, **20**, 8193–8202.

Li W, Dehnade F and Zafarullah M. (2001). *J. Immunol.*, **166**, 3491–3498.

Li W, Liang X, Kellendonk C, Poli V and Taub R. (2002). *J. Biol. Chem.*, **1**, 1–10.

Liu J, Clegg JC and Shoyab M. (1992). *Cell Growth Differ.*, **3**, 307–313.

Lin J, Jin X, Rothman K, Liu H, Tang H and Burke W. (2002). *Cancer Res.*, **62**, 376–380.

Liu J, Li C, Ahlborn TE, Spence MJ, Meng L and Boxer LM. (1999). *Cell Growth Differ.*, **5**, 15–18.

Liu J, Spence MJ, Wallace PM, Forcier K, Hellstrom I and Vestal RE (1997). *Cell Growth Differ.*, **8**, 667–676.

Mahboubi K and Pober J. (2002). *J. Biol. Chem.*, **277**, 8012–8021.

Makogonenko E, Tsurupa G, Ingham K and Medved L. (2002). *Biochemistry*, **41**, 7907–7913.

Marsters P, Morgen K, Morley S, Gent D, Hejazi A, Backx M, Thorpe E and Kalsheker N. (2002). *Biochem. J.*, **1**, 1–10.

Minami M, Inoue M, Wei S, Takeda K, Matsumoto M, Kishimoto T and Akira S. (1996). *Proc. Natl. Acad. Sci. USA*, **93**, 3963–3966.

Noda A, Toma-Aiba Y and Fujiwaba Y. (2000). *Oncogene*, **19**, 21–31.

Rayanade RJ, Ndubuise MI, Etlinger JD and Sehgal PB. (1998). *J. Immunol.*, **161**, 325–334.

Rayanade RJ, Patel K, Ndubuise M, Sharma S, Omura S, Etlinger JD, Pine R and Sehgal PB. (1997). *J. Biol. Chem.*, **272**, 4659–4662.

Sauter E, Yeo U, SteMM A, Zhu W, Litwin S, Tichansky D, Pistritto G, Nesbit M, PiNkel D, Herlyn M and Bastian B. (2002). *Cancer Res.*, **62**, 3200–3206.

Schaefer L, Wang S and Schaefer T. (2000). *Cytokine*, **12**, 1647–1655.

Sherr C and Roberts J. (1999). *Genes Dev.*, **13**, 1501–1512.

Sinibaldi D, Wharton W, Turkson J, Bowman T, Pledger W and Jove R. (2000). *Oncogene*, **19**, 5419–5427.

Spence MJ, Vestal RE and Liu J. (1997). *Cancer Res.*, **57**, 2223–2228.

Strand K, Murray J, Aziz S, Ishida A, Rahman S, Patel Y, Cardona C, Hammond W, Savidge G and Wijelath E. (2000). *J. Cell. Biochem.*, **79**, 239–248.

Wagner B, Hayes T, Hoban C and Cochran B. (1990). *EMBO J.*, **13**, 4477–4484.

Wahl A and Wallace PM. (2001). *Ann. Rheum. Dis.*, **60**, iii75–iii80.

Yamada T, Tobita K, Osada S, Nishihara T and Imagawa M. (1997). *J. Biochem.*, **121**, 731–738.

Zarling JM, Shoyab M, Marquardt H, Hanson MB, Lionbin MN and Todaro GJ. (1986). *Proc. Natl. Acad. Sci. USA*, **83**, 9739–9743.

Zhang XG, Gu JJ, Lu ZY, Yasukawa K, Yancopoulos GD, Turner K, Shoyab M, Taga T, Kishimoto T, Bataille R and Klein B. (1994). *J. Exp. Med.*, **179**, 1343–1347.

Zhang D, Sun M and Samols D. (1996). *J. Biol. Chem.*, **271**, 9503–9509.

ORIGINAL PAPER

Identification of PRC1 as the p53 target gene uncovers a novel function of p53 in the regulation of cytokinesis

Cong Li[1], Meihong Lin[1] and Jingwen Liu*,[1]

[1]Department of Veterans Affairs Palo Alto Health Care System, 3801 Miranda Avenue, Palo Alto, CA 94304, USA

Our previous studies conducted in MCF7-ptsp53 cells have demonstrated that overexpression of the wild-type (wt) p53 at permissive temperature 32°C leads to growth arrest at the G2/M phase of the cell cycle. To identify novel p53-regulated genes that are responsible for the p53-induced G2/M arrest, we conducted cDNA microarray analyses. The array results indicated that the mRNA level of protein regulator of cytokinesis (PRC1) was significantly decreased when the p53 transactivation activity was turned on, suggesting that PRC1 transcription could be downregulated by p53. In this study, we have extensively examined the functional role of p53 in the regulation of PRC1, a cell cycle protein that plays important roles during cytokinesis. We demonstrate that increased expression of the wt p53 either by exogenous transfection or chemical induction results in reduced mRNA and protein expression of PRC1 in HCT116 p53$^{+/+}$, HCT116 p53$^{-/-}$, MCF-7, T47D, and HeLa cells. Importantly, we show that the decreased PRC1 expression is accompanied by the appearance of binucleated cells, indicating the process of cell division after mitosis being inhibited. By isolation and characterization of a 3 kb genomic fragment containing the 5'-flanking region and part of exon 1 of PRC1 gene, we demonstrate that p53 directly suppresses PRC1 gene transcription. We further locate the p53-responsive sequence to the proximal promoter region −214 to −163, relative to the transcriptional start site. The in vivo interaction of p53 with PRC1 gene promoter is further demonstrated by chromatin immunoprecipitation assay. Taken together, these new findings suggest that p53 may have important roles in the regulation of cytokinesis through controlling the transcription of PRC1.
Oncogene (2004) 0, 000–000. doi:10.1038/sj.onc.1208114

Introduction

The protein p53 is the most important tumor suppressor identified to date. The essential roles of p53 as a gatekeeper to maintain mammalian cell homeostasis and to prevent malignant transformation (Levine, 1997) is well indicated by its frequent mutations occurring in the majority of human tumors including breast tumor (Vogelstein and Kinzler, 1992; Harris et al., 1996; Tarapore and Fukasawa, 2000). The loss of wild-type (wt) p53 is clearly an important event in breast tumorigenesis (Malkin et al., 1990; Hollstein et al., 1991). However, the exact mechanisms by which loss of p53 normal function leads to cancer formation and progression are not fully understood. In mammalian cells, the correct cell division is controlled by checkpoints at G1/S transition, G2/M transition, and mitosis. Many studies have indicated p53 being an important integral part of these checkpoints (Bargonetti and Manfredi, 2002). Accumulated p53 in response to DNA damage or through experimental overexpression has been shown to cause growth arrest at G1 (Agami and Bernards, 2000; Wesierska-Gadek and Schmid, 2000; Willers et al., 2000) and/or G2 (Agarwal et al., 1995; Taylor et al., 1999; Taylor and Stark, 2001; Nakamura et al., 2002) or to induce apoptosis (Vousden, 2000; Kokontis et al., 2001). In some cases, overexpression of the wt p53 induces cellular senescence (Sugrue et al., 1997; Dubrez et al., 2001; Jung et al., 2001). However, at present, it is not fully understood what factors are involved in the determination of cell fate in response to high cellular levels of p53. Moreover, the p53 downstream target genes mediating different cellular responses to p53 have not been completely characterized.

We have stably transfected a temperature-sensitive (ts) p53 mutant p53Val^{135} in MCF-7 breast cancer cells to establish a cell system (MCF7-ptsp53) where the transactivating function of p53 can be turned on or turned off by culturing cells at either permissive temperature 32°C or at the nonpermissive temperature 37°C (Michalovitz et al., 1990; Milner and Medcalf, 1990; Martinez et al., 1991). Interestingly, flow cytometric analysis of the DNA content shows that overexpression of the transcriptionally active p53 at 32°C arrested the growth of MCF-7 cells by exclusively increasing the percentage of cells in the G2/M phase without affecting G0/G1 phase or inducing apoptosis (Li et al., 2003). Thus, this cell line provides us a relatively unique system to characterize p53-initiated molecular events occurring at the G2/M phase. In order to identify novel p53-regulated genes that are responsible for the p53-mediated G2/M arrest, we performed

*Correspondence: J Liu; E-mail: jingwen.liu@med.va.gov

cDNA microarray analyses to compare the gene profiles of MCF7-ptsp53 cells cultured at either 37°C or at 32°C. Using the criteria of twofold as a cutoff line, the expressions of 14 genes were shown differentially regulated by wt p53 overexpression but not by nonspecific temperature switch (Li et al., 2003). Interestingly, none of the p53-regulated genes is related to apoptosis. However, four genes that previously have demonstrated to be involved in G2/M arrest were affected by the overexpression of wt p53 including p21, cdc2, cyclin B2, and PRC1. The former three genes have been demonstrated in a number of studies to be involved in p53-mediated G2 arrest (Dulic et al., 1998; Taylor et al., 1999; Kruse et al., 2000; Manni et al., 2001; Yin et al., 2001). However, PRC1 is a newly characterized cell cycle protein and its regulation by p53 or by other agents that affect cell cycle have not been reported.

The terminal stage of the cell cycle is cytokinesis. During the process of cytokinesis, cells divide their organelles, cytoplasm, plasma membrane, and other cell contents into two daughter cells (Stright and Field, 2000). PRC1, a recently characterized mitotic spindle-associated Cdk substrate, has been shown to have an exclusive role in cytokinesis (Jiang et al., 1998; Mollinari et al., 2002). Microinjection of anti-PRC1 antibodies into HeLa cells blocked cellular cleavage without affecting nuclear division, which resulted in binucleated cells (Jiang et al., 1998). The essential role of PRC1 in cell cleavage was also demonstrated by using PRC1 small interfering RNA (siRNA) to block its expression (Mollinari et al., 2002). It was shown that in the absence of the PRC1 protein, cells were able to progress normally in mitosis to metaphase and underwent normal chromatid segregation in anaphase. However, cells lacking PRC1 always showed aberrant anaphase spindle morphology and became increasingly binucleate with time. Further studies demonstrate that PRC1 regulates cytokenesis by stabilizing the midzone microtubule bundle and permitting completion of cell cleavage. The requirement of PRC1 for cell cleavage can also be inferred from its expression pattern. PRC1 expression levels are high during S and G2/M and drop dramatically after cells exit mitosis and enter G1 (Jiang et al., 1998). However, the factors that control the cell cycle-specific expression of PRC1 are largely unknown.

In this study, we have extensively examined the functional role of p53 in the regulation of PRC1 expression. Through several different lines of investigation, we provide strong evidence to demonstrate that PRC1 gene transcription is negatively regulated by p53. Our new findings suggest that p53 as the gatekeeper to maintain mammalian homeostasis may exert its function to control the final checkpoint for cell division at the stage of cytokinesis by transcriptional suppression of PRC1.
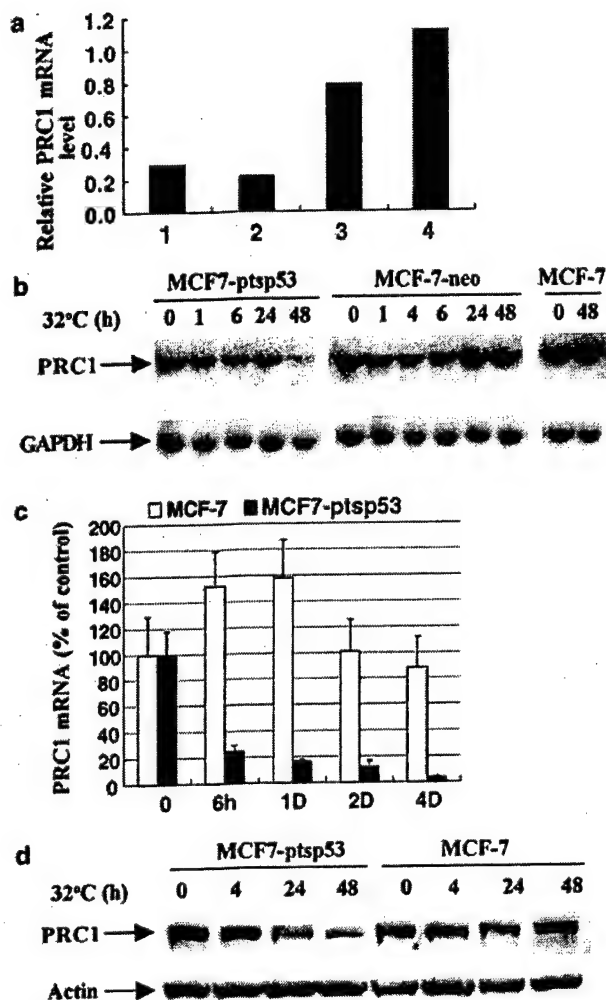
Results

Overexpression of p53 downregulates PRC1 gene expression in MCF-7 cells

To identify specific wt p53-regulated genes, we performed four sets of microarray analysis. First, gene expression profiles of MCF7-ptsp53 grown at 32°C and 37°C were compared. Second, MCF7-ptsp53 grown at 32°C was compared to untransfected parental MCF-7 cells grown at 37°C. Third, MCF7-ptsp53 grown at 37°C was compared to untransfected parental MCF-7 cells grown at 37°C. The last set of experiment was designed to assess the effect of temperature switch (37 → 32°C) on general gene expression of MCF-7 cells, as a negative control for the specific changes induced by p53 overexpression. The array results showed that the PRC1 mRNA level in MCF7-ptsp53 cells cultured at 32°C was decreased by 70% as compared to cells cultured at 37°C (Figure 1a, bar 1) and was decreased by 78% as compared to MCF-7 cells cultured at 37°C (bar 2). On the contrary, the temperature switch had no effect on PRC1 mRNA expressions in MCF-7 cells (bar 4). The data also indicated that overexpression of mutant p53 (ptsp53 ^{Val135}) did not significantly affect PRC1 mRNA expression, as MCF7-ptsp53 and MCF-7 cells cultured at 37°C expressed similar amounts of PRC1 mRNA (bar 3). These results demonstrated an inverse relationship between p53 transcriptional activity and PRC1 expression.

To follow up on this observation, Northern blot analysis was performed to detect the changes of PRC1 mRNA levels after the ptsp53 cells were switched from 37–32°C. The results in Figure 1b show that the PRC1 mRNA was downregulated by wt p53 in a time-dependent manner. The level of PRC1 mRNA began to drop by 6 h of culturing in the permissive temperature. By 24 h at 32°C, only 40% of the mRNA remained, and a residual level of the PRC1 mRNA could be detected after 48 h. Again, the temperature switching had no effect on PRC1 mRNA expression in the parental and the mock-transfected control clone (neo). We further conducted a quantitative real-time PCR assay using cDNAs prepared from mRNAs isolated from different samples. The results confirmed the kinetics of p53-mediated downregulation of PRC1 mRNA expression (Figure 1c). Examination of PRC1 protein levels in these cells led to corroborated findings in that the PRC1 protein level was decreased to 31% of control at 24 h and further decreased to 15% at 48 h by temperature shift-down (Figure 1d) only in MCF7-ptsp53 cells but not in parental MCF-7 cells.

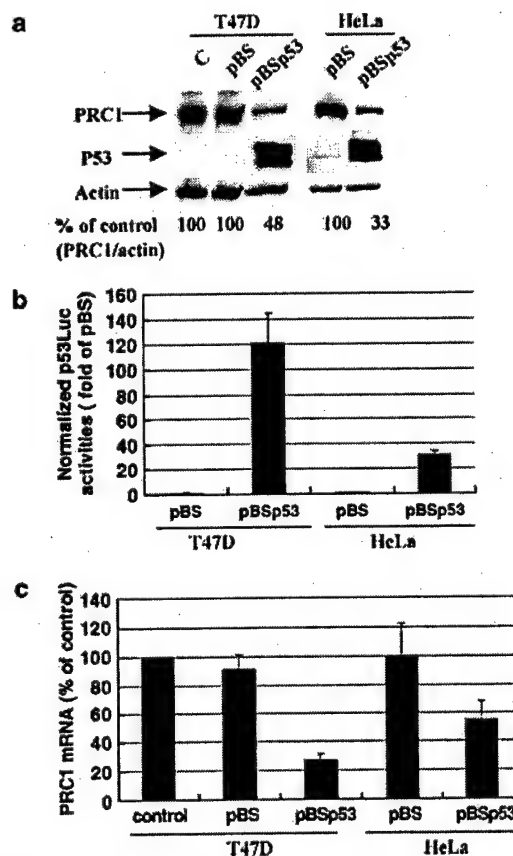### Overexpression of p53 downregulates PRC1 gene expression in other cell lines

The above experiments were carried out in MCF-7 breast cancer cell line. To further confirm the correlation between p53 overexpression and downregulation of PRC1 gene expression, different cell systems were used. T47D and HeLa cells were cotransfected with a wt p53

expression vector pBSp53 and pEGFP or mock transfected (pEGFP plus pBS empty vector). Two days post transfection, cells were subjected to cell sorting using green fluorescent protein (GFP) as a marker for transfection. After separation, GFP-positive cells were collected and total cell lysates as well as total RNA were harvested. Figure 2a (middle panel) and Figure 2b confirmed the increased protein levels and the transactivating activities of p53 in pBSp53-transfected cells. Figure 2a also shows that exogenously expressed wt p53 reduced PRC1 protein level by 52% in T47D and by 67% in HeLa cells, as compared to that in untransfected or mock-transfected cells.

Real-time PCR to detect PRC1 mRNA levels in pBSp53 transfected cells confirmed the results of

Figure 1 Overexpression of the wt p53 downregulates PRC1 gene expression in MCF-7 breast cancer cell lines. (a) Comparison of the PRC1 mRNA levels by microarray. MCF7-ptsp53 and MCF-7 cells were cultured at 37°C or 32°C for 4 days, respectively. Total RNA isolated from both cell lines were labeled with either cy3-dCTP or cy5-dCTP according to different experimental designs. The graph illustrates the ratio of PRC1 mRNA expression level in the paired samples. Bar 1, MCF7-ptsp53 at 32°C versus MCF7-ptsp53 at 37°C; Bar 2, MCF7-ptsp53 at 32°C versus MCF-7 at 37°C; Bar 3, MCF7-ptsp53 at 37°C versus MCF-7 at 37°C; Bar 4, MCF-7 at 32°C versus MCF-7 at 37°C. (b) Northern blot: MCF-7, MCF-7-neo, and MCF7-ptsp53 were seeded at 37°C. After switching to 32°C, cells were harvested at different times as indicated. Total RNA was isolated and 15 *i*g per sample was analysed for PRC1 mRNA by Northern blot. The membrane was stripped and hybridized to a human GAPDH probe. (c) Real-time PCR: The relative amounts of PRC1 mRNA harvested from MCF-7 or ptsp53 cells cultured at 32°C for various times were measured by a quantitative real-time RT-PCR assay using a PRC1-specific fluorogenic probe from Gorilla Genomics. The amount of PRC1 mRNA in cells cultured at 37°C was defined as 100, and the amount of PRC1 mRNA at different time points was plotted relative to that value. The data shown are derived from three separate experiments. (d) Western blot: MCF7-ptsp53 or MCF-7 seeded at 37°C were switched to 32°C at the same time and total cell lysates were harvested at different time points as indicated. In all, 50 μg protein/sample was analysed for PRC1 protein expression by Western blot. The membrane was stripped and reprobed with anti-*á*-actin for normalizing differences in protein loading

Figure 2 Suppression of PRC1 expression by p53 in different cell lines. T47D or HeLa cells were cotransfected with pBSp53 and pEGFP vector or mock transfected with pBS empty vector plus pEGFP. At 2 days after transfection, pEGFP-expressing cells were selected by fluorescent-activated cell sorting. Two-third of sorted cells were used for protein extraction and the rest of the cells were lysed for RNA isolation. Total cell lysate and total RNA were also harvested from untransfected cells as control. (a) The PRC1 protein was detected by Western blotting with anti-PRC1 rabbit serum and the p53 protein was detected with DO-1 antibody (Santa Cruz). (b) T47D and HeLa cells were cotransfected with p53Luc plus pBS vector or pBSp53 along with the normalizing vector pRSVluc. At 48 h after transfection, the luciferase activities were analysed. (c) The relative amount of PRC1 mRNA was measured by the real-time quantitative RT–PCR. The amount of PRC1 mRNA or protein signals in untransfected cells (T47D) or mock-transfected cells (HeLa) was defined as 100%
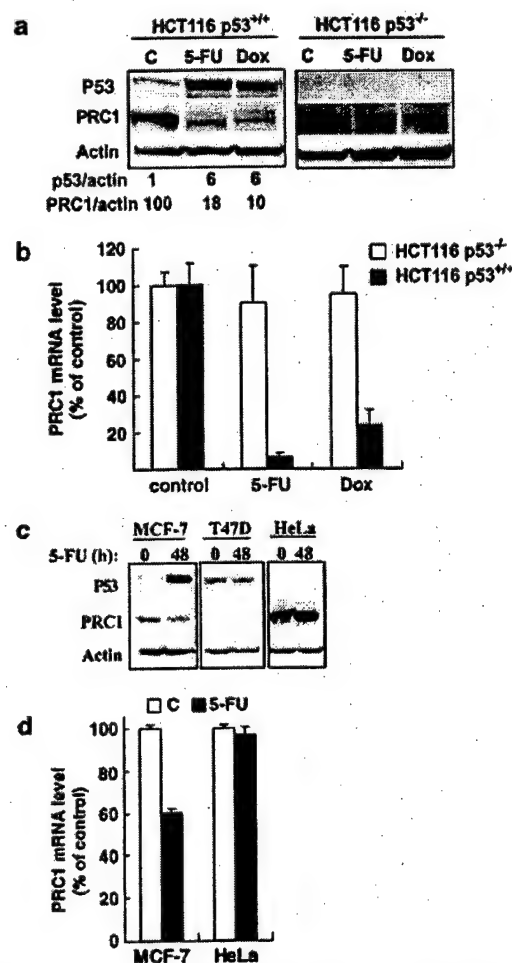

4

Western blot (Figure 2c). Together, these results demonstrate that downregulation of PRC1 mRNA and protein expression by p53 are not limited to MCF7-ptsp53 cells.

Suppression of PRC1 expression upon treatment with chemotherapeutic drugs 5'-fluorouracil (5-FU) and doxorubicin (Dox)

In addition to overexpression of the wt p53, we were interested in determining whether PRC1 expression could be repressed in a physiological environment with an elevated level of endogenous p53. To investigate this, we treated HCT116 p53$^{+/+}$ and HCT116 p53$^{-/-}$ with the therapeutic drugs 5-FU at 50 μg/ml or Dox at 2 μg/ml for 24 h. We also treated MCF-7, T47D, and HeLa cells with 5-FU at an effective dose of 10 μg/ml, which has been shown to increase cellular p53 protein levels in several cell lines (Chun and Jin, 2003). Following the treatment, the p53 and PRC1 protein levels were examined by Western blotting. Figure 3a and c (top panel) showed that the therapeutic drugs only effectively induce endogenous p53 expression in HCT116 p53$^{+/+}$ and MCF-7 cells that have functional p53; whereas p53 was not induced in HCT116 p53$^{-/-}$ cells which are p53 null, and T47D which does not have functional p53. P53 protein level in HeLa cells was also not induced due to the expression of the human papillomavirus E6 protein, which targets p53 for degradation. The induction of endogenous p53 by 5-FU or Dox considerably repressed PRC1 protein expression in HCT116 p53$^{+/+}$ and MCF-7 cells, whereas the PRC1 expressions in HCT116 p53$^{-/-}$, T47D, and HeLa cells were not changed by the same treatment (Figure 3a and c middle panel). The real-time PCR assay to measure PRC1 mRNA levels in different cell lines after the drug treatments obtained similar data (Figure 3b and d). These results are consistent with those achieved by exogenous expression of p53 and clearly demonstrate a regulatory role of p53 on PRC1 expression.

Downregulation of PRC1 gene expression by p53 overexpression results in binucleation

PRC1 is a microtubule binding and bundling protein essential to maintain the mitotic spindle midzone. Mollinari *et al.* (2002) have shown that complete suppression of PRC1 by siRNA in HeLa cells resulted in about 10% cells becaming binucleated after 24 h treatment of siRNA. We sought to determine whether the decreased PRC1 expression caused by p53 over-expression has similar inhibitory effects on cell division. First, by performing wt p53 immunostaining and DAPI staining, we examined the cell p53 level as well as the nuclei of MCF7-ptsp53 and regular MCF-7 cells that had been cultured at 32°C for 2 days. Under this condition, we found that over 95% of the ptsp53 cells cultured at 32°C overexpressed wt p53 and approximately 3% of these cells had two nuclei per cell (Figure 4, top panel). In contrast, we could not find any binucleated cells in MCF-7 cells (image not show).

Figure 3 Repression of PRC1 expression by endogenous p53 activated in response to chemotherapeutics. HCT116 p53$^{+/+}$ and HCT116 p53$^{-/-}$ cells were treated with 5-FU (50 μg/ml) or Dox (2 μg/ml) for 24 h. MCF-7, T47D, and HeLa cells were treated with 10 μg/ml of 5-FU for 48 h. Total cell lysate as well as total RNA were isolated from these samples. (**a**) Western blot analyses of p53, PRC1 protein expressions in HCT116 p53$^{+/+}$ and HCT116 p53$^{-/-}$ cells treated or untreated with drugs. The amount of p53 in untreated cells is expressed as 1; the amount of PRC1 in untreated cells is expressed as 100%. Note that p53 was not induced by chemotherapeutics in p53-null cells and PRC1 level in this cell line was not changed either. (**b**) Real-time quantitative PCR analyses of PRC1 mRNA levels in HCT116 p53$^{+/+}$ and in HCT116 p53$^{-/-}$ cells untreated and treated with drugs. The amount of PRC1 mRNA level in untreated cells is expressed as 100%. (**c**) Western blot analyses of p53 and PRC1 protein expressions in MCF-7, T47D, and HeLa cells treated or untreated with 5-FU. P53 protein was induced by 5-FU in MCF-7 cells but was not changed in T47D and HeLa cells; and the PRC1 level in MCF-7 was decreased by 60% after the drug treatment but was not changed in other cell lines. (**d**) Real-time quantitative PCR analyses of PRC1 mRNA levels in MCF-7 and HeLa cells untreated and treated with 5-FU. PRC1 mRNA levels in untreated cells are expressed as 100%

We have tried to detect the cell PRC1 level by immunostaining, but we could not obtain a specific staining by the current PRC1 antibody. Next, we extended this observation to HCT116 p53$^{-/-}$ cells after transfection of pBSp53 and pEGFP and enrichment of
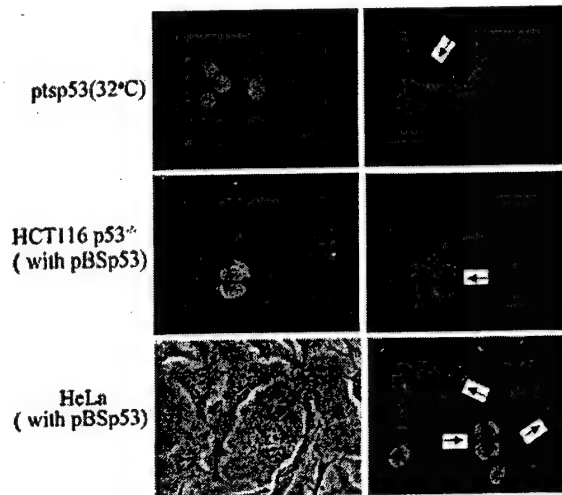
Figure 4 Suppression of PRC1 expression by p53 leads to binucleation. To detect binucleated cells after p53 expression, MCF7-ptsp53 cells cultured at 37°C were switched to 32°C for 2 days prior to staining with pAb246 p53 antibody (Green) and DAPI (blue) (top panel). HCT116 p53$^{-/-}$ (middle panel) and HeLa cells (bottom panel) were transfected with pBSp53 or the empty vector in the presence of pEGFP. At 2 days after transfection, positive transfected cells were selected by cell sorting and were cultured overnight. Next day, cells were fixed with cold methanol and stained with DO-1 p53 antibody and FITC-conjugated rabbit anit-mouse IgG (green) and DAPI to visualize the DNA (blue). The green signal of EGFP could not be detected after fixing cells, so the green signals are solely due to the positive staining of p53. Cell images under phase contrast and under fluorescent microscope were recorded by a CCD digital camera PENGUIM 600CL. Red arrows indicate binucleated cells

transfected cells by cell sorting. We found that about 95% of the transfected cells overexpressed wt p53 and 2% of these cells became binucleated (Figure 4 middle panel), whereas in mock-transfected HCT116 p53$^{-/-}$ cells, few cells showed binucleation. Similar experiments of transfection and cell sorting were performed in HeLa cells. We detected binucleation in 5.4% of HeLa cells after transfection with the wt p53 as compared to the mock-transfected HeLa cells that contained less than 0.5% of binucleated cells. Figure 4 bottom left panel showed the phase contrast image of pBSp53-transfected HeLa cells, and the bottom right showed DAPI staining.

p53 suppresses PRC1 promoter activity

To determine an inhibitory effect of p53 on PRC1 gene transcription, we first isolated a 3 kb genomic fragment of PRC1 gene covering from −2964 to +76 relative to the transcription start site. This was accomplished by a PCR reaction using RPCI 11 human genomic clone as a template. The PCR product was subcloned into the pGL3-basic luciferase reporter. The resulting plasmid was named PRC1-3kb. The ATG translation start codon was excluded from the fragment to ensure the correct translation of luciferase gene product.

HCT116 p53$^{-/-}$, MCF-7, T47D, and HeLa cells were cotransfected with PRC1-3 kb along with the pRSV-Luc

normalizing vector. In all four cell lines, PRC1-3 kb showed the luciferase activities. In MCF-7, the PRC1-3 kb luciferase activity was 20-fold of the promoterless vector pGL3-basic. In HCT116 p53$^{-/-}$, T47D, and HeLa cells, the PRC1-3 kb luciferase activities were over 100-fold of pGL3-basic (data not shown). These results indicate that the isolated 3 kb fragment contains the functional PRC1 promoter. The fact that the PRC1 promoter activity was fivefold lower in MCF-7 cells that express functional wt p53 than that in HCT116 p53$^{-/-}$, HeLa, and T47D cells implies that the PRC1 promoter activity is subjected to the negative regulation by endogenous p53.

To examine the effect of p53 on PRC1 transcription, we transfected PRC1-3 kb in the presence of different amounts of pBSp53 into HCT116 p53$^{-/-}$ or T47D cells. At 2 days after transfection, the PRC1 promoter activities in transfected cells were determined. Figure 5a and b show that p53 inhibited PRC1-3 kb promoter activity in a dose-dependent manner in HCT116 p53$^{-/-}$ and T47D cells. PRC1-3 kb promoter activity was nearly completely suppressed by the highest dose of pBSp53 in both cell lines. In a parallel experiment, p53 reporter vector p53Luc was cotransfected with different amounts of pBSp53 into HCT116 p53$^{-/-}$ cells. The result in Figure 5c demonstrated the dose-dependent increase of p53 transactivating activity in these transfected cells. We also determined the time-dependent effect of p53 expression on PRC1 promoter activity in T47D cells. PRC1 promoter activity was decreased to 34.1% of control at 16 h and further decreased to 6.1% at 48 h by exogenous expression of p53 (Figure 5d). At each time point, pBS empty vector was used as a control to pBSp53.

The effects of p53 overexpression on PRC1 promoter activities in MCF-7 and HeLa cells were further examined. In MCF-7, cotransfection of pBSp53 with PRC1-3 kb reduced the luciferase activity by 49% as compared to that of the empty vector-transfected cells. In HeLa cells, 45% reduction in PRC1 promoter activity was observed after cotransfection of PRC1-3 kb with pBSp53 (data not shown).

Localization of the p53-responsive region to the proximal section of the PRC1 promoter

To understand how p53 regulates PRC1 transcription, the identification of p53-responsive *cis*-regulatory elements on PRC1 promoter is of importance. To this end, serial deletions of the 5′-flanking region of PRC1-3 kb promoter were made. Figure 6 illustrates the nucleotide sequence spanning the PRC1 proximal promoter region from −281 to +76 and a schematic diagram of the deletion constructs. T47D cells were transfected with these truncated constructs individually with pBSp53 or with the empty vector pBS, and assayed for luciferase activities. Figure 7a compared the basal promoter activity of the deletion constructs with the activity of the full promoter construct PRC1-3 kb. These results, summarizing six separate transfections, showed that deletion of the 5′-flanking region from 3 kb to −282 did
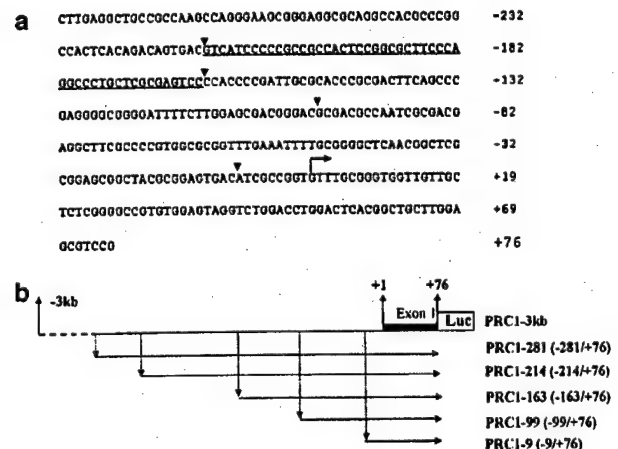
6

not affect the PRC1 promoter basal activity at all. However, additional deletion of 67 nucleotides drastically reduced the promoter activity by more than 80%. Further deletions to −9 gradually reduced the promoter activity to the baseline. These data demonstrate that the functional regulatory elements controlling the basal transcription of PRC1 gene reside within a 272 bp region
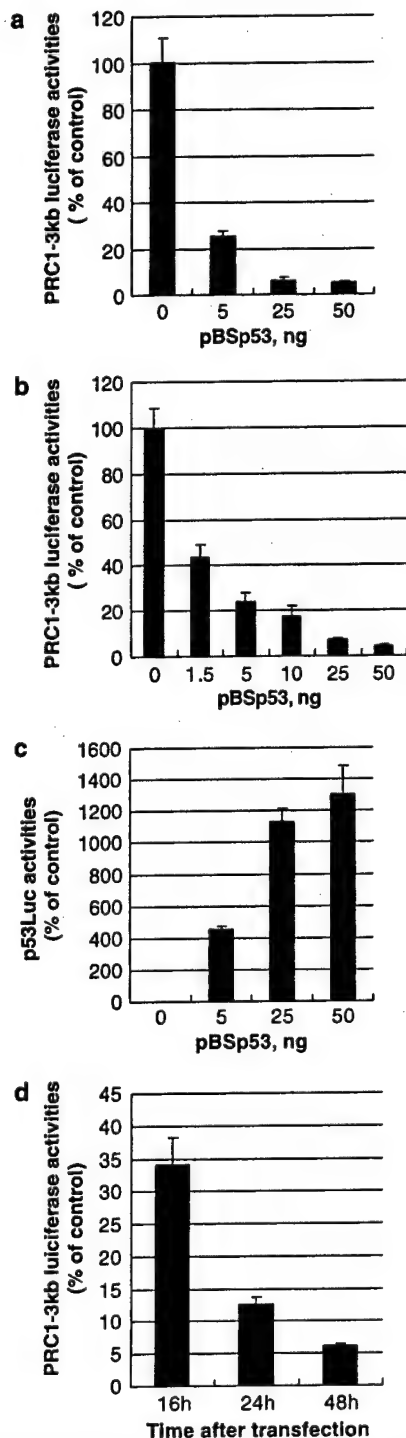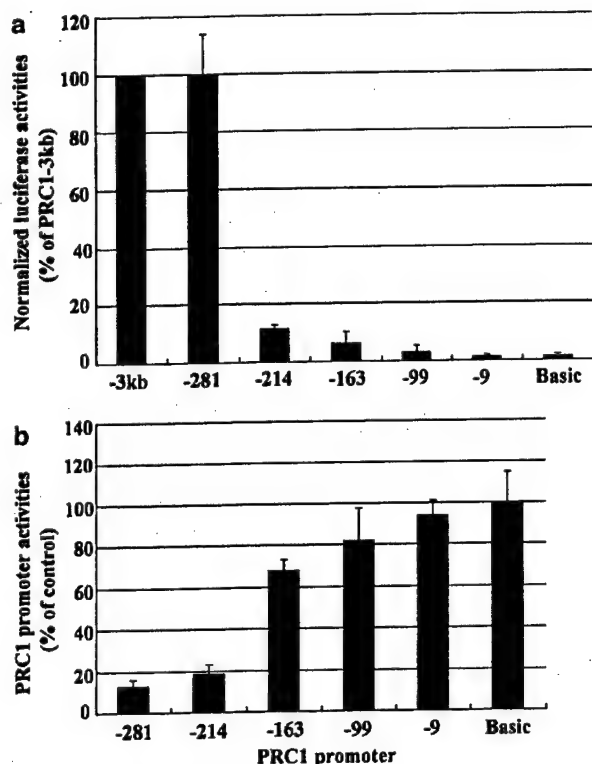

between −281 and −10. P53 was able to repress the promoter activities of PRC1-281 and PRC1-214 to the same extent as PRC1-3 kb (Figure 7b), but it lost responsiveness to the promoter constructs PRC1-163, PRC1-99, and PRC1-9. To confirm the presence of the p53-responsive element within the region of −214 to −163, we made an internal deletion construct (PRC1-281-del) that does not contain the fragment between −216 and −161. The results in Figure 8 show that deletion of this region increased the basal promoter activity (Figure 8a) but significantly reduced the response to p53-mediated suppression (Figure 8b). These data provide additional evidence to support the functional role of this region in p53-mediated down-regulation of PRC1 transcription.

Sequence analysis using MatInspector failed to detect a consensus or a homologous p53-binding site within the whole 272 bp basal promoter region or within the p53-
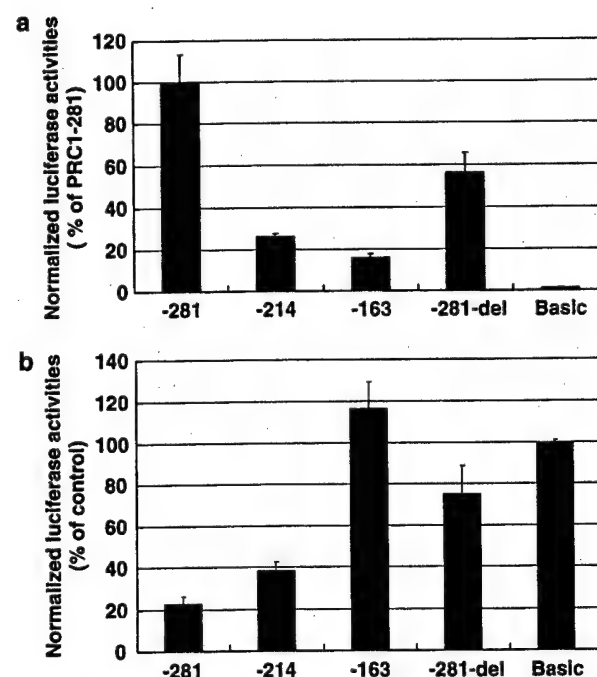

Figure 6 Nucleotide sequence of the proximal 5′-flanking region of PRC1 gene and a diagram of the PRC1 promoter deletion constructs. In (a), the first nucleotide in exon 1 is putatively signed as the transcription start site and is indicated by an arrow. The arrowheads indicate the truncation sites. The defined p53-responsive region is bold and underlined. In (b), PRC1 genomic fragments with different 5′ deletions were cloned into pGL3-basic luciferase vector

Figure 5 P53 suppresses PRC1 promoter activity. (a, b) Dose-dependent suppression of PRC1 promoter activity by p53: HCT116 p53−/− (a) or T47D cells (b) seeding in 24-well culture plates were cotransfected with PRC1-3 kb reporter DNA, pBSp53 (with indicated amount of plasmid), and a normalizing vector pRSV-Luc for 48 h. The normalized PRC1 promoter luciferase activity in the absence of p53 expression is expressed as 100%. (c) Dose-dependent activation of p53Luc by p53. HCT116 p53−/− cells seeding in 24-well culture plates were cotransfected with p53Luc reporter DNA, pBSp53 (with indicated amount of plasmid), and a normalizing vector pRSV-Luc for 48 h. The normalized p53 reporter luciferase activity in the absence of p53 expression is expressed as 100%. (d) Time-dependent suppression of PRC1 promoter activity by p53 in T47D: T47D cells seeding in 24-well culture plates were cotransfected with PRC1-3 kb reporter DNA, pBSp53 (or pBS vector as control), and normalizing vector pRSV-Luc. Cells were harvested at different intervals after transfection. At each time point, the normalized PRC1-3 kb luciferase activity in the pBS empty vector-cotransfected cells is expressed as 100%

7

Figure 7 Truncation analyses of PRC1 basal promoter activity and p53-mediated suppression of the PRC1 promoter activity. (a) Comparison of the PRC1 promoter activities driven by different lengths of the 5'-flanking sequences: T47D cells were transfected with different PRC1 promoter deletion constructs along with the pRSV-Luc normalizing vector. Cell lysates were harvested 48 h after transfection and the firefly luciferase activity and the renilla luciferase activity were measured using the dual luciferase assay kit. The data shown are summarized results of six independent transfection assays in which triplicate wells were used in each condition. The PRC1-3 kb promoter activity is defined as 100%, other promoter constructs' activities are presented as percentage of that value. (b) Localization of the p53-responsive region of PRC1 promoter: T47D cells were transfected with different PRC1 promoter constructs and pRSV-Luc with pBSp53 or with pBS empty vector. At 48 h post transfection, cells were harvested and the luciferase activities were analysed. The normalized luciferase activity of each construct in the pBSp53-transfected cells was compared to that of the pBS vector which is expressed as 100%. The data shown are summarized results of four independent transfection assays in which triplicate wells were used in each condition. The different responses to p53 between PRC1-214 and PRC1-163 are statistically significant ($P < 0.05$). In these assays, pGL3-basic vector is included to filter out nonspecific effects of p53 on luciferase activity

Figure 8 Loss of p53 response by deletion of the PRC1 promoter region from −216 to −163. (a) Comparison of the basal PRC1 promoter activities in different constructs. The function of −214 to −163 region on the basal PRC promoter activity was assessed by transient transfect PRC1-281-del (the region from −216 to −161 was deleted from PRC1-281) as well as other PRC1 promoter constructs into the T47D cells. PRSV-Luc was cotransfected as a normalizing plasmid. Cell lysates were harvested 48 h after transfection and the luciferase activities were measured using the dual luciferase assay kit. The normalized PRC1-281 promoter activity is defined as 100%, other promoter constructs' activities are presented as percentage of that value. (b) p53-mediated suppression. T47D cells were transfected with different PRC1 promoter constructs and pRSV-Luc with pBSp53 or with pBS empty vector. At 48 h post transfection, cells were harvested and the luciferase activities were analysed. The normalized luciferase activity of each construct in the pBSp53-transfected cells was compared to that of the pBS vector which is expressed as 100%

responsive region (−214 to −163). This p53-responsive region, however, does contain a GC-rich sequence (−206 to −199) and a putative NF-κB site (−195 to −181). Thus, site-directed mutagenesis on the promoter construct PRC1-281 was performed to individually mutate the GC-rich stretch (muGC) or the NF-κB site (muNF-κB). The contributions of these sequences to the basal and p53-repressed PRC1 promoter activity were assessed by transfection of the wt and the mutated constructs into T47D cells in the absence or the presence of pBSp53. The upper panel of Figure 9 shows that

nucleotide alternation within the GC-rich sequence reduced the basal PRC1 promoter activity by 65% and mutation within the NF-κB site moderately lowered the promoter activity by 37%. However, none of these mutations individually abolished the p53-mediated repression of the promoter activity (Figure 9, lower panel). These data suggest that the GC-rich region and the NF-κB site are important for the PRC1 promoter basal activity, but they are expendable for the p53-mediated suppression of the PRC1 transcription.

p53 interacts with PRC1 promoter in vivo

To determine whether p53 could interact with the proximal region of the PRC1 promoter *in vivo*, we performed chromatin immunoprecipitation (ChIP) experiments. The MCF7-ptsp53 cell system was used for this purpose. MCF7-ptsp53 cells cultured at 37°C or 32°C for 48 h were treated with formaldehyde to

a

b
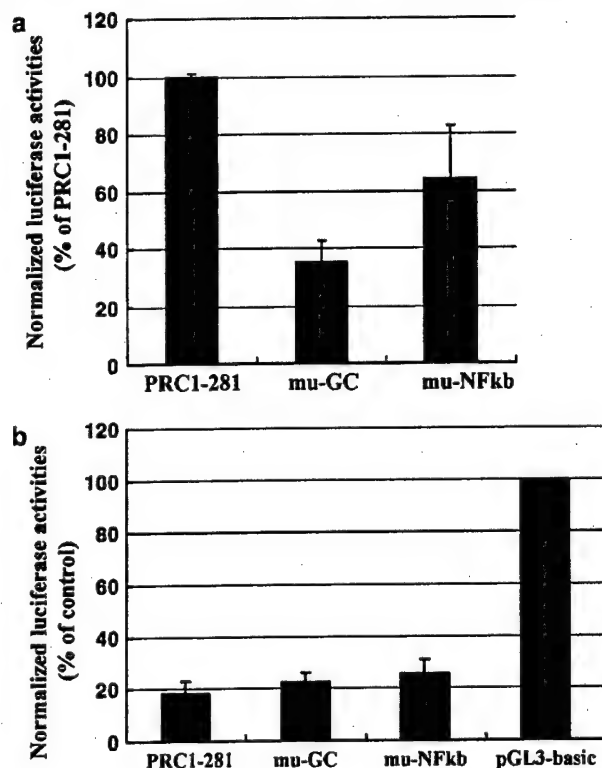
Figure 9 The proximal GC-rich motif and NF-κB site are important for basal PRC1 transcriptional activity but they are not essential for p53-mediated suppression. The effects of p53 on the wt PRC1 promoter construct PRC1-281 and the two mutant constructs were assessed by transient transfection of these plasmids with pBSp53 or with pBS control vector, respectively, into T47D cells. Luciferase reporter assays were conducted as described in Figure 7. The data (mean±s.d.) were derived from four separate transfection experiments. In the upper panel, the normalized luciferase activity of PRC1-281 is expressed as 100%. In the lower panel, the luciferase activity of each vector in pBS control-transfected cells is expressed as 100%

generate covalently crosslinked DNA–protein complex within the cells. Crosslinked chromatin was then immunoprecipitated with antibody against p53. Normal rabbit IgG was used as a nonspecific binding control. PCR amplification was then performed on the immunoprecipitated DNA and on the total input DNA. Primers were designed to amplify the region from −281 to +76 of the PRC1 gene that contained the full promoter activity as well as the p53-responsive region. Primers to amplify the p53-responsive region within the p21 promoter were used as a positive control (Kaeser and Iggo, 2002). Figure 10 showed that PRC1 and p21 chromatins were specifically immunoprecipitated with anti-p53 antibody only from MCF7-ptsp53 cells maintained at 32°C (Figure 10, right panel) that express the functional p53 but not from cells cultured at 37°C that expressed the mutant p53 (Figure 10, left panel). These data clearly indicate the *in vivo* association of wt p53 with PRC1 gene promoter and provide additional evidence to support the regulatory role of p53 in PRC1 gene transcription.
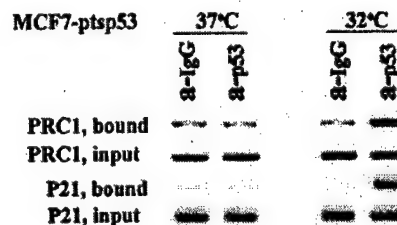
Figure 10 ChIP of PRC1 promoter. MCF7-ptsp53 cells were cultured at 37°C or at 32°C for 2 days. ChIP was performed with antibody against p53. Normal rabbit IgG was included in the assay as a negative control for nonspecific binding. P53 binding was tested by using PRC1-specific primers; p21 primers were used as a positive control for p53 binding. *Bound* represents the DNA coimmunoprecipated with antibody, while *input* represents the starting material before immunoprecipitation

Discussion

Mammalian cells proceed through the cell division cycle in a strictly ordered fashion. To do so, cells must precisely duplicate their chromosomal DNA during S phase, segregate the sister chromatids to opposite poles of spindle during mitosis, then proceed with the process of cytokinesis that finally leads to daughter cell separation. P53, the cellular gatekeeper for growth and division, is known to play key roles in the checkpoints of G1 to S phase transition and G2 to M phase transition. The p53-mediated G2/M checkpoint is thought to account for the phenotype of genetic instability that is commonly associated with a p53 mutation (Cheng and Loeb, 1993). In this study, we demonstrate a new function of p53 in cytokinesis through its action as a negative regulator of PRC1, a protein that plays important roles in cytokinesis.

Exogenous overexpression of the wt p53 resulted in decreases of PRC1 mRNA and protein levels not only in MCF-7 or T47D breast cancer cells but also in HeLa and the p53 null HCT116 p53$^{-/-}$ cells, thereby suggesting that the ability of p53 to regulate PRC1 is a general property of this tumor suppressor protein. The decline in PRC1 protein and mRNA expression in responses to elevated endogenous p53 level in HCT116 p53$^{+/+}$ and MCF-7 cells after therapeutic drugs treatment provide additional support to this newly characterized function of p53 (Figure 3). Although in our studies we did not use mutant constructs of p53 containing different mutations, the microarray experiments comparing MCF7-ptsp53 overexpressing the ts mutant of p53 with the p53 wt MCF-7 revealed similar levels of PRC1 mRNA, thus suggesting that the function of p53 in suppression of PRC1 gene transcription is specific for the wt p53.

Since high levels of PRC1 at the G2/M phase have been shown to be required for HeLa cells to exit mitosis, the suppressed PRC1 expression in MCF7-ptsp53 cells cultured at the 32°C likely contributes to the growth arrest of these cells at the G2/M stage of the cell cycle. In HeLa cells, the inhibited expression of PRC1 by siRNA gave rise to binucleated cells, and the percentage of binucleation increased with time. In our studies, we have detected binucleated cells in all four cell lines within 2–3

days after overexpression of the wt p53, either by temperature switching of MCF7-ptsp53 cells, or by transient transfection of pBSp53 into HCT116 p53$^{-/-}$, HeLa, and T47D cells. In general, 2–5% of p53-overexpressed cells were shown to become binucleated. This was in sharp contrast with the mock-transfected cells in which binucleated cells were rarely found under the same experimental conditions. In our experimental settings, overexpression of the wt p53 deceased the PRC1 protein levels by 70–80% after 2 days, the incomplete suppression of PRC1 expression may explain the relatively low percentage of binucleated cells. Alternatively, some other cellular genes that are not downregulated by p53 may also need to be inhibited in order to completely stop cell division. Owing to the limitations of transient transfection, we could not examine this binucleation phenomenon over a longer period of time in HCT116p53$^{-/-}$, HeLa, or T47D cells. In MCF7-ptsp53 cells, soon after temperature shift down, cells became growth arrested with little proliferative activity. Thus, we could not observe increased population of binucleated cells even after 1 week of culturing at the permissive temperature.

In an attempt to further characterize the regulatory function of p53 on PRC1, we have made a construct encoding a his-tagged PRC1. Transient transfection of this vector into cells generated the typical phenotype as previously observed in HeLa cells (Mollinari et al., 2002). Revealed by immunostaining with anti-His antibody, PRC1 formed brightly stained fiber rings surrounding the nucleus (data not shown). We were interested in determining whether enforced expression of PRC1 could override the p53-induced G2/M arrest by establishing stable PRC1 expression clones of MCF7-ptsp53. However after transfection of His-PRC1 into cells, the transfected cells grew very slow and we could not isolate positive clones after antibiotic selection. It is possible that overexpression of PRC1 has a negative impact on cell growth.

P53 exerts its functions by engaging in complexes with other proteins (Espinosa and Emerson, 2001) or by acting as a transcriptional activator or repressor (Levine, 1997). As a transcription activator, p53 binds DNA in a sequence-specific manner (Vogelstein and Kinzler, 1992; Levine, 1997). However, as a transcription repressor, different DNA motifs have been shown to be involved in p53-mediated suppression (Seto et al., 1992). Compared to the gene activation through a direct binding of p53 to its recognition sequence, the mechanisms of transcriptional suppression by p53 are much more complex and are less clearly defined (Harris et al., 1996; Manni et al., 2001). In this study, we have isolated PRC1 promoter and demonstrate that p53 suppress PRC1 promoter activity in dose- and time-dependent manners, thus proving that p53 suppresses PRC1 expression by modulating its transcription.

Our deletion analyses have clearly defined the region from −281 to −9 of the 5'-flanking sequence being the functional region of the PRC1 promoter. Interestingly within this 272 bp section, almost 80% of the transcriptional activity is driven by regulatory elements located

with a 70 bp section (−281 to −214). Several transcription factor-binding sequences are clustered within this region including a muscle initiation sequence, a Sp1-binding site, a CAT box, and a Ap1/CREB site. The contribution of these regulatory sequences in the control of PRC1 transcription during cell cycle awaits further investigation.

With regard to p53, we have searched for the regulatory sequences responsible for p53 suppression. Our transient transfection results point to the sequences between −214 and −163 as the p53-responsive region. This region does not contain a classical p53-binding sequence nor the newly identified p53-repressive element in MAD1 promoter (Chun and Jin, 2003). As other studies have demonstrated that p53 could inhibit gene transcription through interruption of positive transcription factors such as Sp1 to bind its recognition sequence, and this p53-responsive region contains a classical Sp1-binding motif and a putative NF-κB-binding site, we mutated both sites to examine their roles in the basal transcription and in the p53-mediated suppression of PRC1 transcription. While mutations at either site lowered the basal PRC1 promoter activity, neither mutation abolished the p53 suppression (Figure 9). Collectively, these results suggest that p53 may repress PRC1 transcription through distinct mechanisms.

In order to assure the functional role of p53 in PRC1 transcription, ChIP assays were performed. As shown in Figure 10, p53 antibody could only precipitate the PRC1 chromatin in MCF7-ptsp53 cells maintained at 32°C that express the functional p53 but not in cells cultured at 37°C that express the mutant p53. Similar results were found with p21 chromatin, which has a well-defined p53-responsive element. ChIP assay further confirmed that PRC1 is a p53-targeted gene and p53 regulates PRC1 expression at a transcriptional level.

We have attempted to detect the binding of p53 to the defined p53-responsive region of PRC1 promoter by conducting gel shift assay using recombinant p53 protein. While p53 could bind strongly to a wt p53 consensus sequence, we could not detect p53 binding to the oligonucleotide probe containing the PRC1 p53-responsive region (−216 to −163) (data not shown). These preliminary results suggest that the interaction of p53 with PRC1 promoter may occur in the presence of other cofactors. Studies to fine map the p53-responsive sequences and to identify the cofactors that are involved in the p53-mediated suppression of PRC1 transcription are under further investigation in our laboratory.

In conclusion, we have identified a new p53 target gene PRC1 whose transcription is subject to the negative regulation of p53. Regarding the physiological significance of PRC1 repression by p53, we hypothesize that in addition to G1/S and G2/M checkpoints, p53 as the most important tumor suppressor that may provide a final checkpoint control for cell division at the stage of cytokinesis by repressing the transcription of the PRC1 gene whose expression is required for cell cleavage at the end of mitosis, thereby preventing premature entry into another round of cell proliferation. Hence, the effects of p53 on blocking cytokinesis may provide additional

10

protection to maintain genomic integrity and to prevent cancer formation in situations of failed G1 or G2 checkpoints.

Materials and methods

Cells and reagents

Human cancer cell lines MCF-7, T47D, and HeLa were obtained from American Type Culture Collection (Manassas, VA, USA). All cell lines were cultured in RPMI-1640 medium supplemented with 10% FBS. Stable MCF7-ptsp53 clone constitutively expressing p53Val[135] mutant was generated in our laboratory and were cultured in RPMI-1640 medium containing 10% FBS and G418 (300 µg/ml) (Li *et al.*, 2003). The HCT116 human colon adenocarcinoma cells and a derivative with a homozygous disruption of the p53 gene were a generous gift from Dr Bert Vogelstein (Johns Hopkins University School of Medicine, Baltimore, MD, USA) and were grown in MaCoy's 5A medium supplemented with 10% FBS and antibiotics. The rabbit anti-PRC1 serum was a generous gift of Dr Tony Hunter (The Salk Institute).

Microarray analysis

The human cDNA array containing some 40–45 K genes was obtained from the Microarray Core Facility at Stanford University School of Medicine. Detailed procedure for probe labeling and hybridization were as described previously (Li *et al.*, 2003). Briefly, MCF7-ptsp53 and MCF-7 cells in RPMI-1640 with 10% FBS were cultured at 37°C or 32°C for 4 days. In all 60 µg of total RNA per sample was used to generate the first-strand cDNA probe in the presence of cy3-dCTP (for MCF7-ptsp53 or MCF-7 at 37°C) or cy5-dCTP (for MCF7-ptsp53 or MCF-7 at 32°C) in the reaction of RT. Labeled cDNA probes were purified and hybridized to an arrayed slide overnight at 65°C. The fluorescent images were captured using a GenePix 4000 scanner (Axon Instruments, Foster city, CA, USA). To analyse the array data, the CLUSTER program was applied to obtain an average-linkage hierarchical clustering and the results were displayed by using the program TREE-VIEW (software available at http://genome-www4.stanford.e-du/MicroArray/SMD/restech.html). The fluorescent intensities of cy-5 and cy-3 for each target spot were automatically adjusted by the analysing program in a way that the housekeeping genes for each slide became equal. The genes whose expression varied by at least twofold from the median red/green rating were subsequently selected and grouped according to their primary functions defined by GeneCards (http://bioinformatics.weizmann.ac.il/cards/).

RNA isolation and Northern blot analysis

MCF-7, MCF-7-neo, and MCF-7-ptsp53 were seeded in 60 mm dishes in RPMI-1640 media supplemented with 10% FBS at 37°C. The cells were switched to 32°C at the same time and were harvested at different times as indicated. Cells were lysed in Ultraspec RNA lysis solution (Biotecxs Laboratory, Houston, TX, USA), and total cellular RNA was isolated according to the vendor's protocol. Approximately 15 µg of each total RNA was used in Northern blot analysis. The PRC1 mRNA was detected with a 340 bp ^{32}P-labeled cDNA probe corresponding to the region 558–897 of PRC1 cDNA sequence. The membrane was stripped and reprobed with a human GAPDH probe to ensure equal amount of loading. The hybridization signals were visualized by a BioRad

PhosphoImager and were quantified by the program of Quantity One.

The PRC1 probe was generated by reverse transcription (RT)–PCR reaction followed by purification with DNA Clean & Concentrator™-5 Kit (Zymo research, CA, USA). The total RNA isolated from MCF-7 cells was used in the RT reaction. The sequences used in the RT–PCR of the probe and other experiments are listed in the table. The conditions for the PCR reactions were as follows: 94°C 1.5 min followed by 94°C 20 s, 60°C 20 s, 72°C 30 s for 30 cycles and a final extension at 72°C for 5 min. PCR product was sequenced to ensure the correct sequence.

Selection of pBSp53-transfected cells

T47D and HeLa cells were cotransfected with pEGFP and pBSp53 or pBS empty vector by FuGENE 6 reagent (Roche). The ratio of pEGFP and pBSp53 or pBS is one to two. At 2 days after transfection, cells were removed from dishes by trypsin and resuspended in fresh medium. The pEGFP-positive cells were selected by flow cytometry (FACS Vantage SE, Becton Dickinson). Approximately 0.5×10^6 cells were used for real-time PCR and the rest of the cells were cultured overnight for p53 immunostaining and DAPI staining.

Quantitation of PRC1 mRNA expression

To quantitatively measure PRC1 mRNA levels in MCF7-ptsp53 and MCF-7 cells cultured at 37°C or 32°C for different intervals as well as in selected pBSp53 or mock-transfected T47D, HeLa, HCT116 p53$^{-/-}$ cells, and HCT116 p53$^{+/+}$ cells treated with 5-FU or Dox, real-time PCR was conducted. Total RNA was isolated from different cell samples by RNAeasy kit (Qiagen). cDNAs were prepared by using Eppendorf kit (Brinkmann Instruments, Inc., NY, USA). Real-time PCR was performed on the cDNA using the ABI Prism 7900-HT Sequence Detection System and Universal MasterMix (Applied Biosystems). PRC1 and GAPDH mRNA expression levels were assessed using the human PRC1 and GAPDH Pre-Developed Ω Becon Gene Expression Set (Gorilla Genomics).

Western blot analysis

Cells were lysed with 1× cold lysis buffer containing a complete mini protease inhibitor cocktail (Roche Molecular Biochemicals) as previously described (Li *et al.*, 2003). Approximately 50 µg protein of total cell lysate was separated on 4–20% SDS–PAGE, and transferred to nitrocellulose membranes. The membranes were blotted with the rabbit anti-PRC1 serum used at a 1 : 10000 dilution, and the signals were detected with an enhanced chemiluminescence (ECL) detection system (Amersham). Membranes were stripped and reblotted with anti-α-actin antibody (Chemicon) to ensure equal amount of protein loading. The signals were quantitated with a BioRad Fluo-S Multi Imager System.

Detection of binucleated cells by p53 immunostaining and DAPI staining

The MCF7-ptsp53 and MCF-7 cells at 37°C or 32°C for 2 days, as well as selected pBSp53- or pBS-transfected HCT116 p53$^{-/-}$, HeLa, and T47D cells were cultured on coverslips. The cells were washed with ice-cold PBS and fixed in cold methanol (−20°C) for 10 min. After two washes with PBS, cells were incubated for 1 h in blocking buffer (0.4% Triton X-100, 0.1% gelatin, 1% BSA in PBS). For MCF7-ptsp53 or MCF-7 cells, anti-p53 antibody Pab246 (Santa Cruz) was used, for all other

Table 1 Sequences of oligonucleotides used in cloning and ChIP assay

Primers	Nucleotide sequence (5' to 3')
PRC1 northern probe (340 bp)	
PRC1F 5'	CTATGATATTGACAGTGCCTCAGTGC
RRC1R 5'	TATTTGCAACCTGTCCCAGAGCTCTCG
PRC1 full promoter	
PRC1 −2964 5'	TCTCCTCACCATCCCTACGACAGAGGTCT
PRC1 +76 3'	CGGACGCTCCAAGCAGCCGTGAGTCC
PRC1 deletion primers	
PRC1-281 5'	GCTGGCTTGGGAGAGGggtaccTTGAGGCTGCCGCCAAG
PRC1-214 5'	CCGGCCACTCACAGACAggtaccTCATCCCCCGCCGCCAC
PRC1-163 5'	TCCCAGGCCCTGCTCGCGggtaccCGACGCCGATTGCGCAC
PRC1-99 5'	GGATTTTCTTGGAGCGACCggtaccCGACGCCAATCGCGACG
PRC1-9 5'	CGGAGCGGCTACGCGGAggtaccTCGCCGGTGTTTGCGGGTG
PRC1-216 5'	GGCCACTCACAGACAGacgcgtCATCCCCCGCCGC
PRC1-161 5'	GCTCGCGAGTCCCCAacgcgtTTGCGCACCCGCGAC
PRC1 mutation oligos	
PRC1-281-mu-GC2 5'	CAGTGACGTCATCCCCatCtGCCACTCCGGCGCTTCC
PRC1-281-mu-NF-κB 5'	GCCGCCACTCCGGCGCTaCgCgtGCCCTGCTCGCGAGTC
PRC1 ChIP primers	
Sense strand	CTTGAGGCTGCCGCCAAGCCAG
Antisense strand	CGGACGCTCCAAGCAGCCGTGAG
P21 ChIP primers	
Sense strand	GTGGCTCTGATTGGCTTTCTG
Antisense strand	CTGAAAACAGGCAGCCCAAG

The generated *Kpn*1 or *Mlu* site is lower case and bold. The mutated nucleotides are lower case, bold, and italic

cell lines, anti-p53 antibody DO-1 (Santa Cruz) was used. The cells were incubated with the primary antibodies at $2 \mu g/ml$ for 1 h at room temperature. After washing with PBS, the cells were incubated with FITC-conjugated secondary antibody (1 : 200 dilution) for 1 h at room temperature. After two washes with PBS, cells were stained with DAPI at a concentration of $1 \mu g/ml$. After rinsing with PBS and drying the coverslips, the coverslips were mounted in an antifading reagent (Molecular Probes, OR, USA). Images were recorded by a Penguin 600CL digital camera connected to an inverted fluorescent microscope.

Cloning of the 5'-flanking region and portion of exon 1 of the human PRC1 gene

Human genomic clone RPCI-11 was obtained from the Bacpac Resources (Children's Hospital Oakland Research Institute, Oakland, CA, USA). Using the genomic clone RPCI-11 as the template, a PCR reaction was performed to amply a 3030 bp fragment containing the 5'-flanking region and portion of exon 1 (−2964 to +76 relative to the transcription starting site). The resulting DNA fragment was first subcloned into the pCR2.1-TOPO vector using TOPO TA cloning kit (Invitrogen) and then was released by cutting with *Kpn*I and *Xho*I. The 3 kb fragment was then inserted into a luciferase vector pGL3-basic at the *Kpn*1 and *Xho*1 sites. The resulting vector was named PRC1-3 kb. The correct orientation of the PRC1 promoter was verified by enzymatic mapping. Note that the portion of exon 1 does not include the ATG translation start codon to guarantee the correct translation of luciferase gene product.

Generation of PRC1 promoter deletion reporter constructs

To construct a series of PRC1 promoter luciferase reporters with different 5' deletions, site-directed mutagenesis was conducted on the template DNA PRC1-3 kb by using the QuickChange™ Site-directed Mutagenesis Kit (Strategen, San Diego, CA, USA) to introduce a unique *Kpn*1 site at

different locations within the PRC1 promoter sequence. The 5' region (from −2964 to different unique *Kpn*1 site) was released by cutting with *Kpn*1. The remaining fragment was religated by Takara ligation kit (Takara shuzo co., LTD., Japan).

To construct PRC1-281-del, site-directed mutagenesis was conducted on the template DNA PRC1-281 to introduce a unique *Mlu*1 site at −216. By using the resulting plasmid as template, another *Mlu*1 site at −163 was created. The region from −216 to −163 was released by cutting with *Mlu*1, the remaining fragment was religated by Takara ligation kit.

The PRC1-281-mu-GC2 and mu-NFkB were conducted by site-directed mutagenesis to mutate the core region of the transcription factor-binding site. The altered sequences were scanned by TRANSFAC software to ensure no new transcription-binding sites being created.

Transfection assay

Cells were seeded in 24-well plates and incubated for 24 h in RPMI-1640 medium containing 10% FBS before transfection. A total of 200 ng DNA/well was transfected into cells using FuGENE 6 transfection reagent (Roche, # 1814443). The DNA ratios of the analysing firefly luciferase reporter to expression vector and to renilla luciferase reporter, pRSV-Luc, were 65 : 25 : 10. Transfected cells were incubated for 48 h prior to cell lysis. Luciferase activities were measured using the Promega Dual Luciferase Assay System.

ChIP assays

Experiments were performed with the ChIP kit (Upstate Biotechnology, Lake Placid, NY, USA) according to the manufacturer's instructions. Briefly, MCF7-ptsp53 or MCF-7 cells cultured at 37°C or 32°C for 2 days were crosslinked with 0.37% formaldehyde and the genomic DNA was sheared by sonication. The samples were then immunoprecipitated with antibody against p53 (FL-393, Santa Cruz). Normal rabbit IgG (Santa Cruz) was used as a negative control. The immunocomplex was heated at 65°C for 4 h to revert the

crosslinking between DNA and proteins. The purified bound DNA was dissolved in 20 μl of Tris buffer (10 mM Tris, pH 8.5). The input DNA was diluted 100 × prior to PCR. The bound and the input DNA were analysed by PCR (32 cycles) with primers that amplify a 357 bp fragment of the human PRC1 proximal promoter region from −281 to +76, relative to the major transcription start site. The PCR conditions were 95°C for 1.5 min, 95°C for 20 s, 65°C for 20 s, 72°C for 40 s, and 72°C for 5 min. As a positive control, the primers that amplify the p21 promoter fragment were used for PCR (Kaeser and Iggo, 2002). The sequences of the primers were presented in Table 1. The PCR products were visualized on a 2% agarose gel stained with ethidium bromide. The intensity of the PCR products was scanned with a BioRad Fluro-S MultiImager System and quantified by the Quantity One Program. Different amounts of template DNA were tested in the PCR reaction to ensure a linear range of DNA amplification.

References

Agami R and Bernards R. (2000). *Cell*, **102**, 55–66.
Agarwal M, Agarwal A, Taylor W and Stark GR. (1995). *Proc. Natl. Acad. Sci. USA*, **92**, 8493–8497.
Bargonetti J and Manfredi J. (2002). *Curr. Opin. Oncol.*, **14**, 86–91.
Cheng KC and Loeb LA. (1993). *Adv. Cancer Res.*, **60**, 156.
Chun ACS and Jin DY. (2003). *J. Biol. Chem.*, **278**, 37439–37450.
Dubrez L, Coll J, Hurbin A, Fraipont, Lantejoul S and Favrot M. (2001). *Gene Ther.*, **8**, 1705–1712.
Dulic V, Stein GH, Farahi FD and Reed SI. (1998). *Mol. Cell. Biol.*, **18**, 546–557.
Espinosa JM and Emerson BM. (2001). *Mol. Cell*, **8**, 57–69.
Harris CC. (1996). *J. Natl. Cancer Inst.*, **88**, 1442–1455.
Harris LC, Remack JS, Houghton PJ and Brent TP. (1996). *Cancer Res.*, **56**, 2029–2032.
Hollstein M, Sidransky D and Vogelstein B. (1991). *Science*, **253**, 49–53.
Jiang W, Jimenez G, Wells N, Hope T, Wahl G, Hunter T and Fukunaga R. (1998). *Mol. Cell*, **2**, 877–885.
Jung MS, Yun J, Chae HD, Kim JM, Kim SC, Choi TS and Shin DY. (2001). *Oncogene*, **20**, 5818–5825.
Kaeser MD and Iggo RD. (2002). *Proc. Natl. Acad. Sci. USA*, **99**, 95–100.
Kokontis JM, Wagner AJ, O'Leary M, Liao S and Hay N. (2001). *Oncogene*, **20**, 659–668.
Kruse K, Wasner M, Reinhard W, Ulrike H, Dohna C, Mössner J and Engeland K. (2000). *Nucleic Acids Res.*, **28**, 4410–4418.
Levine AJ. (1997). *Cell*, **88**, 323–331.
Li C, Shridhar K and Liu J. (2003). *Breast Cancer Res. Treat.*, **80**, 23–37.
Malkin D, Li FP and Strong LCEA. (1990). *Science*, **250**, 1233–1238.

Manni I, Mazzaro G, Gurtner A, Mantovani R, Haugwitz U, Krause K, Engeland K, Sacchi A, Soddu S and Piaggio G. (2001). *J. Biol. Chem.*, **276**, 5570–5576.
Martinez J, Georgoff I and Levine AJ. (1991). *Genes Dev.*, **5**, 151–159.
Michalovitz D, Halevy O and Oren M. (1990). *Cell*, **62**, 671–680.
Milner J and Medcalf E. (1990). *J. Mol. Biol.*, **216**, 481–484.
Mollinari C, Kleman JP, Jiang W, Schoehn G, Hunt T and Margolis RL. (2002). *J. Cell Biol.*, **157**, 1175–1186.
Nakamura S, Gomyo Y, Roth JA and Mukhopadhyay T. (2002). *Oncogene*, **21**, 2102–2107.
Seto E, Usheva A, Zambetti GP, Momand J, Horikoshi N, Weinmann R, Levine AJ and Shenk T. (1992). *Proc. Natl. Acad. Sci. USA*, **89**, 12028–12032.
Smith ML and Fornace Jr AJ. (1995). *Curr. Opin. Oncol.*, **7**, 69–75.
Stright AF and Field CM. (2000). *Curr. Biol.*, **10**, R760–R770.
Sugrue MM, Shin DY, Lee SW and Aaronson SA. (1997). *Proc. Natl. Acad. Sci. USA*, **94**, 9648–9653.
Tarapore P and Fukasawa K. (2000). *Cancer Inves.*, **18**, 148–155.
Taylor W, DePrimo S, Agarwal A, Agarwal M, Schönthal A, Katula K and Stark G. (1999). *Mol. Biol. Cell*, **10**, 3607–3622.
Taylor WR and Stark GR. (2001). *Oncogene*, **20**, 1803–1815.
Vogelstein B and Kinzler KW. (1992). *Cell*, **70**, 523–526.
Vousden K. (2000). *Cell*, **103**, 691–694.
Wesierska-Gadek J and Schmid G. (2000). *J. Cell. Biochem.*, **80**, 85–103.
Willers H, McCarthy E, Wu B, Wunsch H, Tang W, Taghian D, Xia F and Powell S. (2000). *Oncogene*, **19**, 632–639.
Yin XY, Grove L, Datta NS, Katula K, Long MW and Prochownik EV. (2001). *Cancer Res.*, **61**, 6493.